Investigations on Rheological and Thermomechanical Properties of LLDPE - Fumed Silica Nanocomposites for Rotational Molding

THESIS

Submitted in partial fulfillment of the requirements for the degree of

DOCTOR OF PHILOSOPHY

by

GIRISH CHANDRAN V

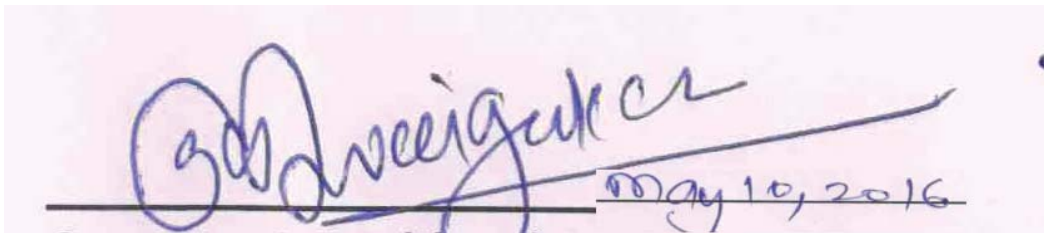Under the Supervision of

Dr. Sachin D Waigaonkar

BITS Pilani
Pilani | Dubai | Goa | Hyderabad

BIRLA INSTITUTE OF TECHNOLOGY AND SCIENCE, PILANI
2016

BIRLA INSTITUTE OF TECHNOLOGY AND SCIENCE, PILANI

CERTIFICATE

This is to certify that the thesis entitled "**Investigations on Rheological and Thermomechanical Properties of LLDPE - Fumed Silica Nanocomposites for Rotational Molding**" and submitted by **Girish Chandran V**, ID NO **2011PHXF407G** for award of Ph.D. of the Institute embodies original work done by him under my supervision.

[signature] May 10, 2016

Signature of the Supervisor

Dr. SACHIN D WAIGAONKAR

Assistant Professor

Department of Mechanical Engineering

Date:

To my family.

Acknowledgement

I would also like to express my gratitude to **Mr. Blaise Costabir**, Managing Director GMI Zarahak Moulders Pvt. Ltd. Goa for providing their facilities for the industrial verification of our laboratory scale studies. I would also like to express my thanks to **Mr. Pradeep** and **Mr. Jhonson** at GMI Zarahak Moulders Pvt. Ltd. Goa for their support.

I would also like to thank **Mr. Praveen Kumar**, Kenwood Industries, Goa for providing their extrusion and pulverizing facilities.

I would also like to thank **Dr. Madhusoodan**, Goa University for his help in using Scanning Electron Microscope for the micro structural studies.

I would also like to express my sincere thanks to **Dr. Kapil Joshi**, Application Specialist and **Mr. Saurabh Mehta**, Product Specialist Anton Paar India Ltd, for their help in conducting parallel plate rheometry at their service laboratory.

I would also like to thank **Mr. Ravi Mehra**, Chairman, Affiliation of Rotational Moulding Organisations (ARMO) for allowing me to participate in various ARMO events which helped me to understand the latest developments in rotational molding.

I would like to thank first degree students **Mr. Vishal Ahuja**, **Mr. Avinash Mittal**, **Ms. Anjali Srivastava**, **Mr. Abhijeeth Selhi** for their support in carrying out my research.

I would like to thank those unknown reviewers for their constructive criticisms and valuable suggestions during the review of my papers which helped me to improve my work further.

I sincerely thank each and every one, who have helped me either directly or indirectly at different stages of my research work.

Finally but not the least, I would like to express my thankfulness towards my lovely wife **Sudha M P**, son **Abhinav G Pisharody** and **my family** for their understanding and support through out my journey.

Girish Chandran V

Abstract

Rotational molding (RM) is a high-temperature, low-pressure, thermo-plastic processing method for the production of hollow or double-walled parts, usually of large dimensions. Polyolifines like linear low density poly ethylene (LLDPE) are commonly used as raw materials for the process. Rotationally molded parts find applications in many engineering and domestic outdoor applications requiring improved mechanical properties, which is limited by the choice of materials and the process itself as it demands high thermal stability of the polymer over a large temperature range. The normal trend of researchers is to focus on process parameters and new polymer blends with micro scale additives to improve the mechanical properties of the product. However, the use of nanocomposites for RM have not been adequately addressed. In this research work, nanocomposites of fumed silica (FS) have been used along with LLDPE. Detailed investigation is required to understand the alteration of rheological and mechanical properties of the polymer with the addition of nano particles. This work is focused on experimental investigations of RM of LLDPE - FS nano composites to improve the melt flow characteristics of the polymer as well as mechanical properties of the product.

Melt flow index (MFI) is commonly used to ascertain the melt characteristics of thermoplastic polymers. For RM using LLDPE, MFI values between 3.5 to 5 g/10 min (at 2.16 kg/190ºC) are preferred. The MFI values of LLDPE and FS blends were measured and proper blends for RM were identified. RM being a low shear process, parallel plate rheometry studies were conducted to study the melt rheology of LLDPE - FS blends and zero shear viscosity was found out. Based on the zero shear viscosity inferences were drawn about the interaction between the nano particles and LLDPE chains. In order to analyze the variations in melt torque during compounding of LLDPE, torque rheometry studies were performed.

The effect of FS on the mechanical and visco elastic properties of LLDPE has been further investigated. It included the effect of FS on static mechanical properties of RM product like tensile, flexural, and impact strengths. The effect of FS on crystallinity of LLDPE is studied by conducting X-ray diffraction studies. The micro structural studies using scanning electron microscopy were conducted to study the dispersion of FS in LLDPE and correlated with the mechanical properties of the nano composites. Dynamic mechanical analysis (DMA) was also carried out to find the time – temperature dependent mechanical properties viz. storage modulus ($E^{'}$), loss modulus ($E^{''}$), and tan delta for LLDPE - FS blends. DMA

studies were extended to perform accelerated stepped isothermal creep studies to find out the influence of FS on creep strains.

As RM suffers a drawback of longer cycle times, the effect of FS on the processibility was also studied apart from the material properties and attempts were made to reduce the cycle time. This was done by preparing an innovative fixture with internal heating and temperature monitoring capabilities, that can be used on a standard universal testing machine. The mold release force was measured for both steel and aluminum molds at different temperatures and pulling rates. The cycle time reduction was achieved by finding minimal pulling force for successful demolding at higher temperatures than (currently) used in industry.

Having arrived at a suitable LLDPE - FS composition at laboratory scale, the same was tested for an engineered product at industrial scale. The industry trials were conducted using a three arm bi-axial rotational molding machine by carefully monitoring the internal air temperature within the mold at GMI Zarahak Moulders Pvt. Ltd, Goa. The effect of 4% FS on powder flow quality (dry flow and bulk density), MFI, static mechanical properties (tensile strength, modulus, toughness, flexural strength and impact strength) as well as dynamic mechanical properties (storage and loss modulus), along with creep and relaxation were investigated. Morphological studies were conducted to correlate the above findings with the dispersion of the nano particles within LLDPE matrix. Finally, the comparative studies between the laboratory findings and scaled up industry trials have been carried out.

Since rotational molding industry is looking for alternative and newer materials with improved properties, the proposed research work is expected to be beneficial to industry as well as the society as majority of the rotationally molded products are used in infrastructural applications.

Contents

List of Figures

List of Tables

Nomenclature

η	Viscosity
η_0	Zero shear viscosity
η^*	Complex viscosity
$\eta^{'}$	Real viscosity
$\eta^{''}$	Imaginary viscosity
γ	Shear strain
$(\frac{d\gamma}{dt})$	Shear strain rate
$\tau)$	Shear stress
t_0	Relaxation time
σ	Stress
ε	Strain
ε_f	Flexural strain
ω	Angular frequency
δ	Phase lag
a_T	Shift factor
ΔP	Pressure drop across die
d	Deflection
n	Flow index
s	Factor of standard time (10 min)
E	Elastic modulus
$E^{'}$	Storage modulus
$E^{''}$	Loss modulus
E^*	Complex modulus
F	Applied force
$G^{'}$	Storage modulus in shear
$G^{''}$	Loss modulus in shear
G^*	Complex modulus in shear
K	Flow consistency
Q	Melt volume rate
R	Radius of die
T_g	Glass transition temperature

List of Acronyms

ABS	Acrylonitrile Butadiene Styrene
ATGO	Attached Graphene Oxide
BET	Brunauer–Emmett–Teller
DMA	Dynamic Mechanical Analysis
HDPE	High Density Polyethylene
ESCR	Environmental Stress Cracking Resistance
FS	Fumed Silica
IAT	Internal Air Temperature
LDPE	Low Density Polyethylene
LLDPE	Linear Low Density Polyethylene
MFI	Melt Flow Index
MVR	Melt Volume rate
PA	Polyamide
PC	Poly Carbonate
PE	Polyethylene
PEG	Polyethylene Glycol
PEN	Polyethylene Naphthalite
PEO	Polyethylene Oxide
PET	Polyethylene Terephthalate
PIAT	Peak Internal Air temperature
PMMA	Polymethyl Methacrylate
PP	Polypropylene
PS	Polystyrene
PVC	Polyvinyl Chloride
RM	Rotational Molding
SAN	Styrene Acrylonitrile
SEM	Scanning Electron Microscope
SIM	Stepped Isothermal Method
TLCP	Thermotropic Liquid Crystalline Polymer
TTSP	Time Temperature Superposition Principle
UTM	Universal Testing Machine
UV	Ultra Violet
XRD	X Ray Diffraction

Chapter 1

Introduction

Rotational molding (RM) is a zero or low shear polymer processing method that uses rotation of mold in a heated chamber for producing hollow seamless products. Unlike other polymer processing technologies, RM uses no pressure, resulting in products with no residual stress [1]. This also makes the design and manufacturing of the molds simple and inexpensive. Being free from the residual stresses (due to the zero or low shear), rotationally molded products are used in a wide variety of domestic and engineering applications like water storage tanks, storage tanks for chemicals, automotive parts like fuel tanks, recreational equipment like kayaks, toys, etc. The process has the capability of producing objects having complex shapes and sizes with ease at lesser costs. It can also accommodate the variation in product thickness with ease. Globally RM industry is steadily growing with an annual consumption of 1.3 million tonnes in 2012 and is expected to consume 1.8 million tonnes by 2017 [2]. Out of the global market North America accounts for 33% of total consumption while Asia Pacific and Europe accounts for 29% and 15% respectively. The total consumption by Indian RM stood at 135 Kilo tonnes in 2012 with around 300 manufacturers. The estimated yearly growth in the sector stands at 8% annually with a predicted consumption of 160 kilo tonnes by 2017 [2]. In Indian RM industry water tanks accounts for 80% of production volume while other applications like automotive parts, sanitary equipment, recreation are on rise. Government focus on sanitation and telecommunication sector is providing wide opportunities for products like inspection / telecommunication manholes, portable toilets, etc. This research is aimed to get better insight and control of sintering process and to investigate the potential of nano-scale reinforcement of fumed silica (FS) in RM.
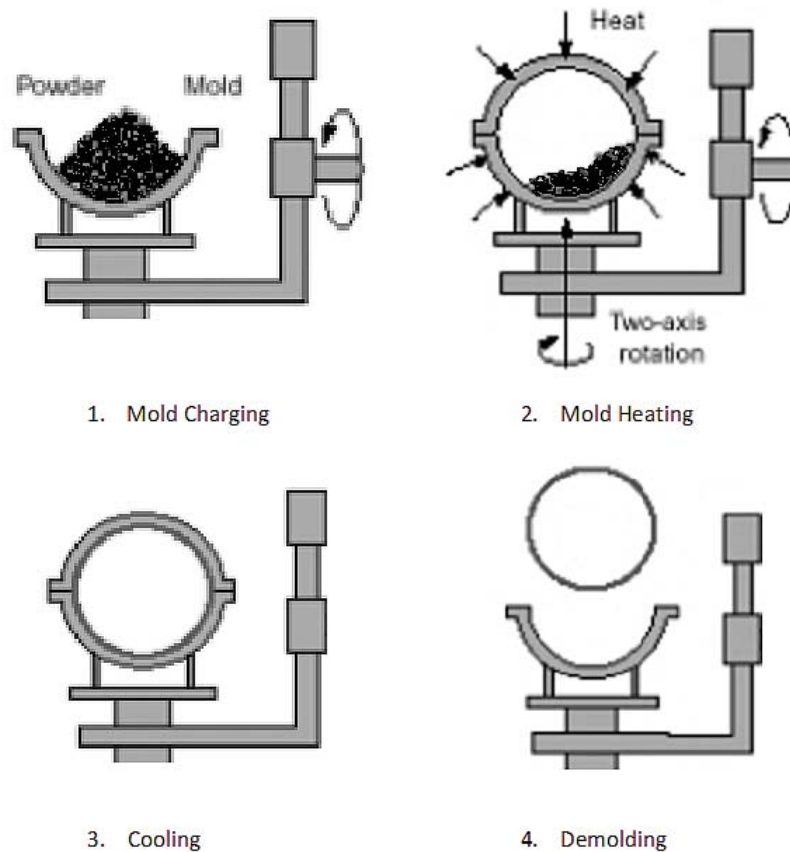
Figure 1.1: Principle of rotational molding

1.1 Rotational Molding of Plastics

Rotational molding of plastics has different activities and can be explained in four principal steps as shown in Figure 1.1 [1].

1. Mold Charging

2. Mold Heating

3. Mold Cooling

4. Demolding or Part Ejection

Mold charging involves application of mold release agents to mold and loading of a measured quantity of rotationally moldable polymer in the form of powder (500 μm), into a hollow mold as shown in Figure 1.1a. The mold is then rotated bi-axially or uni-axially and rocked about two principal axes at lower speeds

as it is heated in a heating chamber. The loaded powder material tumbles within the mold and melts to form layers by adhering to the mold surface for achieving desired thickness. The heating is stopped once proper sintering of material is achieved. The mold rotation is continued during the cooling process for the polymer to retain the desired shape of the mold as it solidifies. When the polymer is sufficiently rigid, external cooling and rotation of the mold is stopped for facilitating product removal from the mold.

The RM cycle time is generally large as the polymer powder is melted, sintered and cooled in the mold during the process. The heating cycle is the longest part of RM and therefore need to be controlled for lowering cycle times. Though the process of heating the polymer and fusing the particles normally take 7 to 15 minutes, 30 minute cycles are also not uncommon. Larger parts with thick walls take even longer times. Effective cooling is important in RM as the rate of cooling affect the crystallinity of polymer and changes the mechanical properties. Higher rate of cooling causes the part to be more amorphous with lesser shrinkage. Higher cooling rates are achieved by using spraying cold water over mold surface. Higher rate of cooling lowers the cycle time but results in warpage of the part. The molded part is then removed manually or with mechanical assistance during the part ejection stage.

Rotational molding is generally done at near atmospheric pressure and produces nearly stress free parts. Owing to the large heating cycle to melt the powder and to form the required shape, the polymer has to withstand temperature in excess of its melting point for relatively long time. This requires polymers with broad processing temperature range. Since RM is a non pressurized process, the molds usually have thin walls and are relatively simple to design and fabricate at low costs. Mostly steel and aluminum are used as mold materials. Mold design is very important in RM for making complex shapes and large volume products. With proper molding complex stress free products with uniform wall thickness can be easily produced unlike other processing methods like blow molding.

Rotational molding uses rotation of mold to distribute the molten polymer along the mold surface. This rotation is generally bi-axial at low speeds. Molds may have 360° rotation on both axis or have partial rocking on secondary axis. The powder undergoes a regular tumbling and mixing action in the mold without relying on the centrifugal force to throw powder against the mold surface. The powder usually lies at bottom of the mold and the mold surface make contact with the

powder pool during rotation. The frequency of this coating of mold surface depends on the speed ratio of the major axis and minor axis or rocking axis. Generally a speed ratio of 4:1 is used to ensure uniform thickness in RM [1]. Depending on the shape and design requirements the speed ratio may be altered to achieve the required results. When the mold rotates in oven, the powder melts and sticks to mold surface due to its tackiness building up a loose powdery mass against the wall. The major portion of heating cycle is then taken up for sintering of these lose powder to form a homogeneous melt. The irregular pockets of entrapped gasses formed during the initial build up is removed over a period of time and vanishes almost completely when optimum cure is obtained. These pockets of gasses are referred as pin holes or bubbles in the finished product. Prolonged heating tend to oxidize the polymer material in contact with air. If the final product is devoid of any pin holes in the cross section, then the product is likely to be over cooked indicating degradation on inner surface. If excess of pin holes are visible in cross section the product is likely to be under cooked. To obtain optimum mechanical properties and desired quality of final product a small number of bubbles on inner free surface is desired. To achieve this an optimum peak internal air temperature (PIAT) for the polymer need to be maintained. Mold pressurization also helps in removal of bubbles [3, 4]. To check the product quality for optimum curing an inspection of inner surface is done. If the inner surface is rough and powdery, the product is under cooked. It will also show a large number of pin holes. On the other hand if the inner surface is very glossy with an acrid smell, the product is likely to be over cooked.

To obtain a good quality finished product, cooling stage is also very important like the heating stage. In RM cooling is done from outside the mold leading to differential cooling of the product. This reduces the rate of cooling and the unsymmetrical nature of cooling results in warpage and distortion of finished product [5, 6]. The outer surface of product in contact with mold is cooled at faster rate there by having a higher degree of crystallinity. For products with larger thickness the cooling rate of inner surface will be significantly lesser than the outer surface leading to an increased amorphous structure. Thus the crystalline outer half will shrink more than the inner surface causing tensile stress at the interface. This will distort the product leading to warped surfaces . As a general rule, the warped section will curve towards the cooler surface (mold). For parts with larger thickness to reduce the effects of warping it is desirable to cool both inner and outer surfaces at same rates. if inside cooling is not possible slow cooling of outer surface is preferred to reduce the effects of warping. Use of jigs and fixtures to counter warping induce undesirable residual stresses in parts and need to be avoided if possible.

The major advantages of RM in comparison with other polymer processing methods like injection molding, blow molding, etc. includes production of seamless large and complex stress free hollow parts at low costs. The molds are also made at relatively low costs at shorter manufacturing lead time. RM allows to produce multi layered parts for better aesthetics and product performance. The efficiency of the process is close to 100% as there is no wastage or minimum wastage of raw material in manufacturing the final product. Several improvements in RM industry is carried out to improve productivity of process focusing on improved materials, process monitoring, development of improved mold release agents mold coatings. Mold release agents reduce the cycle time, defects and browning of finished products. The sacrificial mold coatings are primarily silicone based and is applied each time to mold prior to molding. This was the most commonly used mold coatings due to its price advantage. Semi permanent coatings will last for a number of cycles before requiring to be reapplied. These coatings are based on polysiloxane. Currently this type of coating is most widely used in RM industry. Permanent coatings are mostly based on Teflon (Poly tetra fluro ethylene) and is directly applied to mold. This is rather expensive and care has to be taken to prevent damage to mold coating while demolding.

The improvements in RM machine also ensures improved productivity and better quality control. Currently various types of RM machines like rock and roll, clam-shell, shuttle, carousel, swing arm, vertical, etc. are available for the required product size and production rate. The improvements in product design and mold has ensured RM process to produce a wide variety of products for varying domestic and engineering applications. The improvements in colorants and anti oxidants has ensured better aesthetics to RM products.

There are several challenges faced by both industrialists and researchers in RM. The availability of materials for RM is one amongst a few. The choice of materials often restrict the use of rotationally molded products in many applications due to the inferior mechanical properties. Generally, linear low density polyethylene (LLDPE) is used for RM due to its good thermal stability during processing, good mechanical properties and low cost. Even though it has good mechanical properties for domestic applications, several engineering applications calls for enhanced mechanical properties. Polymers like polypropylene (PP), nylon, acrylonitrile butadiene styrene (ABS), etc. provide improved mechanical properties but are less commonly used and for unique applications due to its increased cost, lower thermal stability, ultra violet (UV) resistance, etc. Along with the materials, larger cycle time hampers the production rate. The cycle time

reduction may be achieved by developing proper materials, mold release agents, efficient heating and cooling systems and process monitoring devices. The available wireless temperature monitoring devices do help in process monitoring but requires refinement for improving cycle times. The warpage, shrinkage, presence of pin holes, non uniformity in color and surface finish are few defects normally observed in rotationally molded products. The study of powder quality, melt characteristics and flow characteristics of powder provide some insights to these problems along with the product and mold design.

1.2   Need for Nanocomposites in Rotational Molding

More than 90% of the material used for RM is from the polyethylene (PE) family. PE (density 0.93 to 0.94 g/cc) is primarily used in RM due to its ability to withstand high processing temperatures (greater than melting point) for longer period of time along with its chemical and UV resistance and relatively lower material cost. However, it cannot provide thermal stability, creep resistance, surface hardness, impact resistance and high strength, restricting its use in many engineering applications. Currently researchers are working on methods for synthesizing RM powders that will withstand the aggressive working conditions. The use of additives, nano scale reinforcement of polymer chains, reactive mixtures, co-polymers, cross linked polymers, etc. along with new polymers are tried in RM for improving the product performance in various environmental conditions. PP do have higher melting point and higher chemical resistance than PE but are susceptible to higher oxidation at temperatures above 100°C. With the use of antioxidants PP provides a choice of material were temperatures are higher and provide much needed chemical resistance. However, it has poor UV resistance. Use of co-polymers of high density PE and PP is preferred but is substantially more expensive than the homo polymer.

Other polymers used for RM includes poly vinyl chloride (PVC), nylon, polycarbonate(PC), acrylics, polystyrene liquid polymers. etc. These polymers are used for unique applications due to their specific properties. PVC in the form of plasticized drysols are used to produce semi flexible products due to its higher tensile and tear strengths. Nylons are used at higher temperature and have good chemical resistance to hydro carbons making it suitable for producing fuel tanks. PC and acrylics show good weather resistance and is suited for out door applications but has lower chemical resistance and increased cost. RM of polystyrene like ABS were done commercially in 1960s and 1970s. Since the improvements in styrenes

for obtaining high impact strength it is rarely rotationally molded in recent times. During molding the impact resistant styrenes are oxidized and is degraded. With the reduction in cycle time and improved styrenes for RM it is used in low volumes for RM. Polymers in powder form with average particle size of 500 μm (35 mesh) are used in RM.

Generally different additives are mixed with the base polymer during the compounding of rotationally moldable polymers. These additives include antioxidants, colorants, UV stabilizers, fillers, environment resistors, etc. The additives are selected based on the product requirements such as aesthetics, reduced cost, environment resistance, etc. These micro scale additives may adversely affect the mechanical properties owing to its size and hardness. However, elastomeric additives improves the toughness and impact resistance but compromises on the strength. Nano scale additives on other hand provide reinforcement to polymer chains owing to its relative size enhancing the mechanical properties of the natural polymer.

With the limited availability of polymers other than polyolefines, use of nano particles for polymer reinforcement is preferred. Nano particles of metals, metal oxides, inorganic and materials along with carbon and other non metallic and semi conducting materials are used with polymers. These nano particles adhere to the polymer chains and alter the mechanical,rheological, optical and many other intrinsic properties of the natural polymer. Use of nano particles can improve the existing materials and provide a different grade of rotationally moldable materials. Nano particles of silica, titanium dioxide, calcium carbonate, etc. can be used as potential nano scale reinforcement for RM.

The removal of bubbles without overheating of molds is still a challenge in RM. The use of fine particles in RM has reduced the presence of pin holes in the finished product [7]. The use of nano particles in polymer matrix further reduces the size of pin holes as it aids in nucleation during polymer crystallization on cooling. The presence of nano particles also changes the free flow of powder during tumbling and the melt viscosity of polymer melt. These changes not only alters the surface finish of the product but also makes an impact on cycle time, rheological properties and mechanical properties of the finished product.

1.3   Scope and Objectives of the Present Study

This study focuses on the synthesis and characterization of nanocomposites based on rotationally moldable LLDPE and FS for RM applications. The composition of the LLDPE - FS blends, and appropriate processing conditions along with their suitability for industrial use is identified through this research. The scope of this research work includes producing rotationally moldable nanocomposite of LLDPE - FS with improved mechanical properties for industrial application. The objectives of this research work are as follows:

1. To investigate the effects of FS in rotationally moldabe LLDPE on melt and rheological characteristics using melt flow index (MFI), parallel plate rheometry and torque rheometry studies.

2. To investigate the dynamic mechanical (viscoelastic)and thermo-mechanical properties of LLDPE with the addition of FS.

3. To investigate the mechanical properties and crystallinity of LLDPE - FS nanocomposites.

4. To study the creep and stress relaxation behavior of LLDPE - FS nanocomposites.

5. To study the morphology of LLDPE - FS nanocomposites to examine the dispersion of FS in LLDPE and correlate with mechanical properties.

6. To study the effect of FS in LLDPE on cycle time reduction and the pulling force requirement during mold release.

7. To test LLDPE - FS nanocomposite at industry scale and to compare the results with the laboratory scale findings.

1.4   Organization of Thesis

To achieve the stated objectives in a logical order , the thesis is organized into following chapters:

Chapter 1 introduces the RM process along with its potential applications and the need of using nano scale reinforcements to improve the process characteristics. The advantages of RM and its disadvantages in comparison with other polymer processing methods are also discussed. The need of using

nanocomposites with LLDPE as a principal raw material in RM has been specified and the scope and objectives of the research work have been delineated.

In Chapter 2 the scope and objectives are supported by a detailed literature survey showing the progress of research in RM along with the use of FS as a potential nano scale additive. The visco elastic properties, rheological properties, mechanical properties, creep, stress relaxation, etc. with the addition of nano particles and particularly of FS in polymers are researched. The important results obtained by different researchers in this field have been discussed in detail and research gaps in terms of use of nano scale reinforcements for improving the processibility as well as mechanical properties of rotationally molded products have been found out.

Chapter 3 discusses the rheological characteristics of LLDPE - FS nanocomposites. The influence of FS and blending methods in melt flow characteristics of LLDPE are studied by measuring the MFI of LLDPE - FS blends. Thermal transitions in the LLDPE - FS nanocomposites were investigated and correlated with their melt flow characteristics. The dynamic viscosity of molten LLDPE and LLDPE - FS blends were measured by conducting dynamic rheological studies and was correlated with the MFI studies. The effect on melt processing during RM and compounding, were analyzed by torque rheometry studies.

Chapter 4 presents the visco elastic properties of LLDPE - FS nanocomposites. The response of the LLDPE - FS nanocomposites to dynamic sinusoidal oscillations are studied to evaluate the effects of FS in natural LLDPE. The response of material to varying frequencies are also studied. Creep studies were also conducted on LLDPE - FS nanocomposites to ascertain their time dependent behavior under stress.

Chapter 5 represents the study of mechanical properties of LLDPE - FS nanocomposites. Different mechanical properties like tensile modulus, tensile strength, elongation at break, flexural modulus, tensile toughness, impact toughness are investigated. This chapter also includes X ray diffraction studies to determine the effect of FS in the crystallinity of LLDPE. To correlate the visco elastic properties of LLDPE - FS nanocomposites, morphological studies using scanning electron microscope (SEM) were performed.

Chapter 6 studies the effect of FS on mold release time. A special fixture with internal heating and provisions to monitor polymer melt temperature, mold temperature and heating rate was developed for this purpose to be mounted on a conventional UTM. The mold release force was studied in the regime of mold release temperature, rate of pulling, etc. apart from FS composition. The suitability of mold release at higher temperature for LLDPE - FS nanocomposite is investigated for reduction in RM cycle time.

Chapter 7 shows the scaled up the findings form laboratory to industrial scale. LLDPE - FS blend was melt mixed, pulverized and rotationally molded in a 3 arm bi axial RM machine (CACCIA RT 2203B). The internal air temperature during RM was monitored carefully using wireless temperature monitoring system for proper process control. The powder characteristics and melt flow characteristics of powder were documented along with the mechanical and visco elastic properties. A comparative study between laboratory scale and industry scale finding has been carried out.

Chapter 8 includes major conclusions of the work carried out, the salient features, final outcomes and contributions of the work. Scope for the future work is also projected in this chapter.

The research methodology followed in the research is given in next section.

1.5 Research Methodology
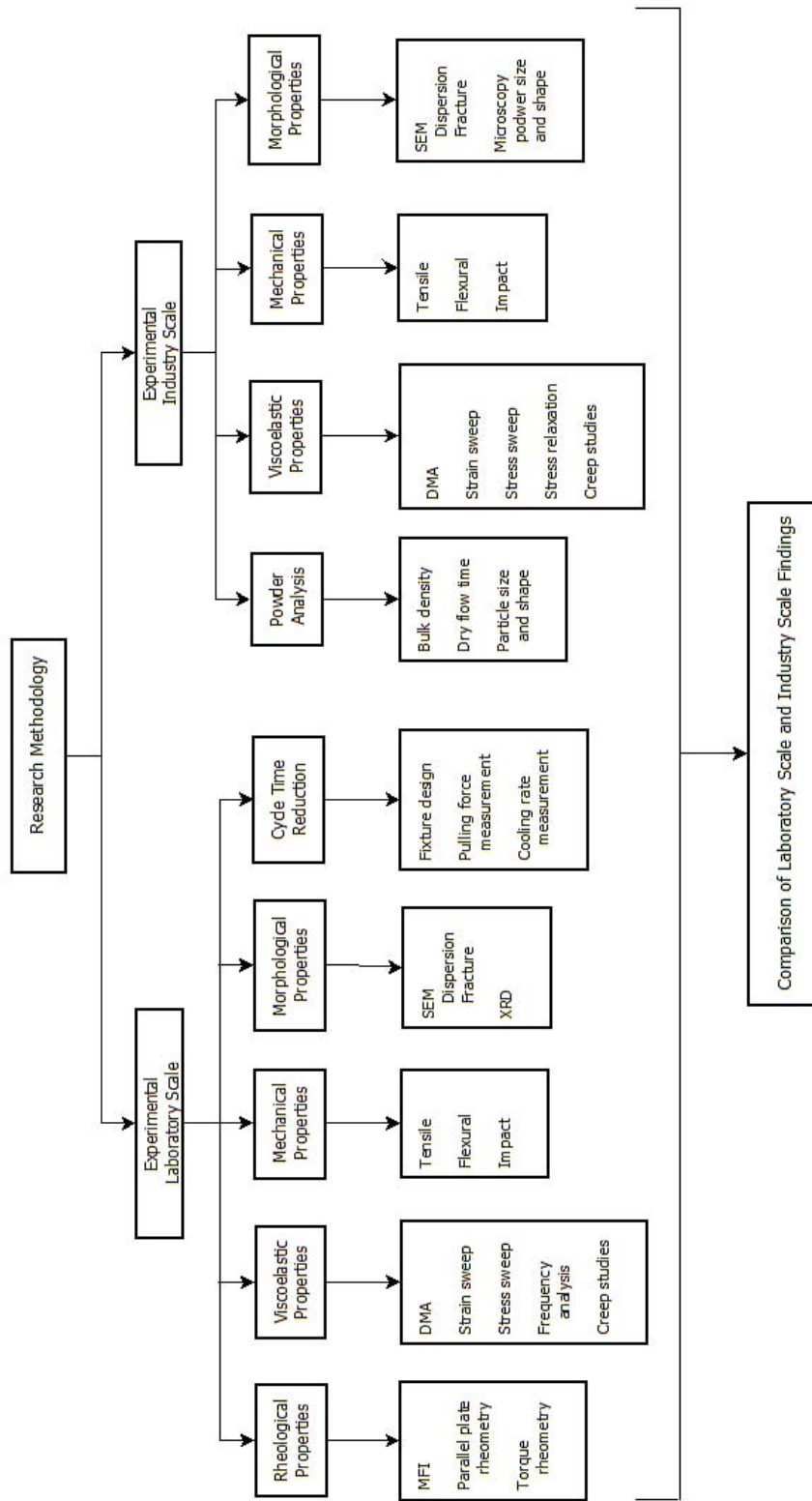
Figure 1.2: Research methodology

Chapter 2

Literature Survey

2.1   Introduction

Rotational molding of polymers begun in 1930s using highly plasticized liquid polyvinyl chloride. The earlier RM equipment consisted of hollow metal molds rotating over open flame. In 1950s hot air ovens were introduced. The advent of polyethylene powders in 1950 revolutionized RM industry. The tailored polyethylene powders for RM expanded the scope and application of RM products. Currently RM products are used in various application sectors like water and waste management, solid waste management, infrastructure, recreation, automotive, retail, industrial, telecommunication manholes, etc. In the 1980s new plastics like PC, polyester and nylon were introduced to RM. In late 1980s more precise monitoring equipment for the control of heating and cooling process was developed. Wireless temperature monitoring systems were developed to monitor the internal air temperature (IAT) and PIAT of 200°C was considered the optimum curing point of LLDPE. Currently commercial wireless temperature monitoring systems like ROTOLOG^{TM}, TEMPLOGGER, K-PAQ^{TM} are available and is used independently or being integrated with the RM machine [8].

The research studies in RM mainly focus on reducing cycle time, improving product quality and improved materials for RM. Even though RM is traditionally a zero shear process, mold pressurization is attempted to accelerate the coalescence of polymer particles during melting [9, 10]. Mold pressurization reduces the number of bubbles due to the faster bubble shrinkage under pressure leading to fewer pin holes in the final product. Mold pressure also delays the separation of part from the mold surface during cooling process. However, the molds are to be re-engineered to handle the excess pressure leading to increased mold cost and possible explosion of the pressurized part. This has prevented RM manufacturers from adopting mold pressurization on large scale.

Another improvement in RM industry is the development of improved mold release agent and mold coatings [11]. Mold release agents reduce the cycle time, defects and browning of finished products. The mold coatings are primarily silicone based and is applied each time to mold prior to molding. This was the most commonly used mold coatings due to its price advantage. Semi permanent coatings will last for a number of cycles before requiring to be reapplied. These coatings are based on polysiloxane. Currently this type of coating is most widely used in RM industry. Permanent coatings are mostly based on Teflon (Poly tetra fluro ethylene) and is directly applied to mold. This is rather expensive and care has to be taken to prevent damage to mold coating while demolding.

Generally, additives like antioxidants, colorants, UV, stabilizers, organic and inorganic fillers, etc. are blended with naive polymers to obtain the desired product performance. These additives are usually micro sized or nano sized particles having specific properties. They are usually blended to natural polymers either by melt mixing or dry mixing depending on the applications. In RM, these additives are melt-mixed in an extruder before pulverized to fine powder. These additives have a profound influence on melt characteristics and thermo-mechanical properties of natural polymer.

This chapter provides an in-depth literature survey of FS nano particle used as nano scale reinforcement for LLDPE and its significance in RM.

2.2 Nano Particles and its Advantage in Polymer Composites

The term nano particle covers a wide range of materials which can be metallic, non metallic, mineral and polymer-based or a combination of materials. Nano particles include metal (Cu, Au, Pd, Pt, etc.), semiconductor (ZnS, CdSe, CdS, etc.), metal oxides (FeO_2, Al_2O_3, ZnO, TiO_2, etc.), organic and inorganic particles like organo clays, carbon nano tubes, calcium carbonate, FS (SiO_2), etc. [12–17]. Nano materials and particles have attracted a great deal of attention as they enhance the performance of materials. Some unique properties, such as magnetic, optical, mechanical and electronic properties changes abruptly at the nano scale. They have wide range of uses such as mechanical reinforcement, catalysts, drug delivery mechanisms, dyes, sunscreens, filters and much more.

The nano size material can be generally any particle or collection of particles having at least one dimension (length, width, thickness) in nano scale (1 to about 30 nm). If one dimension is in the nano meter range, the nano particle is present in the form of sheets of one to a few nano meters thick to hundreds or thousands nano meters long, such as platelet clays and layered silicates (phylo-silicates) [18]. Thin (nano) films used in computer chips and fuel cell applications represent one-dimensional nano materials. When the two dimensions are in the nano meter scale and the third is larger, the material forms an elongated structure, for example carbon nano tubes, oxide-based nano tubes, nano wires made of silicone, gallium nitride and indium phosphide, cellulose whiskers, etc. When the three dimensions are in the order of nano meters, the material is present in the form of spherical nano particles, such as silica or zeolite, or even can include semi conductory nano clusters. Nano particles exist in three dimensions having diameters less than 100 nm. This includes engineered particles such as the fullerenes and quantum dots [19–23].

Among numerous applications of nano materials, reinforcement of polymer matrix is also gaining significant interest among researchers. Traditionally micro sized additives are blended with polymer to enhance its mechanical properties, aesthetics, anti-oxidation characteristics, UV protection, etc. along with reduced overall cost [24–26]. These additives, apart from giving the desired effect, may also tend to deteriorate the mechanical properties owing to their size, shape and hardness. The elastomeric additives provide better impact resistance but tend to reduce the tensile strength. For example, the addition of butadiene in polystyrene (PS), increased the stiffness and tensile strength while reducing the impact toughness and elongation at break [27]. However, at concentrations above 10 wt% of butadiene the tensile strength and modulus were reduced. The increase in mechanical properties such as tensile strength, impact toughness, creep, stress relaxation, etc. were reported with addition of various nano fillers. Literature studies show the evidence of improvement in the thermo mechanical properties of molded products when reinforced with nanocomposites like metal nano particles, metal oxides, organo clays, calcium carbonate, FS, etc. Sahebian *et al*. showed that the addition of calcium carbonate nano particles to high density polyethylene and polypropylene has increased the heat capacity, sensible heat and crystallinity index along with the dimensional stability of the natural polymer [15]. The addition of copper nano particles (up to 25 vol.%) by Molefi *et al* in low density polyethylene (LDPE) and high density polyethylene (HDPE) matrix showed an increase of tensile modulus, loss and storage modulus, while decreasing its elongation at break[28]. Similarly, Esthapan *et. al* demonstrated that the mechanical properties like modulus, elongation at break and time to rupture for polypropylene fiber

was enhanced with the addition of nano titanium dioxide up to a concentration of 3% [29]. The tensile modulus showed a significant improvement of 45% at 3% concentration of titanium dioxide concentration whereas, elongation at break and time to rupture showed an increase of 15% at a concentration of 1.5%.Cassagnau and Mélis also showed a substantial increase in shear elastic and loss modulii with the addition of FS in molten ethylene vinyl acetate, PS and PP. By adding FS in thermoplastic poly (dimethylsiloxane-urea) tensile and viscoelastic properties were significantly improved as demonstrated by Yilgor *et. al* [30]. An increase of storage modulus from 2 MPa for poly (dimethylsiloxane-urea) to 6 MPa for the composite was observed. Addition of nano particles also affected the optical properties, electrical conductivity, gas and solvent transport and many other intrinsic and extrinsic properties with relatively low level of dispersion in polymers like phenyl C61-butyric acid methyl ester, poly(p-phenylene-vinylene), PS, poly methyl methacrylate (PMMA), etc. [24]. In contrast to the micro scale additives, nano scale additives have Brunauer–Emmett–Teller (BET) surface area in the range of 50 - 400 m^2/g. For a comparison, the size of micro scale additive, individual polymer chain and nano particles are shown in Figure 2.1. The large polymer chain - nano particle interface area in the case of nanocomposites in comparison to micro composites, makes the effects appearing significant in nanocomposites [31]. These chain - particle interactions provide hindrance to polymer chain movements altering the rheological, viscoelastic and mechanical properties of the nanocomposites.
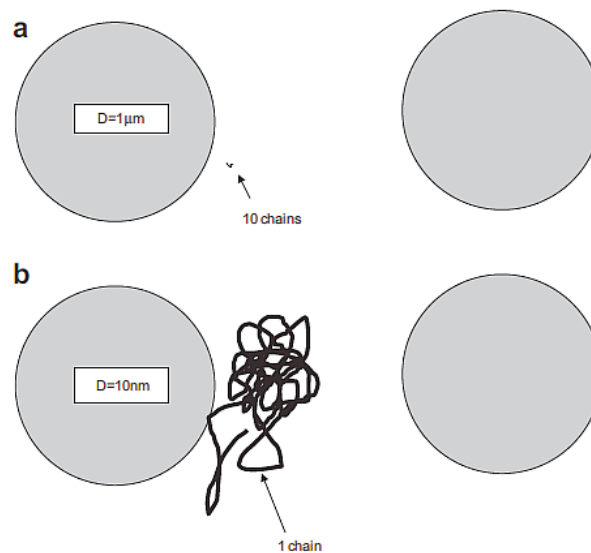
Figure 2.1: Relative sizes of polymer chain and nano particle
a) Polymer chain with Rg = 5nm and particle with diameter D = 1μm
b) Polymer chain with Rg = 5nm and particle with diameter D = 10nm

The addition of nano particles with large surface area (BET surface area)

15

to thermoplastic polymer matrices like LLDPE, led to the change in material properties like viscosity, melt strength, resistance to shear, etc. resulting from interactions between chains and nano particles. Nano particles in polymer matrices like PE and epoxy composites have the tendency to associate into extended structures with polymer chains that can alter the rheological, and viscoelastic properties of the polymer matrix [24]. In polypropylene- calcium carbonate nanocomposites the shear modulus increased by 20% with increase in nano filler concentration [32]. However, this increase was greater in the high frequency region. There was also a significant increase in complex viscosity of the nanocomposites with increasing calcium carbonate concentration. The rheological behavior of the nanocomposites was more sensitive to nano particle concentrations at low frequencies below 1 Hz. This increase in complex viscosity (10 times increase for a concentration of 5 to 15% calcium carbonate in PP) of was attributed to the frictional interactions between the nano particles and also between the polymer chains and nano particles [33]. The rheological properties of polymer composites are thus attributed to the adhesion of filler material to the polymer matrix [34]. Large increase in the storage modulus at lower frequencies, exhibiting as a secondary plateau and a drop in storage modulus at larger strain are commonly observed with the addition of nano particles in polymer matrix [35, 36]

The rheology of filled thermoplastics is affected by the presence of nano fillers and its dispersion in the polymer matrix. The dispersion of nano particles, further depends on the extent of filler/filler and polymer/nano particle interactions. Dispersion in polymer matrix is further facilitated by improving the stress transfer between polymer and nano particles during melt compounding. [37]. The improvements seen in the viscoelastic properties with the incorporation of nano particles, are attributed to the hydrodynamic effect caused by the nano particles, and at higher concentrations (above 5 wt %, or 2 vol %) to the propensity of the particle aggregation leading to brittleness [38]. Thus a direct consequence of incorporation of nano fillers in polymers was seen as change in steady state shear viscosity and viscoelastic properties [14, 35].

2.3   Fumed Silica in Polymer Processing

Fumed Silica is a preferred nano scale nano reinforcement used in polymer composites owing to its easy availability, particle size and shape [39]. FS particles are formed by the pyrolisis of chlorosilanes, like silicon tetra chloride, in a flame of air an hydrogen resulting in FS and hydrogen chloride. FS nano particles are

industrially available in a wide range of sizes and with surface treatments from hydrophilic to hydrophobic. Strong polymer/nano particle interactions may occur between hydrophilic nano silica with a high specific surface area and a polar matrix [40]. Similar interactions are also seen when bi functional coupling agents are used to modify nano silica in order to form covalent bonds with the functional groups present in the polymer matrix [41, 42]. These interactions may lead to the formation of an immobilized layer or "bound" polymer surrounding the filler particles. FS is available as individual particles ranging from 5-50 nm and if dispersed properly it attains an aggregate size of 10-50 nm in polymer matrix. Due to this, FS is able to self-aggregate when dispersed in polymer matrices, forming an interconnected network of interacting particles and polymer chain. This results in altering the melt viscosity, dynamic mechanical properties, glass transition temperatures, etc. of the naive polymer [43]. Recent investigations in morphological studies of nano silica filled LDPE using atomic force microscopy revealed suppression of spherulitic formation in comparison with natural LDPE. These studies also revealed the presence of FS in the sandwiched amorphous areas between crystalline lamellae of LDPE. These existed as strips with varying thickness from 10 to 30 nm [44]. These spherulites grew during the solidification of the molten polymer until they collide with adjacent ones. The spherulitic boundary thus formed, by adjacent spherulites, in large numbers result in lower mechanical properties. The addition of FS in low concentrations induces well organized lamellar stacks and reduces the spherulitic formation. The decreased spherulitic growth rate is attributed due to the dispersion and size of nano particles in LDPE matrix. These structures of FS formed with LDPE, causes increased adhesion and melt viscosity in comparison with natural LDPE.

2.3.1 Effect of FS Nano Particles on Mechanical Properties

Researchers had shown FS nano particles, when blended with polymers provide high rigidity, impact toughness and increased tensile strength. The mechanical properties such as impact strength, tensile strength, and elongation at break of the poly amide-6 - silica nanocomposites showed a tendency to increase, with the addition of the nano silica up to 5% and declined thereafter [45, 46]. The incorporation of FS in polyethylene terephthalate (PET) has increased the mechanical properties like toughness and tangent modulus at low filler content [47]. It also increased the intrinsic viscosity of the blends. Further, the Young's modulus showed increase from 1316 MPa to 1522 MPa for addition of 0.5% FS. However, the Yield strength reduced from 33.7 KPa to 30.9 KPa. Mechanical behaviors of FS - poly carbonate blends in uni-axial tension and three point bending revealed increased yield strength and enhancement of strain at break [48]. The tensile

strength and modulus of 3-aminopropyl triethoxysilane functionalized silica nano particles attached graphene oxide (ATGO) in epoxy were reported to be significantly higher in cryogenic temperature in comparison with room temperature [49]. Also, the fracture toughness (K_1C) obtained from the single edge notched bending test increased sharply with an increase in ATGO loading in the epoxy up to 1%. In epoxy nanocomposites using nano-silica (upto 30%), the visco elastic properties such dynamic storage modulus and tensile modulus were reported to increase with silica content showing a max. of 30% increase [50]. However, at 20% of silica content dynamic storage modulus decreased to 1380 MPa from 1410 MPa for epoxy with no silica content. The behavior could be explained by considering the polymer – filler interactions limiting the degree of cross-linking attained by the polymer matrix during curing. This can be due to the large viscosity increase due to FS particles during composite preparation. Scanning electron microscopy (SEM) of the fractured surfaces and dynamic mechanical multi-frequency tests suggested the presence of strong polymer – filler interactions in case of 30% filled samples.

It was generally observed from linear viscoelastic measurements that the filler structure was not stable upon the cessation of the flow. In the case of platelet nano-composite (organo-clays, graphite oxide) a two-step process of recovery was generally reported: the first one was the disorientation of the fillers followed by a second phenomenon of aggregation / clustering [35]. The non-linear viscoelastic behavior and modulus recovery studies in FS filled ethylene vinyl acetate, PP and PS, mentioned the filler network breakdown in describing the strain-dependence of viscoelastic properties of composites. The strain / creep recovery tests performed by subsequent strain sweep or time sweep experiments showed that the initial equilibrium network structure was unable to completely restore even after several hours [51].

In HDPE nanocomposites containing up to 5 wt% of FS, both tensile strength and tensile modulus were increased [52]. Also, the thermal stability of HDPE was enhanced by the addition of FS nano particles. Effect of FS nano filler on deformation response and morphology of LDPE, HDPE and isotactic PP was investigated by Kalfus *et al* [31]. It was established that the degree of polymer matrix reinforcement was significantly affected by the extent of polymer matrix crystallinity. Kalfus *et. al* also reported that by adding FS to the molten polymer, mobility of polymer chains in contact with FS particles was hampered, causing significant changes in morphology of these semi crystalline nanocomposites. In nano silica filled PP, isothermal and non-isothermal crystallization kinetics were reported [53]. Analysis of the isothermal crystallization showed that the

crystallization phenomenon was characterized by faster rate, as the amount of silica was increased. The nucleation activity of the FS nano-particles on the polymer matrix showed good nucleation up to a filler concentration of 7.5 wt%.

Polymeric composites with high mechanical strength tend to lose their properties on constant loading and exhibit a time-dependent behavior in modulus (creep) and strength (creep rupture), at temperatures greater than glass transition temperature (T_g) [54–56]. Creep studies are often conducted to predict the time-dependent mechanical properties and are also quite useful in designing the product. Typically short isothermal creep tests are conducted at various temperatures above T_g, to create the master curves at a specified reference temperature using time temperature superposition principle [57, 58]. During testing, the test specimen is normally subjected to a tensile stress and the strain variations are measured with precise extensometers over a period of time in isothermal conditions [59–66]. Recently, combination of tensile and compressive creep tests are being conducted using constant stress in cantilever orientations [67], three point bending orientation [55] using dynamic mechanical analyzer. Stepped isothermal method (SIM) creep tests are considered as an enhancement to the traditional creep tests owing to its reduced test time and use of single specimen to minimize the scattering effects [68]. SIM is a well-established method for the accelerated product testing of geosynthetics [69–72]. It was successfully applied for creep studies in polypropylene (PP) [68], aramid fibers [73], and high density polyethylene pipes [56]. The effect of nano particles in creep behavior of polymer composites deserves attention as significant improvements in mechanical properties are observed. FS nano particles, used as a coupling agent for PP-glass composites, significantly increased the creep strength in matrix. Creep compliance reduced by around 20% when untreated PP was blended with 5% FS [74].

2.3.2   Effect of FS nano Particles on Rheological Properties

The addition of nano silica also affected the rheological characteristic of polymer melt . Reviews on melt rheology of FS and organo-clays nanocomposites showed a solid-like rheological response, which include a non-terminal relaxation zone, an apparent yield stress and a strong non linearity behavior (Payne effect) [75, 76]. In the FS nanocomposites, both percolation threshold and limit of linearity increased with the addition of FS by surface grafting of end-tethered chains. In the case of FS nano-composites, filler inter-particle interactions dominate the viscoelastic behaviors. As a consequence, the rupture of the filler network was the first-order mechanism in the Payne effect. On the contrary, the polymer - particle

interactions, which lead to a strong modification of the chain relaxation process, was the dominant mechanism with colloidal silica at identical filler concentrations [77, 78]. Transient shear experiments proved, the network breakdown mechanism between the clay platelet domains (inter-particle interactions) were the driving force of the structural evolution, particularly for the network recovery during rest time [75].

An increasing trend of dynamic viscosity was observed with rising concentrations of silica nano particles in several nanocomposites blends. With the addition of FS in polyester based polyurethane resin showed an increase from 1100 mPa.s to 3100 mPa.s at 10% concentration. The rate of increase of viscosity increased with the nano silica content and was attributed to the increased hydrogen bond between the hydroxyl group in polyester and silica nano particles[79]. Similar increase in viscosity was observed with the addition of nano silica in PS. [80]. The MFI shown a reduction from 81.3 g/10 min for neat PS to 17.5 g/10 min for PS-10% nano silica, measured at 200ºC /5 kg. This increased viscosity was attributed to good chain - nano particle surface interaction leading to limited polymer chain mobility in the melt. This was related to polymer chain – nano particle surface interaction and partial adsorption of fillers on polymer chains, causing their entanglement. For polyolefin-FS blends [81], the degree of reinforcement between matrix and filler got substantially affected by the extent of polymer matrix crystallinity. The addition of FS suppressed spherulitic growth rate caused by the increased melt viscosity of nanocomposites in comparison with natural PE [44]. While most of the research studies have shown an increase in melt viscosity of polymer blends, a few have observed reduction in melt viscosity. With small concentration of FS in Polyethylene naphthalite (PEN), a reduction of 20% in melt viscosity was observed [82]. This was due to the increase in the nucleation effect with increasing silica content in PEN. Similar trend was also observed in PET [83]. The viscosity measured at 10^{-1} rad/s using dynamic oscillatory viscometer showed a decrease from 60 Pa.s for PET to 20 Pa.s for PET-2% FS concentration. Nylon-6 when blended with organo clays also resulted reduction in melt viscosity [45]. Further, the addition of nano silica into in-situ composites of PC and a thermotropic liquid crystalline polymer (TLCP) reduced the viscosity upto a concentration of 9% FS at relatively high shear rates [84]. The addition of 10.7 wt% TLCP and 1 wt% FS led to a 48% viscosity reduction of PC melts, while 9 wt% FS led to further viscosity reduction of 60%. These were attributed to the degradation of the polymer during melt processing and the slip between the polymer chains and filler. With the addition of hydrophobic and hydrophilic FS of different surface area and particle size in solvent based polyurethane additives, a noticeable increase in the viscosity, negative thixotropy and increase in storage modulus was seen [85]. These

modifications were pronounced in the adhesives that contained hydrophilic FS.

Many researchers have formulated various empirical relations to represent the rheological behavior of polymer melts and colloids [81, 86–91]. Molecular dynamics simulations were used to explain the variation of viscosity and glass transition temperature (T_g) with addition of nano particles. The simulation results too suggested that the nano particles increase the entanglement without significantly affecting the bonding in polymer chains [92–97]. In composite micro mechanics, the assumption of statistical homogeneity is used allowing usage of classical continuum mechanics to formulate constitutive equations. Classical continuum mechanics cannot be applied when heterogeneity length scale is below 20 nm, whereas, molecular dynamics simulations are limited to nano-scale and cannot be applied to micro-scale particles. A simple micro mechanics-informed model was developed by Andrea Dorigato *et al.* [98] for predicting the anomalous increase in the nano-composite modulus of LLDPE, assessed as a function of FS composition (1-4 wt%). The model was able to predict the nanocomposite's behavior by using a new structural parameter, α, with a physical interpretation. Since, nano particles are prone to agglomerate, their primary or secondary agglomerates may exist in many nano-composite systems. These interactions and the possible reinforcement mechanism may be responsible for the changes in various properties of nanocomposites reported in literature.

The interaction of FS and polyethylene oxide (PEO) lead to a diminution of the specific surface area and contributions of micro pores (pore radius R < 1 nm) and meso pores (1 < R < 25 nm) to the pore volume [99]. Quantum chemical calculations of a complex PEO fragment with a $\equiv$SiOH group of a silica cluster in the gas phase and with consideration for the solvent (water) effect showed a reduction of interaction energy in the aqueous medium. However, the complex remained strong enough to provide durability of the PEO adsorption complexes on FS; i.e., PEO-FS nanocomposites could be stable in both gaseous and liquid media. The addition of PEO in polymer matrix like PC increased the processability by reducing the viscosity with increased concentrations of PEO [100]. The viscosity values as recorded by capillary rheometer reduced from order of 10^6 poise to 10^5 poise at a true shear rate of 1 s^{-1} for a 30% concentration of PEO in PC.In the case of melt-filled polymers, the viscous forces were dominant and the nano-particles were subjected to strong alignment under flow. It was generally observed from linear viscoelastic measurements that the network structure was broken under flow and rebuilt upon the cessation of flow under static conditions (annealing or rest time experiments). The linear viscoelasticity has been used to

characterize the viscoelastic properties of polymer melts filled with nano-sized fillers (nanocomposites). One of the direct consequences of filler incorporation in molten polymers is the notable change in viscoelastic behavior since they are sensitive to the concentration, particle size and shape (aspect ratio) along with its structure and surface treatment of the fillers.

Along with the rheological characteristics, torque rheometry studies are used to determine the variation of melt shear with time to ascertain the degradation and cross linking of polymers in the presence of additives. It measures the effect on torque increase along with the processing temperatures, due to the usage of filler particles in polymer blend for enhancing mechanical properties, environment resistance and aesthetics. Torque rheometry measures the viscosity-related torque generated by the resistance of a material to the shearing action of the plasticizing process [101]. The addition of nano particles in polymer blend is associated with increase in viscosity and hence increased torque is required for polymer processing. Typical torque rheometry analyses include the study of polymer processing behavior, effect of added fillers, thermal and shear sensitivity during compounding, and others. PVC - nano $CaCO_3$ blend torque rheometry carried out by Gulsen [102] revealed increased torque value during cross linking for decreased particle size of $CaCO_3$. During torque rheometry of PVC-$CaCO_3$ blend at 30 - 90 rpm at a processing temp of 190º C, the torque values initially dropped owing to polymer melt. The torque value stabilized at 2.5 Nm for pure PVC and increased rapidly once the cross linking initiates. It increased to approx 11 Nm at maximum after which degradation of PVC took place. While blending with $CaCO_3$ of varying particle size from 3μm to 25 nm, the max torque value was observed to increase from approx 11 Nm to 14 Nm [103]. Parallel plate and torque rheometry were used to study the chemical cross linking of PVC induced by metallic mercaptides (Ba and Mg salts of 2-dibutylamino-4, 6-dithio-1,3,5-triazine) combined with various thermal stabilizer combinations (calcium / zinc and barium / zinc stearates) [101]. The extent of cross-linking was determined by measuring the solvent (tetrahydrofuran) insoluble gel content. The cross linking reaction measured by torque and parallel plate rheometry, showed that the magnesium salt of the 2-dibutylamino-4, 6-dithio-1,3,5-triazine was more effective than the barium salt in cross-linking the PVC. Hale *et al.* investigated effects of cross-linking reactions and order of mixing on properties of compatibilized Poly Butelene Terephthalate / ABS blends and its impact on mechanical properties using a single screw extruder [104]. The blend viscosity was much higher than that of the individual components indicating the possibility of chemical reaction. The impact strength of ABS-45 / PMMA 30/5 was slightly lower than ABS-45 / Styrene acrylonitrile (SAN) 30/5 blends, indicating that the presence of an acrylic polymer with no epoxy groups, which is miscible with the SAN matrix, did have a small effect

on ABS impact properties. Similar studies on PET / PC blends were carried out using elongation rheometry by Robinson *et al.* [105]. Addition of PC at low levels (l0-20%) permitted the thermo elastic processing of PET over a wider temperature range, and suggested that uni-axial orientation and significant strain-induced crystallization in the PET -phase can be achieved at lower strain levels.

2.4   Nano scale Reinforcements in RM

Currently PE, in its many forms, represents about 80% of rotationally molded polymers in industry [1]. Cross linked grades of PE are also commonly used in RM [78]. PVC plastisols [106] make up about 12% of the world consumption, and PC, nylon, PP[107], unsaturated polyesters, ABS [108], acrylics [109], polybutylenes, PS, polyurethanes [110], etc. make up the rest. Use of reinforced plastic composites has been accomplished by researchers and industrialists for RM, providing materials with much improved properties over pure polymers [107, 111–113]. The micro scale reinforcements in RM do have its advantages and limitations as in other polymer processing technology. The micro scale additives may adversely affect the mechanical properties owing to their hardness, while elastomeric particles may increase toughness but result in reduction of stiffness. Greco *et al.* showed that selective reinforcement using HDPE matrix pultruded tapes increased the stiffness of LLDPE parts during plate bending and pressurization tests [114]. Glass particulate reinforcement of various sizes in LLDPE for RM also showed improvements in tensile modulus up to 20% as reported by Yan *et al.*[115]. O. Kulikov *et al.* found that the use of FS as an additive, at concentrations from 100 to 500 ppm, reduced the number of bubbles formed by entrapped gasses and worked as densification aid [116]. Similarly Spence and Crawford also observed that by increasing the number of fine particles more physically smaller bubbles were produced, while larger particles increased the porous area in the product [7]. However, a balanced mix of these two particles size distributions reduced the porous area significantly. They have also showed that melt viscosity had substantial influence on the powder flow during tumbling inside the mold. This will eventually affect uniformity and variations in product thickness. The nature of powder flow and its effect on the melt deposition of powder materials in rotationally molded parts was examined by Olinek *et al*[112]. The study showed the importance of particle size, flow and shape geometry of LLDPE. He had developed an experimental set-up that allowed analysis of particle deposition pattern in RM process especially to address the problems of thickness distribution, fabricating composites and multi-layered products.Addition of FS nano particles is speculated to increase the flow of the powder in early stages of melting. They have also revealed that viscosity

of melt had significant influence on the flow of powder inside the mold which in turn will affect uniformity in thickness. Pick *et. al.* found that higher number of bubbles result in lower impact toughness [117]. They established a quantitative relationship between the impact performance and thermal transition of LLDPE. In addition to the particle sizes the pressurization of polymer melt during RM resulted in fast bubble shrinkage [9]. The entrapment of bubbles of gasses trapped during sintering of the PE, was prevented by the use of reacting mixtures of polyethylene glycols (PEG) with citric acid as processing additive [116, 118]. The processing additives accelerated sintering of the PE particulates, and greatly reduced the number of bubbles in the melt. However, it was found that its high concentrations impede flow of the particles which is not desired during the processing. The use of PEG as well as PEG-based esters at concentrations from 0.1 to 0.5 wt% reduced the sintering time of the polymer melt but affected free-flow properties of the LLDPE powders [119]. A combination of the PEG and PEG-based esters with FS reduced the amount of trapped gasses, decreased the sintering time while preserving the good free-flow behavior of the LLDPE powders [120, 121].

Rotational molding suffers from a relatively longer cycle time for the removal of entrapped gasses (bubble)and ineffective heating/cooling of mold. The importance of internal cooling of mold was emphasized by Tan *et al.* [122], and suggested rapid and symmetrical cooling across the mold for smaller spherulite size, increased the mechanical properties and less potential warpage or distortion in moldings. The existence of an optimum sintering temperature had been predicted at which the density of the sintered product was maximum for a good quality rotationally molded product [118].

Along with the improvements in materials used for RM, the RM industry has seen rapid technological advances in the past few decades in process control and cycle time reduction. Until recently, the RM process was relying on both trial and error and the experience of the operator to judge the curing of product and hence product quality. This imposed a serious quality control issue when automotive and industrial products were molded. The monitoring of IAT in the mold provided a better control of the process eliminating much of the guess work from the process.Monitoring the IAT and pressure in molds has provided significant improvements in product quality and repeatability [10]. Since, the monitoring of IAT in a bi-axially rotating closed mold in an oven imposed practical difficulties, wireless temperature monitoring systems like ROTOLOG$^{\text{TM}}$, TEMPLOGGER, K-PAQ$^{\text{TM}}$ [8] were developed. The design of molds and choice of mold material along with internal mold coating [8] for quick release of parts ensured reduced cycle time for

the RM process. The quality of polymer powder and aesthetics were improved by the use of mixing colorants in sophisticated pulverizer to obtain the proper powder size and shape. The use of improved process control and adopting variations in materials by use of micro scale and nano scale reinforcements for desired properties make the RM process one of the most important polymer processing method.

2.5 Patent Search on Reinforcements for Polymer Processing

A notable amount of polymer processing patents were dedicated to reinforcement of molded shape and bubble removal: Maziers [123] in his patent mentioned that the micro-pellets exhibited a better bubble removal as a function of temperature in comparison with the powdered products. Swain [124] proposed to use a combination of resin pellets and resin powder (20 to 40 wt%) to make rotationally molded products having improved strength, environmental stress cracking resistance (ESCR) and other strength characteristics. It was proposed by Sowa [125] to use about 0.01 to 0.04 wt% of fatty acid salt such as calcium stearate and lithium stearate per 100 parts by weight of olefin polymer based RM compositions to provide parts with pinhole free surfaces and bubble free product. Needham [126] proposed addition of zinc stearate into RM compositions containing cross linking agents to prevent the formation of voids in the final rotationally molded article. He also proposed to use nucleating, like calcium carbonate, zinc oxide, pigments such as carbon black and titanium dioxide to improve resistance of rotational molded containers to puncture. The supposed nucleating agents had a particle size in the range from about 0.05 to 20 microns, preferably from about 0.1 to 10 microns. Densification aids were proposed recently by Maziers [127]. One densification aid comprised fluro polymer as a major component and in addition comprised a minor component selected from the group consisting of a polyether block co-polymer, thermoplastic polyurethane, a polyester and PEG. Other densification aid comprised a polyether ester, optionally consisting essentially of a mixture of a polyether ester as a major component with a minor component selected from the group consisting of polyether block polyamide (PA), thermoplastic polyurethane, a polyester, PEG and fluro polymer. The PEG used in two referred inventions usually have an average molecular weight from 100 to 2000 g/mol and more preferably from 150 to 700 g/mol.

2.6 Assessment of Literature

It is thus evident that there is a growing interest to use FS in polymer matrix for improving the process and mechanical properties of the product. Also, it can be seen that there is deficiency of studies towards use of nano scale reinforcements for improving the processibility as well as mechanical properties of rotationally molded products. Apart from this, melt compounding using the extruders poses significant problems like agglomeration, separation, etc. It may be due to the fact that control of this process is difficult mainly due to the biaxial rotation of mold in aggressive heating environment which makes the use of conventional temperature measuring devices very difficult. Also, it is speculated that incorporation of such nanocomposites may adversely affect the powder flow characteristics within the mold thus producing a defective mold. Based on the literature survey, following gaps in research are identified:

1. Even though FS nanocomposites were discussed in great detail for enhancement of mechanical properties and nucleation kinetics, it was not reported extensively in LLDPE blends so as to use them in RM process. The normal trend of researchers is to study RM process after powder formulation and once the powder is poured in the mold. The powder formulation to get the desired properties is often overlooked. It had been indicated that during nucleation nano pores were formed when blended with FS which was speculated for easy bubble removal in RM process.

2. Rotational molding being a very low shear process, the changes in zero shear viscosity of melt during molding is critical. With the addition of FS in LLDPE, zero shear viscosity may be altered due to the entanglement of polymer chains. However, studies correlating zero shear viscosity for RM with nano particles are very less. Further torque rheometric studies of rotationally moldable LLDPE have not been adequately emphasized in the literature. Since LLDPE granules are compounded in an extruder before pulverizing, the torque rheometric studies can provide important insights with respect to its processibility.

3. In RM industry, more than 80% of all the material used is from the PE family and few other polymers like PP, nylon, PVC, etc. are proved commercially successful. The enhanced mechanical properties in terms of higher modulus, uni axial strength and impact toughness are much desired in rotational molded components due to the lack of choice of materials available at present. The mechanical properties were improved by addition of additives in micro scale

and controlling the process parameters in commercially proven polymers. The uses of nano sized reinforcements were not investigated in detail for RM.

4. The effect of FS on cycle time reduction is not addressed at length in literature. The cycle time reduction with reinforced LLDPE is quantum leap in RM and has significant commercial implications. Similarly, PIAT studies on FS-LLDPE blends to monitor cycle time and proper sintering is proposed as the same is not available in the surveyed literature.

5. LLDPE being a viscoelastic material, the dynamic mechanical analysis for determining the storage modulus, Loss modulus, creep modulus and thermo-mechanical properties of LLDPE - FS blends are yet to be addressed.

6. The studies of FS in other polymer blends showed positive reinforcement effects at lower concentrations.Morphological studies provide valuable insights into the understanding of mechanical properties of polymer along with the dispersion of nano particles. However, the correlation between the morphological proprieties and mechanical properties for rotationally moldable LLDPE has not been emphasized in literature.

7. Most of the studies have reported the findings at laboratory scale. Since the application of the FS nanocomposites in industrial scale is difficult mainly due to the difficulty in process control, the scaling up of the laboratory scale findings in a RM industry is lacking in existing literature.

This research work is an attempt to bridge the above gaps in literature.

Chapter 3

Rheological Characteristics of LLDPE - FS Nanocomposites

3.1 Introduction

Rheology is defined as the study of the deformation and flow of a fluid. It is a semi-quantitative tool to study the deformation and flow behavior under stress. An important property of a molten polymer is its shear viscosity and the dependence of the viscosity on temperature and deformation rate. Most polymer melts are classified as shear thinning fluids (also known as pseudo-plastics). Shear thinning refers to the reduction of viscosity at increased rate of shearing. At higher shear rates, the polymer molecules orient themselves and the number of entanglements between the polymer chains decreases. This helps the polymer chains to slide and flow past one another resulting in large scale movement and reduction of viscosity. The viscosity also decreases with increasing temperature due to the increase in the kinetic energy of the molecules. A rigorous study must be performed on polymer materials in order to better understand the rheological behavior. The quantitative methods involving polymer structure and measurable properties like viscosity, strain rate and viscoelastic properties are currently investigated by many researchers and remain a challenge to address the commercially available polymers [81, 128]. During the past two decades precise, reliable, economic in-line and on-line rheometers are made to address the needs of commercial and research interests [129].

In a fluid under stress, the ratio of shear stress (τ) to the shear strain rate ($\frac{d\gamma}{dt}$) is called shear viscosity (η) and is analogous to the modulus of a solid. In ideal (Newtonian) fluid, the shear viscosity is a material constant. However, for plastics (molten state) the viscosity varies depending on the stress, strain rate, time, temperature, etc. and is no longer a constant for the material. The viscosity of polymer melt reduces with increased shear rate for constant temperature as given in Figure 3.1 [130]. The dynamic viscosity is independent of shear rate at very low shear rates and the limiting value of viscosity is called zero shear viscosity (η_0) .

This is an important material constant and serves as an indicator of molecular weight of polymer.
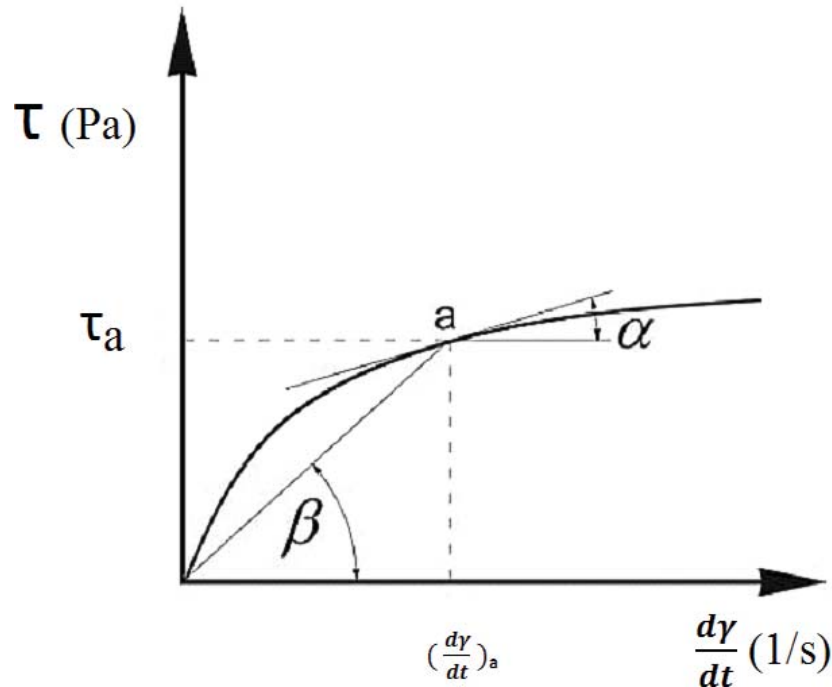
Figure 3.1: Viscosity coefficients $\tan \alpha$ = Dynamic viscosity, $\tan \beta$ = Apparent viscosity

As almost all the polymer processing methods involve melt processing, the study of polymer melt flow is very crucial. RM also being not an exception for this, the rheological characterization of the material is extremely important. In this chapter, the effect of adding FS in rotationally moldable LLDPE, on melt and rheological characteristics are investigated. For this purpose, three different approaches have been followed . These are:

1. MFI Studies

2. Dynamic rheological studies

3. Torque Rheometry

The effect of blending methods for FS in LLDPE, ie dry mixing and melt mixing, in rheological properties are also studied to ascertain proper mixing method for rotationally molding LLDPE - FS nanocomposite.

3.2 Material and Methods

To study the rheological characteristics blends of of LLDPE - FS nanocomposites are prepared. Rotationally moldable grade of natural LLDPE (G-Lene R35A042) having MFI of 4.2 g/10min and density of 935 kg/m^3 was supplied by GAIL India Limited.Detailed specification of R35A042 is given in Appendix A.1. The natural LLDPE is devoid of any additives as per the manufacturer, and the terminology "natural" is used throughout in this thesis to represent the same. Hydrophilic FS of grade Aerosil-200 with a BET surface area of 200 m^2/g and tapped density of 50 g/l was used as for nano reinforcement (Evonik industries). Detailed specification of Aerosil-200 is given in Appendix A.2. The primary particle size was 5 – 50 nm. A few key important material properties are given in Table 3.1.

Table 3.1: Summary of material specifications

Specifications	Unit	Value
Natural LLDPE		
Melt Flow Index	g/10min	4.2
Density @ 23ºC	g/cc	0.935
Vicat Softening Point	ºC	115
Fumed Silica		
Specific Surface Area (BET)	m^2/g	200± 25
Tapped Density	g/l	≈ 50
SiO$_2$ Content	wt.%	> 99.8

LLDPE - FS nanocomposite blends (1 – 8 wt% FS) were prepared by dry mixing and melt mixing using high speed mixer and lab scale single screw extruder. FS was dried at 105ºC in a temperature controlled oven for 2 hours to ensure the removal of entrapped moisture. Dry mixing was carried out in a high speed mixer running at 3000 rpm with fixed intervals of 30 seconds mixing time and 30 seconds cooling time repeated for 4 to 5 times to ensure proper mixing. Melt mixing was done in a three stage single screw extruder as shown in Figure 3.2 running at 25 rpm to obtain the extrudate. These were pelletized using a cutter running at 8 rpm. The pellets were dried at 60ºC in a temperature controlled oven for 1 hour. The specifications of the single screw extruder are given in Appendix A.4.

Figure 3.2: Lab scale single screw extruder

3.2.1 MFI Studies

Being a stress free process, in RM, proper MFI (and hence viscosity of the melt) is very crucial. MFI values of 3.5 to 5 g/10 min are ideal for the process. If the viscosity is very low, the polymer melt will not adhere to the mold causing annulled casting. A high melt viscosity causes inadequate mold flow, increasing the processing time and the amount of entrapped gasses, resulting in defective part. MFI studies were performed using a Dynisco LMI 4000 melt flow indexer with digital encoder as shown in Figure 3.3a. The specifications of Dynisco LMI 4000 are given in Appendix A.5. MFI was measured at 190ºC/2.16 kg, according to ASTM-D1238 [131], method A . The melt density and melt volume rate for the blends were found according to ASTM-D1238, method B. The melt flow indexer is essentially an extrusion plastometer which consists of a chamber for melting the polymer along with a die and dead weight piston arrangement. The melt chamber is cylindrical in shape and thermostatically controlled to ensure a constant set temperature during the testing. According to ASTM-D1238 the steel cylinder is 50.8 mm in diameter, 162 mm in length with a smooth straight hole of 9.5504 $\pm$ 0.0076 mm in diameter, displaced 4.8 mm from the central axis to accommodate thermal sensors. The piston compresses the polymer melt inside this thermally controlled cylindrical melt chamber which has a steel die of 2.0955 $\pm$ 0.0051 mm at the bottom through which the extrudate flows. The load is applied on piston by mounting weights directly on piston or by hydraulic or pneumatic means. The

essential features of the melt flow indexer are given in Figure 3.3b

(a) Melt flow indexer
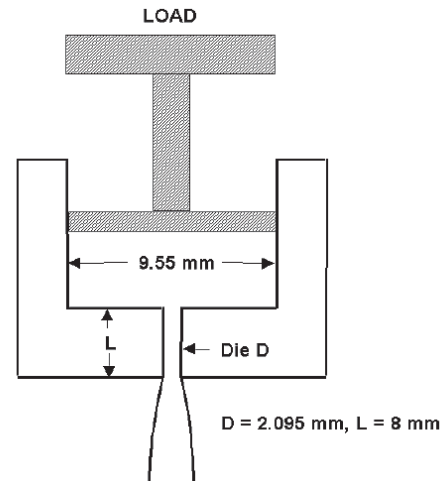
(b) Schematic of melt flow indexer

Figure 3.3: Melt flow indexer and its schematic

There exists both manual (Method A) and automatic (Method B) operation modes for determining the melt flow rates. In manual operation the extrudate is cut at specified time (cut time, usually 20 s) and is weighed in a precision balance to calculate the melt flow rate. In the automatic mode the weighing of extrudate is avoided by specifying the melt density of the polymer as an input in the melt flow indexer. The melt flow indexer measures the melt volume rate (MVR) as the ratio between volume (V) of polymer melt passed through the die at constant temperature and pressure to the time taken and can be calculated by Equation 3.1 [130].

$$MVR(cc/10min) = V.s/t \qquad (3.1)$$

Where s - The factor of standard time (10 min , s=600)
The weight (W) of polymer melt can be measured separately using a precision balance for obtaining the MFI using Equation 3.2.

$$MFI(g/10min) = W.s/t \qquad (3.2)$$

The ratio of MFI to MVR thus gives the polymer melt density. In a melt flow indexer, normally the piston moves at a constant velocity to give a constant melt

volume rate (Q). At low shear rates the flow through the die in melt flow indexer can be approximated as steady flow. Assuming Newtonian flow, the apparent shear rate can be expressed as given in Equation 3.3.

$$\frac{d\gamma}{dt} = \frac{4Q}{\pi R^3} \tag{3.3}$$

Where R is the radius of the die.

The shear stress (τ) can be calculated by knowing the pressure drop (Δ P) across the die from Equation 3.4.

$$\tau = \frac{\Delta P.R}{2L} \tag{3.4}$$

Where L is the length of the die.

Hence apparent viscosity expressed as the ratio of shear stress to apparent shear rate is given by Equation 3.5.

$$\eta = \frac{\pi \Delta P.R^4}{8LQ} \tag{3.5}$$

This is known as Hagen-Poiseuille equation [85, 137], which can be regarded as the basis of rheological measurements, as it is very easy to measure the volume flow rate, and thus viscosity can be calculated by the above equation. The pressure drop across the die can be approximated by the pressure exerted by piston as given by Equation 3.6.

$$\Delta P = \frac{F}{\pi R^2} \tag{3.6}$$

Where F is the load exerted by the piston.

The dynamic viscosity and shear rate at various temperature for the LLDPE - FS blends were calculated along with the MFI using the melt flow indexer. The MFI was measured using Method A (ASTM-D1238) while dynamic viscosity and shear rate calculation was done using Method A/B and Method B.

3.2.2 Dynamic Rheological Measurements

Zero shear viscosity for natural LLDPE and LLDPE - FS blends were measured using an Anton Paar MCR 102 rheometer . The specifications of MCR 102 are given in section A.6. Parallel plate configuration was used for measuring the rheological characteristics. This rheometer allows precise control of gap between the plates and isothermal conditions at desired temperature during the testing. In this study, the tests were done at 5% strain (amplitude) with 1 mm gap between the parallel plates. The temperature was varied from 140^oC to 220^oC in increments of 20^oC. The angular frequency (ω) was varied from 100 to 0.1 rad/s for every temperature step. The experimental set up is shown in Figure 3.4.

Figure 3.4: Parallel plate rheometer MCR 102 set up

3.2.3 Torque Rheometry

Torque rheometric studies were conducted using a twin screw torque rheometer. It is used as an attachment to the single screw extruder and is shown in Figure 3.5. The torque rheometer simulates the melt mixing of polymer blends in extruder and records the reactive torque on rotors as a function of time. The studies were done at 60 rpm at temperatures of 210^oC and 150^oC for 40 minutes. The blends of LLDPE - FS powder was loaded to fill the rheometer roller chamber

upto 70% by volume. A 5 kg weight was used for forcing down the loading ram to close the mixing chamber.

Figure 3.5: Torque rheometer attachment

3.3   Results and Discussions

3.3.1   MFI of LLDPE - FS Nanocomposite

The variations in MFI due to the addition of FS in LLDPE, in dry and melt mixing conditions are shown in Figure 3.6. From the plot, a decreasing trend of MFI was observed with the addition of FS and is summarized in Table 3.2. From Table 3.2 it is clear that the MFI decreases with increasing FS content. This indicates that the viscosity of the polymer melt increases. Further, it was observed that the MFI did not vary significantly for dry as well as melt mixing till 2% FS composition. Thus, with lower FS composition a proper dispersion was achieved with high speed mixing. With increased FS content beyond 2%, the proper dispersion of FS could be possible only through melt mixing using screw extruder. Generally, MFI values between 3.5 to 5 g/10 min are acceptable for RM (for LLDPE at 190°C/2.16 kg). Thus, LLDPE - FS blends up to a limiting value of 4% FS which resulted in MFI of 3.65 g/10 min can be considered suitable for RM. The variation of MFI for different temperatures is shown in Figure 3.7. With this plot, it is easier

to ensure the proper temperature for the processing of these nanocomposites. It can be seen that the increasing FS content reduces the MFI at any given temperature. This is due to restricted movement of polymer chains in the melt. The mobility of polymer chains is affected by the partial entanglement and adhesion of FS to polymer chains. Figure 3.7 shows a consistent trend of increase in MFI with temperature for all the compositions.
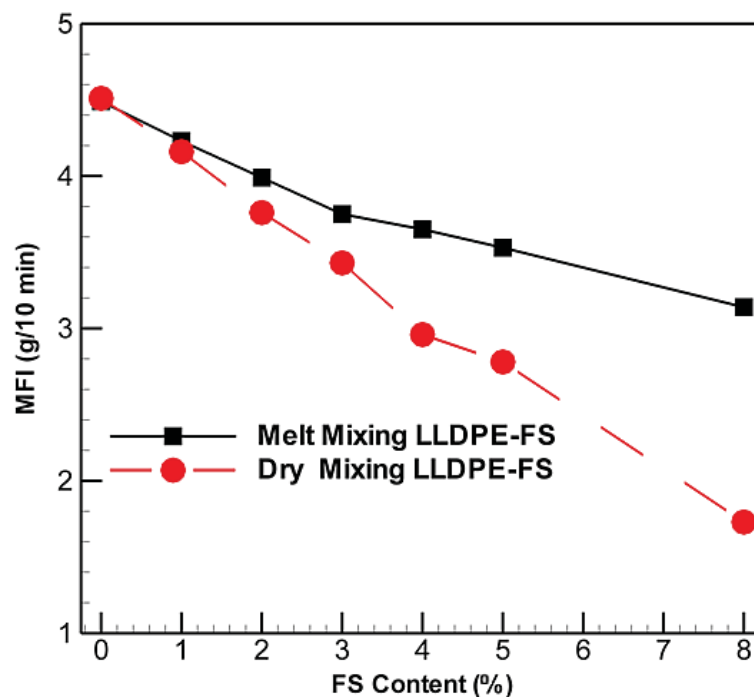
Figure 3.6: Variation of MFI for natural LLDPE and LLDPE - FS blends

Table 3.2: Variation of MFI

	MFI (g/10 min)	
	Melt mixing	Dry Mixing
Natural LLDPE	4.49	4.51
LLDPE + 1% FS	4.23	4.16
LLDPE + 2% FS	3.99	3.76
LLDPE + 3% FS	3.75	3.43
LLDPE + 4% FS	3.65	2.96
LLDPE + 5% FS	3.53	2.78
LLDPE + 8% FS	3.14	1.73

The dynamic viscosity and shear rates for LLDPE - FS blends at various temperatures calculated using Hagen-Poiseuille equations (Equation 3.5) are summarized in Table 3.3. The dynamic viscosity so obtained was used to compare

the flow behavior of LLDPE - FS blends and is plotted in Figure 3.8. As expected, the viscosity of the melt increased with FS content but reduced with temperature. Natural LLDPE at 180°C had a dynamic viscosity of 2178 Pa.s while as LLDPE - 5% FS had a dynamic viscosity of 2877 Pa.s. The melt viscosity reduced to 1205 Pa.s and 1550 Pa.s for LLDPE and LLDPE - 5% FS at 210°C. Similarly, the effect of varying shear rates with change in FS composition and temperature was studied by varying the loads used in MFI testing. The variation of shear rate with temperature is shown in Figure 3.9. It can be seen that due to the reduction in viscosity, the shear rate increases for a constant load. Natural LLDPE at 180°C had a shear rate of 9.04 s^{-1} while as LLDPE - 5% FS had a shear rate of 6.84 s^{-1}. The shear rate increased to 16.3 s^{-1} and 12.7 s^{-1} for LLDPE and LLDPE - 5% FS at 210°C. Since LLDPE with increasing FS has shown lowest shear rate, increased resistance to melt shear could be seen. This can also be attributed to increased viscosity with the addition of FS in LLDPE.
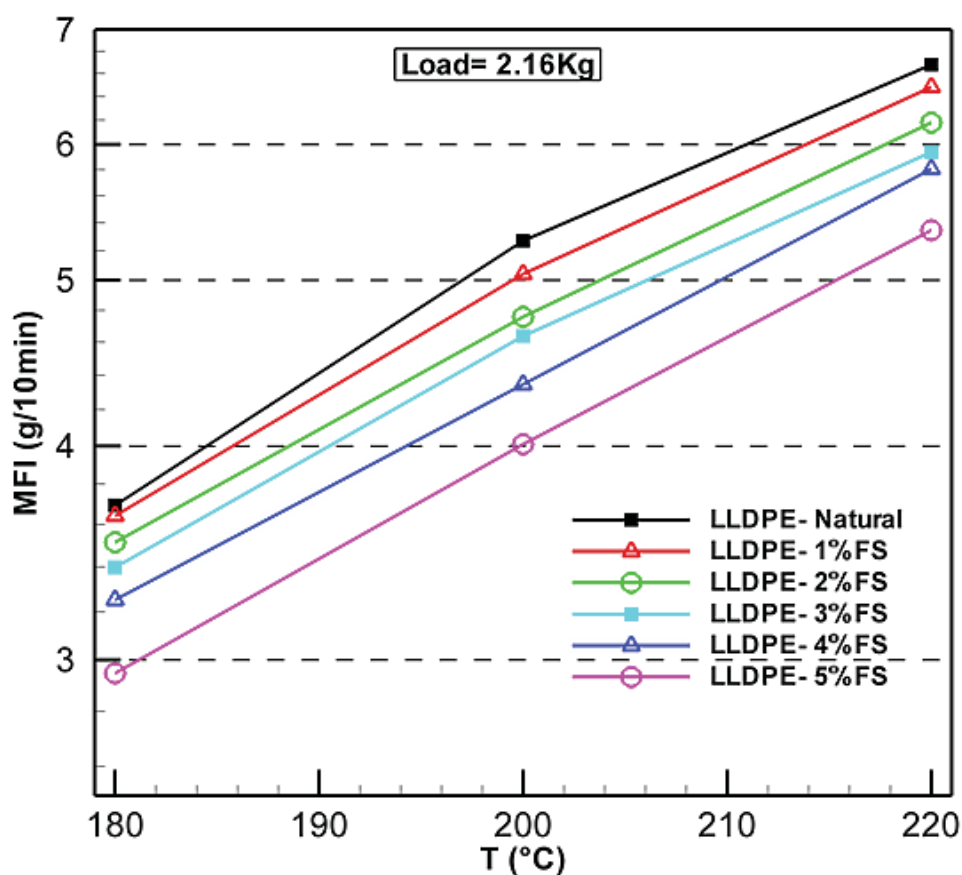
Figure 3.7: Variation of MFI vs. temperature for natural LLDPE and LLDPE - FS blends
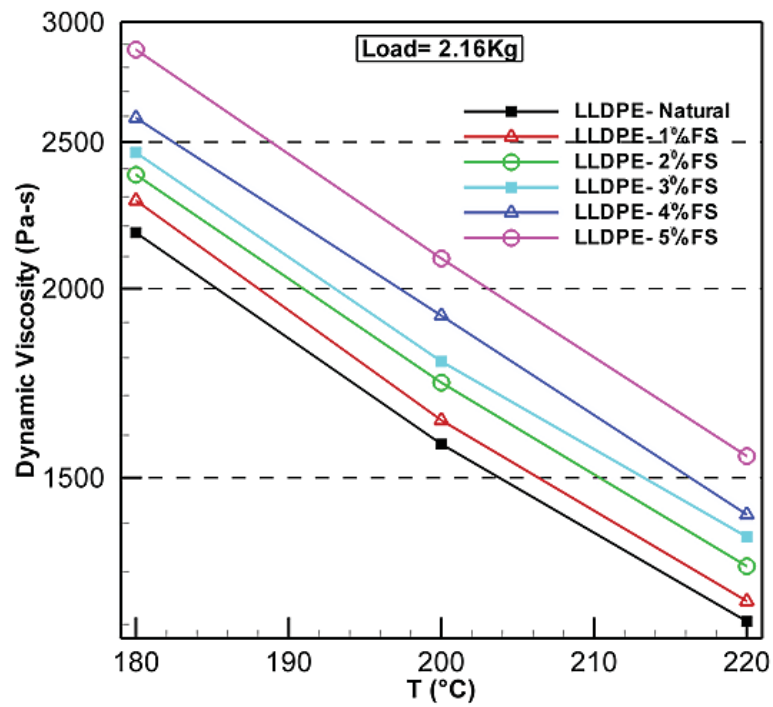
Figure 3.8: Variation of dynamic viscosity vs. temperature for natural
LLDPE and LLDPE - FS blends
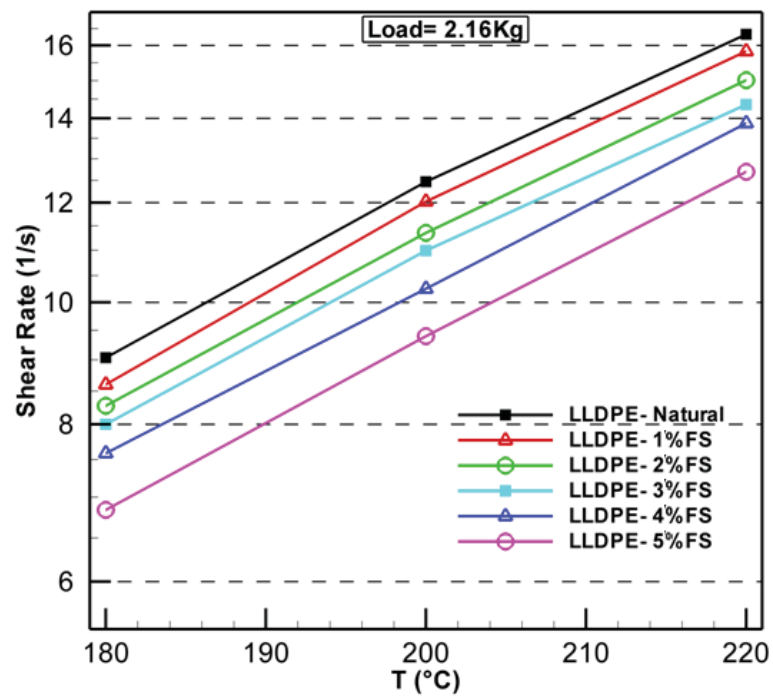
Figure 3.9: Variation of shear rate vs. temperature for natural LLDPE
and LLDPE - FS blends

Table 3.3: Variation of dynamic viscosity and shear rate

	Temperature °C	MVR cc/10 min	Dynamic Viscosity Pa.s	Shear Rate s^{-1}
Natural LLDPE	180	4.89	2177.89	9.04
	200	6.75	1578.71	12.47
	220	8.85	1205.57	16.33
LLDPE + 1% FS	180	4.66	2287.20	8.61
	200	6.51	1637.04	12.02
	220	8.58	1243.29	15.83
LLDPE + 2% FS	180	4.48	2378.51	8.28
	200	6.15	1733.56	11.35
	220	8.13	1311.16	15.01
LLDPE + 3% FS	180	4.33	2460.09	8.00
	200	5.96	1790.31	10.99
	220	7.78	1371.01	14.35
LLDPE + 4% FS	180	4.11	2593.73	7.59
	200	5.56	1919.65	10.25
	220	7.52	1418.36	13.88
LLDPE + 5% FS	180	3.71	2877.15	6.84
	200	5.09	2094.06	9.40
	220	6.88	1550.32	12.69

3.3.2 Dynamic Rheological Studies

Though the MFI studies provide necessary information needed to assess the flow of molten polymer within mold, dynamic rheological studies are needed to get an insight of melt flow particularly in the zero state regime as RM is a very low shear stress process. This is found by dynamic viscoelastic measurements. In the controlled stress measurements shear rate is measured by the angular deflections of the plate using an optical encoder. The shear viscosity is defined by relating the shear stress and the shear rate in a simple power law model [86]. The model can be used to represent the variation of viscosity with shear rate at sufficiently high shear rates. This can be expressed as given in Equation 3.7 [132, 133],

$$\eta = K \left(\frac{d\gamma}{dt} \right)^{n-1} \tag{3.7}$$

Where (n) known as flow index is defined as the slope of the shear thinning region (at high shear rate) which is often used to quantify the degree of shear thinning

for different polymers. 'K' is known as the flow consistency. At very low shear rates in log - log scale, plateau region is exhibited by viscosity plot and is referred as zero-shear viscosity or Newtonian plateau. This can be determined from the modified Cross fit model (Equation 3.8) . This model approach power-law behavior at high shear rate, and the dimensionless material constants (m) is simply related to the power law exponent.

$$\eta = \frac{\eta_0}{1 + \left(t_0 \dfrac{d\gamma}{dt} \right)^m} \tag{3.8}$$

Where (t_0) represents the characteristic relaxation time , and (m) characterizes the slope of the line over the pseudo plastic region in the logarithmic plot. Similarly viscosity is represented as complex viscosity η^* and is given in Equation 3.9

$$\eta^* = \eta' - i\ \eta'' \tag{3.9}$$

Where the real (η') and imaginary (η'') components, which are functions of frequency, are related to the storage modulus (G') and loss modulus (G'') under shear is given in Equation 3.10 and Equation 3.11:

$$\eta' = \frac{G''}{\omega} \tag{3.10}$$

$$\eta'' = \frac{G'}{\omega} \tag{3.11}$$

Further the tangent of phase angle ($\tan\delta$) is defined as the ratio between the loss modulus and storage modulus and is given in Equation 3.12

$$\tan\delta = \frac{G''}{G'} \tag{3.12}$$

For many polymeric systems, comparison of the steady state shear flow viscosity (η) taken as the absolute value of the complex viscosity ($|\eta^*|$), at some shear rate ($\dfrac{d\gamma}{dt}$) and at an angular frequency (ω) which is equal to the same shear rate, has shown relation to each other. A useful empirical relationship is first stated by Cox and Merz [134, 135] which is expressed by Equation 3.13

$$\eta\left(\frac{d\gamma}{dt}\right) = |\eta^*(\omega)|_{\omega = \frac{d\gamma}{dt}} \tag{3.13}$$

Where, $|\eta^*(\omega)|$ is the absolute value of the complex viscosity at angular frequency ω. Cox - Merz equation thus provides a method to correlate dynamic and steady state data. When the shear rate tends to reach zero, it is termed as zero shear viscosity.

The experimentally determined complex viscosity (η^*) and its real ($\eta^{'}$) and imaginary components ($\eta^{''}$) are given in Table 3.4.

Table 3.4: Dynamic rheological measurements - viscosity

Material	T	Angular frequency (ω)	Complex Viscosity (η^*)	Imaginary Viscosity ($\eta^{''}$)	Real Viscosity ($\eta^{'}$)
	°C	rad/s	Pa.s	Pa.s	Pa.s
Natural LLDPE	220	100	593.47	290	517.79
	220	10	1026.4	281.68	987.03
	220	1	1346	172.06	1335
	220	0.1	1569.6	97.164	1566.6
	180	100	742.01	397.73	626.41
	180	10	1428.9	525.24	1328.9
	180	1	2207.8	493.36	2152
	180	0.1	2730	307.68	2712.6
	140	100	981.93	578.68	793.29
	140	10	1976.8	712.94	1843.8
	140	1	2942.3	643.06	2871.2
	140	0.1	3730.1	554.12	3688.7
LLDPE - 2%FS	220	100	742.95	363.97	647.69
	220	10	1289.6	353.2	1240.3
	220	1	1705.8	235.28	1689.5
	220	0.1	2333.6	342.53	2308.4
	180	100	976.54	542.22	985.89
	180	10	1889.8	710.72	1946.6
	180	1	3022.1	1201.1	3014.9
	180	0.1	7270.7	5464.2	4796.4
	140	100	1328.3	837.3	1031.2
	140	10	2890.7	1255.2	2604
	140	1	4992.6	2279.2	4441.9
	140	0.1	13156	10684	7677.3
LLDPE - 4%FS	220	100	789.06	424.86	664.91
	220	10	1494.7	501.53	1408.1
	220	1	2186.1	467.16	2135.6
	220	0.1	3163.1	691.34	3086.7
	180	100	1015.8	594.36	823.75
	180	10	2097.8	887.83	1900.7
	180	1	3684.9	1552.1	3342.1
	180	0.1	7998.6	5631.3	5680.3
	140	100	1349.7	875.85	1027
	140	10	3058.2	1384.4	2726.9
	140	1	5419.2	2381.7	4867.8
	140	0.1	12681	9617.8	8264.6

The variations of melt viscosity for LLDPE, LLDPE - 2% FS and 4%FS blends at various temperature and angular frequency are shown in Figure 3.10, Figure 3.11 and Figure 3.12 respectively. It is known that the angular frequency has analogy with shear rate applied to the polymer melt [134].
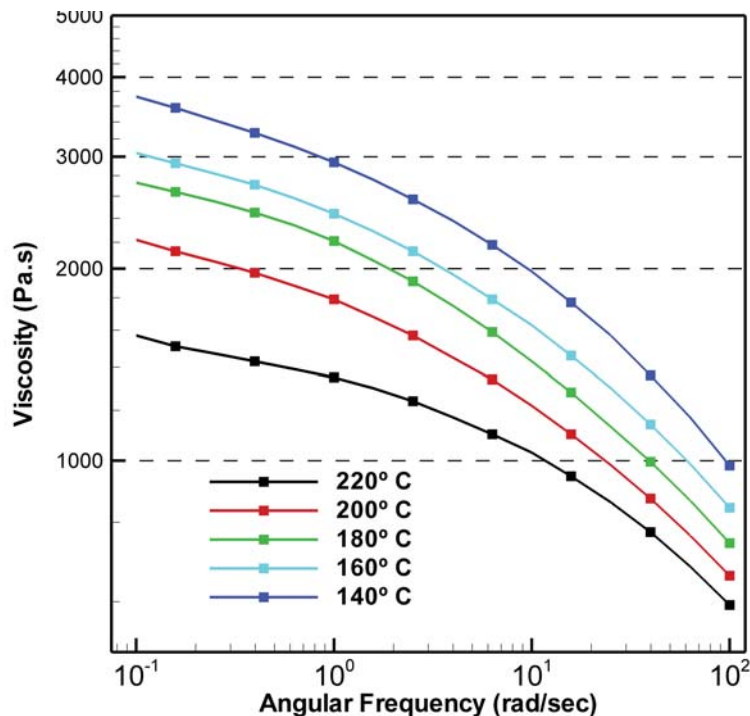
Figure 3.10: Variation of viscosity vs. angular frequency for natural
LLDPE

Table 3.5: Comparison of viscosity - MFI and dynamic rheological measurements

Material	T	MFI studies		Rheometry studies	
		Shear strain	Calculated viscosity (MFI)	Angular frequency	Measured Viscosity (Rheometry)
	°C	s^{-1}	Pa.s	rad/s	Pa.s
Natural LLDPE	220	16.33	1205.6	10	1026.4
	200	12.47	1578.7	10	1215.3
	180	9.47	2177.9	10	1428.9
LLDPE - 2% FS	220	15.01	1311.2	10	1289.6
	200	11.35	1733.6	10	1578.6
	180	8.28	2378.5	10	1889.8
LLDPE - 4% FS	220	13.88	1418.4	10	1494.7
	200	10.25	1919.7	10	1661.5
	180	7.59	2593.7	10	2097.8
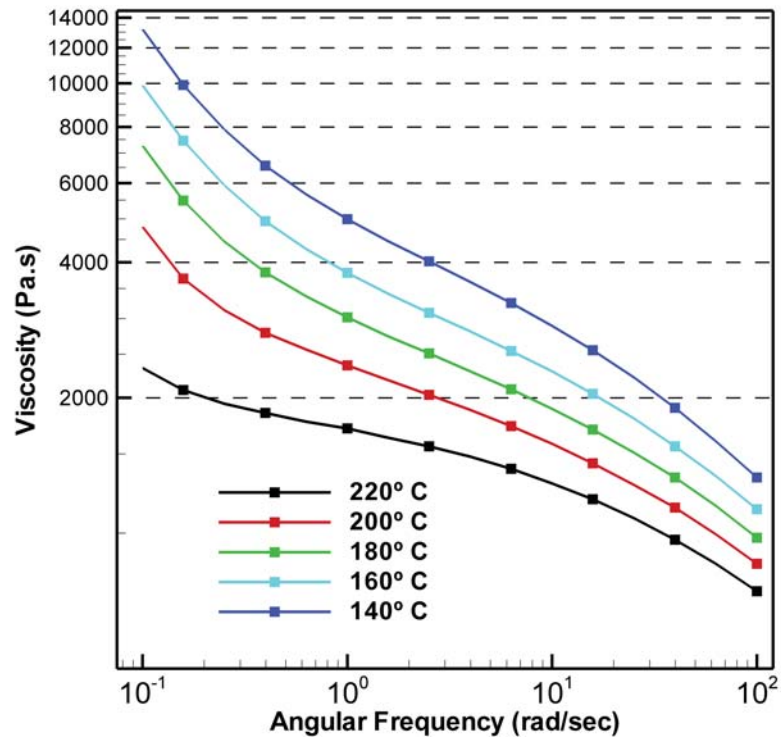
Figure 3.11: Variation of viscosity vs. angular frequency for natural LLDPE - 2%FS blend
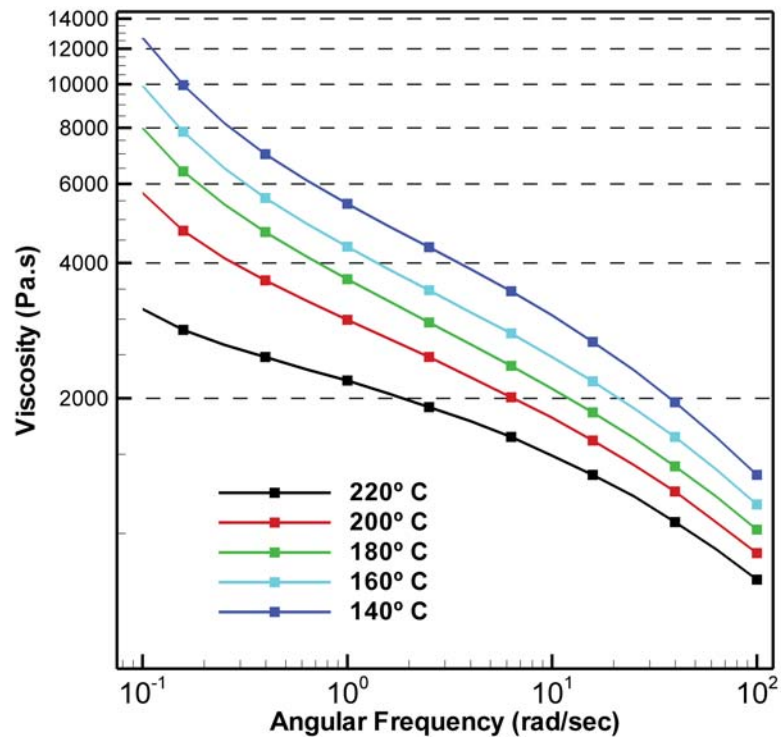
Figure 3.12: Variation of viscosity vs. angular frequency for natural LLDPE - 4%FS blend

As seen from Figure 3.10, at lower angular frequency natural LLDPE showed frequency independent behavior with a dynamic viscosity of 1238.8 Pa.s at 2.4 rad/s. This indicates the suitability of MFI studies to calculate the steady state shear viscosity for LLDPE. Similar trend was observed at 200°C with a reduction in viscosity at elevated temperature, a common characteristic of molten polymers. From Figure 3.12, for LLDPE - 4% FS blends steady state behavior was observed at 220°C and angular frequency of 0.1 - 10 rad/s during testing. In this interval, the calculated viscosity of 1418.4 Pa.s from MFI studies is close to measured viscosity of 1494.7 Pa.s as shown in Table 3.5. However, at lower frequencies (equivalently low shear rates) and reduced temperatures the melt viscosity tend to increase for LLDPE - FS blends as seen in Figure 3.11 and Figure 3.12. From Figure 3.12, it can be seen that the dynamic viscosity increased from 1494.7 Pa.s at 10 rad/s to 3163.1 Pa.s at 0.1 rad/s at 220°C. The results also indicate decreased mobility of polymer chains with the addition of FS causing entanglement of polymer chains.

To calculate the zero shear viscosity for natural LLDPE, time temperature superposition principle (TTSP)was used. Shift factors were calculated using Williams, Landel and Ferry (WLF) equation [136, 137] (TTSP is discussed in detail in chapter 4). The master curves generated at 200°C reference temperature are shown in Figure 3.13. Plateauing of viscosity curves at low shear was observed for natural LLDPE indicating zero shear viscosity value of 3430 Pa.s at 0.01 rad/s. With the addition of FS steady state behavior of viscosity was not observed at very low shear. The viscosity tends to increase with lower shear rates with the addition of FS, due to the dominating nano filler polymer chain interactions. On the other hand at higher shear rates the dominating effects of nano silica was less, leading to a steady state shear flow at 0.5 rad/s to 5 rad/s. This means that the melt strength of the LLDPE - FS composites increases at low shear rates. Since rotational molding is characterized by low shears, the FS can be considered as an useful particulate reinforcement for LLDPE.

To express the viscosity behavior for LLDPE -FS nanocomposites, curve fitting was carried out using regression analysis. The regression equation for viscosity using power law (Ostwald model) for natural LLDPE is given in Equation 3.14.

$$\eta = 1575.6\omega^{-0.185} \tag{3.14}$$

Similarly the regression equation using power law for LLDPE - 2% FS and LLDPE -

4% FS blends are given in Equation 3.15 and Equation 3.16.

$$\eta = 2549.7\omega^{-0.26} \tag{3.15}$$

for LLDPE - 2% FS blends

$$\eta = 2928.7\omega^{-0.261} \tag{3.16}$$

for LLDPE - 4% FS blends

The curve fits with the above equations are shown in in Figure 3.14. The R^2 value of fit and slope of shear thinning region (n) and the constant K are given in Table 3.6. Since power law or flow index 'n' is less than one, shear thinning behavior is expected at high shear rates and steady state viscosity at very low shear rates. The increase in flow consistency or zero shear viscosity is normally associated with increase in molecular weight. Since nano silica particles do not cross link with polymer chains, an increase in average molecular weight will not take place. The increase in viscosity can be then attributed to the entanglement of polymer chains and weak hydrogen bonding between polymer chains and silica group.
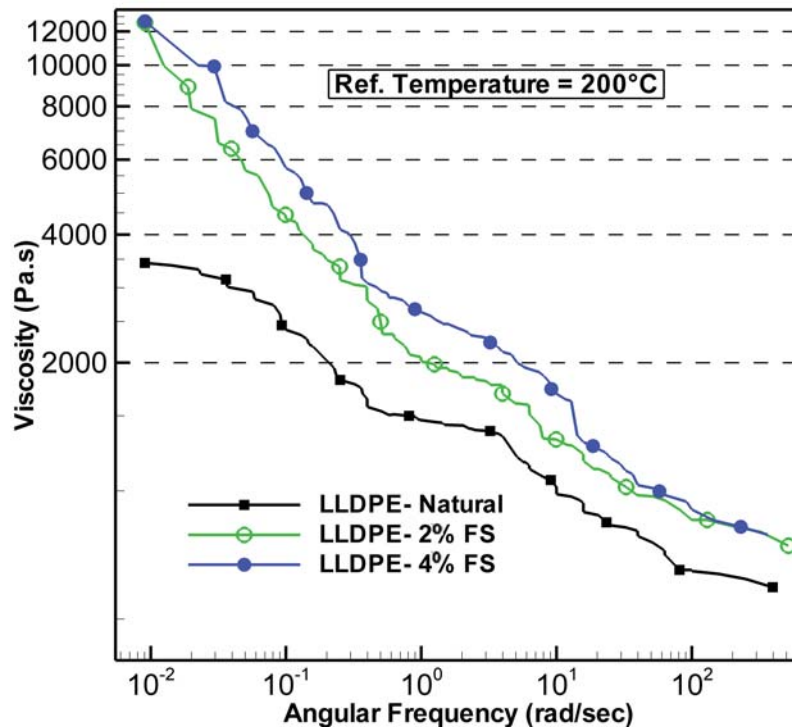
Figure 3.13: Variation of viscosity at 200ºC natural LLDPE and
LLDPE - FS blends
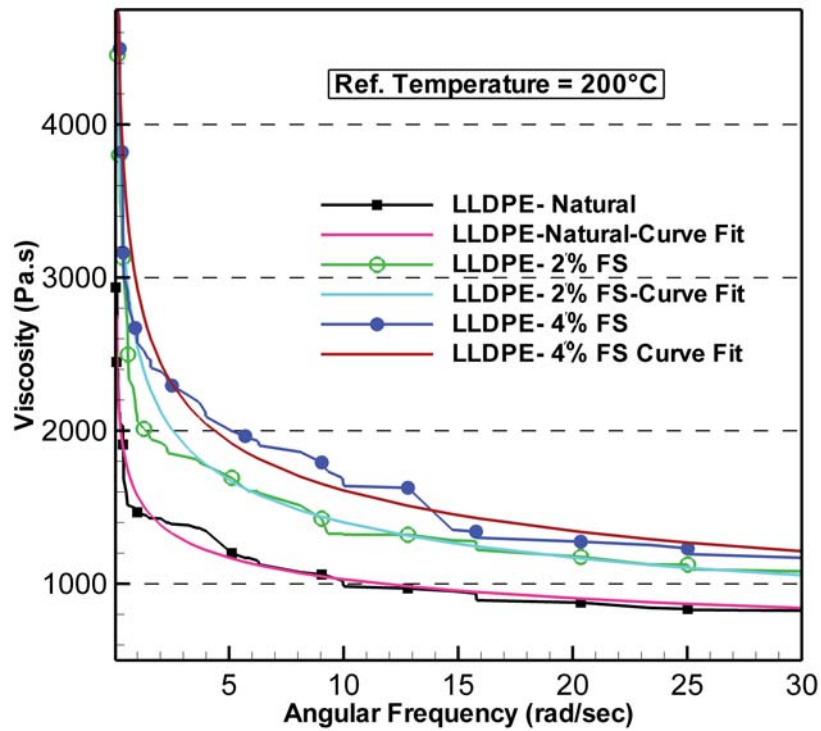
Figure 3.14: Curve fitting for viscosity vs angular frequency - LLDPE - FS blends

Table 3.6: Power law curve fitting data for viscosity

	R^2	Flow Consistency (K) Pa.s	Flow Index (n)
Natural LLDPE	0.9832	1575.6	0.815
LLDPE + 2% FS	0.9647	2549.7	0.740
LLDPE + 4% FS	0.9781	2928.7	0.739

The polymeric melts, being pseudo plastic in nature exhibits both viscous and elastic nature when it is subjected to shear. The variations of modulus and loss modulus at different shear rates and temperature need to studied. Thus, to study the rheological characteristics of polymer melts dynamic oscillatory shear measurements are used[33, 138]. In a dynamic oscillatory shear experiment, the sample is subjected to a homogeneous deformation at a sinusoidally varying shear strain or shear stress. In a controlled strain experiment, one generates a strain that is as close as possible to a sine wave as given in Equation 3.17.

$$\gamma(t) = \gamma_0 \sin(\omega t) \tag{3.17}$$

In the linear shear strain-shear stress region the relation between shear stress (τ_t)

46

and shear strain (γ_t) is given by Equation 3.18 [139].

$$\tau(t) = \gamma_0(G' \sin(\omega t) + G'' \cos(\omega t)) \tag{3.18}$$

G' and G'' is considered as the real and imaginary components of complex modulus G^* in shear and is represented as given in Equation 3.19

$$G^*(\omega) = G'(\omega) + i\,G''(\omega) \tag{3.19}$$

Figure 3.15, Figure 3.16 and Figure 3.17 shows the changes in storage and loss moduli for natural LLDPE, LLDPE - 2% FS and LLDPE - 4% FS respectively. It can be observed that with the addition of FS in LLDPE, both storage modulus and loss modulus showed an increasing trend, indicating melt strengthening due to entanglement of polymer chains with nano silica. The results of parallel plate rheometry with values of elastic, loss moduli and viscosity for LLDPE and LLDPE - FS blends are summarized in Table 3.7. It can be seen that maximum storage modulus (83.73 MPa) was obtained for LLDPE - 4% blends at higher shear rate (100 rad/s) and lower temperatures (140 ºC). This indicates the polymeric melt exhibits increased elastic behavior at high frequencies and low temperature.
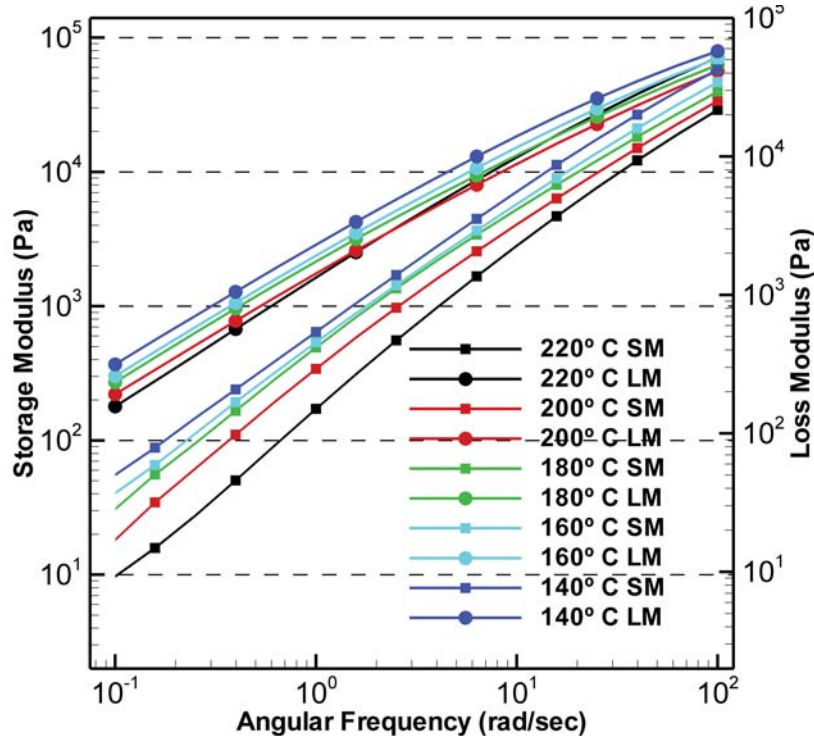
Figure 3.15: Variation of storage and loss moduli vs. angular frequency for natural LLDPE
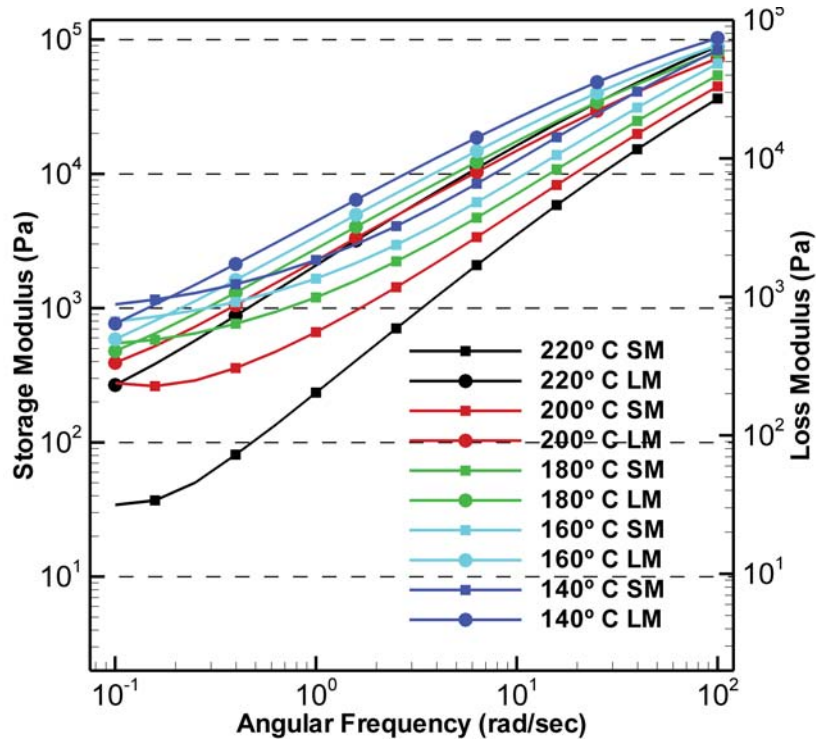
Figure 3.16: Variation of storage and loss moduli vs. angular frequency
for LLDPE - 2%FS blend
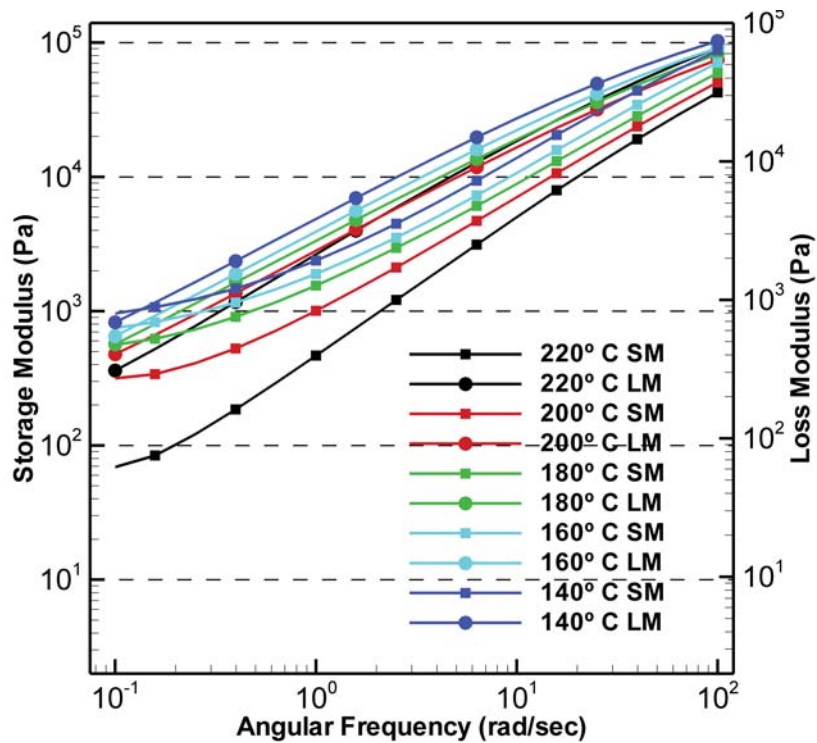
Figure 3.17: Variation of storage and loss moduli vs. angular frequency
for LLDPE - 4%FS blend

Table 3.7: Viscoelastic properties of LLDPE - FS polymer melt.

Material	T	Angular frequency	Storage Modulus	Loss Modulus
	°C	rad/s	Pa	Pa
Natural LLDPE	220	100	29000	51779
	220	10	2816.8	9870.3
	220	1	172.06	1335
	220	0.1	9.7164	156.66
	180	100	39773	62641
	180	10	5252.4	13289
	180	1	493.36	2152
	180	0.1	30.768	271.26
	140	100	57868	79329
	140	10	7129.4	18438
	140	1	643.06	2871.1
	140	0.1	55.412	368.87
LLDPE - 2%FS	220	100	36397	64769
	220	10	3532	12403
	220	1	235.28	1689.5
	220	0.1	34.253	230.84
	180	100	54222	81217
	180	10	7107.2	17511
	180	1	1201.1	2773.2
	180	0.1	546.42	479.64
	140	100	83730	103120
	140	10	12552	26040
	140	1	2279.2	4441.9
	140	0.1	1068.4	767.73
LLDPE - 4%FS	220	100	42486	66491
	220	10	5015.3	14081
	220	1	467.16	2135.6
	220	0.1	69.134	308.67
	180	100	59436	82375
	180	10	8878.3	19007
	180	1	1552.1	3342.1
	180	0.1	563.13	568.03
	140	100	87585	102700
	140	10	13844	27269
	140	1	2381.7	4867.8
	140	0.1	961.78	826.46

3.3.3 Torque Rheometry Studies

Normally the melt mixing of LLDPE with fillers or additives is carried out in a screw extruder. Hence, the resistance offered to the rotation of the screw by the melt gives an indication of resistance to melt shear. Torque rheometry can be used to assess this resistance. Torque rheometry indicates the changes in torque while blending the mixture in melt extruder. This simulates real life process conditions found in small or large internal production mixers or extruders [140]. Torque rheometers designed to create turbulent flow and high shear action for providing an optimal mix of all heterogeneous components in polymer melt. The resistance of the test sample against being mixed is proportional to its viscosity and is measured as the reactionary torque on the rheometer rotors. This torque is recorded as a function of time in torque rheometry studies. This also thus records any cross linking effects or degradation of samples by the increased torque values with time. A torque rheometer consists of a temperature controlled mixing chamber along with two parallel rotors coming in close contact during some time of its rotation. The schematic of torque rheometer chamber is shown in Figure 3.18 [140]. These rotors rotate in counter clock wise direction at a specified speed ratio. The shape of the rotors (eg. roller blade, cam blade, banburry blade, etc.) are designed to provide optimal mixing both axially and radially at the specified speed ratio. The designed rotors along with the specified volume of chamber ensures minimum and maximum gap sizes between rotors and mixing chamber.
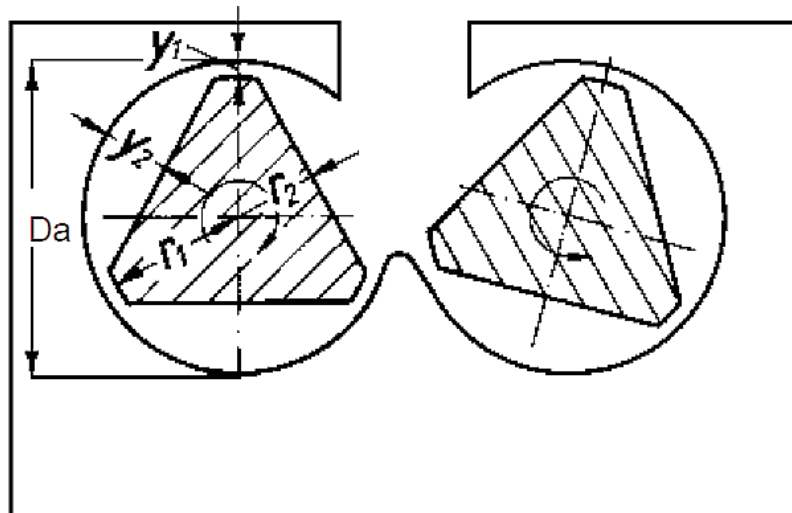
Figure 3.18: Torque rheometer schematic

The experiments were conducted at 60 rpm at temperatures of 210°C and 150°C for 40 minutes. The blends of LLDPE - FS powder were loaded to fill the rheometer roller chamber upto 70% by volume. A 5 kg weight was used for forcing

down the loading ram to close the mixing chamber. Figure 3.20 and Figure 3.19 shows torque values at 150°C (completion of melting) and 210°C (proper sintering of LLDPE in RM) respectively. For the sake of clarity, the torque values up to 200s and the average melt torque values (for a time interval of 200s - 2500s) are shown in the graphs. It can be seen that the melt torque increases with the addition of FS in LLDPE. At 4% FS composition, initial torque recorded 45-50 Nm at 150°C and 30-35 Nm at 210°C. In torque rheometry, the initial torque increase suggests the resistance offered to screw rotation due to loading of polymer blend inside the chamber. For this composition, a maximum of 10% increase in melt torque was observed when compared with natural LLDPE. After melting, the torque generally remained constant, indicating the thermal stability of the material (Ref. section B.1). The increased torque needs to be accounted for polymer compounding. Though it can be lowered by raising the temperature, it may not be suitable, as the polymer blends tend to degrade at higher temperature. During torque rheometry a rise in torque indicates cross linking of polymer or polymer degradation. The cross linking behavior is witnessed in PVC.

The degradation of polymer in the presence of additives can be observed as a spike in torque values.The degradation takes place at lower temperatures when FS content is high. It was found that the polymer blends with 4% and above FS, tends to degrade at 210°C under shear and prolonged exposure to heat as shown in Figure 3.21. Since FS has lower heat capacity (740 J/kg K) than LLDPE (2080 J/kg K), it tends to attain higher temperatures in the polymer matrix for the same heat input. The poor heat dissipation tends to melt the lower molecular weight polymer chains and the side chains of the long polymer chains in the vicinity of FS nano particles. The polymer chains in close contact with FS will thus tend to oxidize causing discoloration and degradation. Though the use of antioxidants may reduce this phenomena to some extent (which were not used in this study), it necessitates a close control over the process. Since RM is a zero shear process, the effect of FS in polymer degradation needs to be further investigated.The RM process requires polymer to be melted in the mold and held for sufficient time at required PIAT for optimum cure. PIAT of the mold is recognized as the process control tool for RM. For RM of LLDPE, PIAT of 210°C provides good sintering with very less amount of entrapped gasses [10]. In the RM process PIAT is maintained for a very small duration. Since the LLDPE - 4% blends degrades only at prolonged exposure at 210°C it is thermally stable during the RM process. Thus it ensures proper viscosity and high melt shear strength without degradation. The possible reduction in PIAT focusing on bubble removal and enhanced mechanical properties along with cycle time reduction needs to be further investigated.
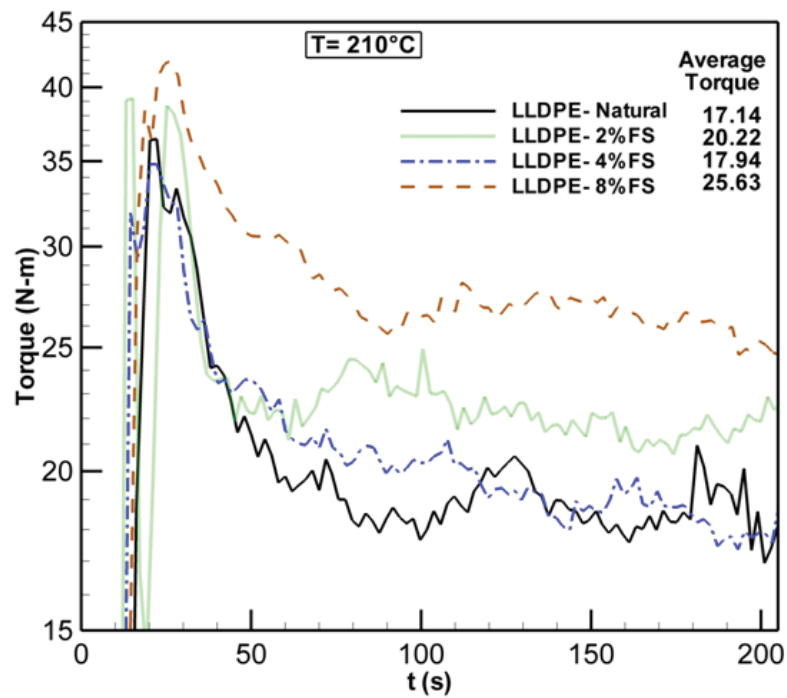
Figure 3.19: Variation of torque vs. time at 210°C for natural LLDPE and LLDPE - FS blends.(Y axis in log scale)
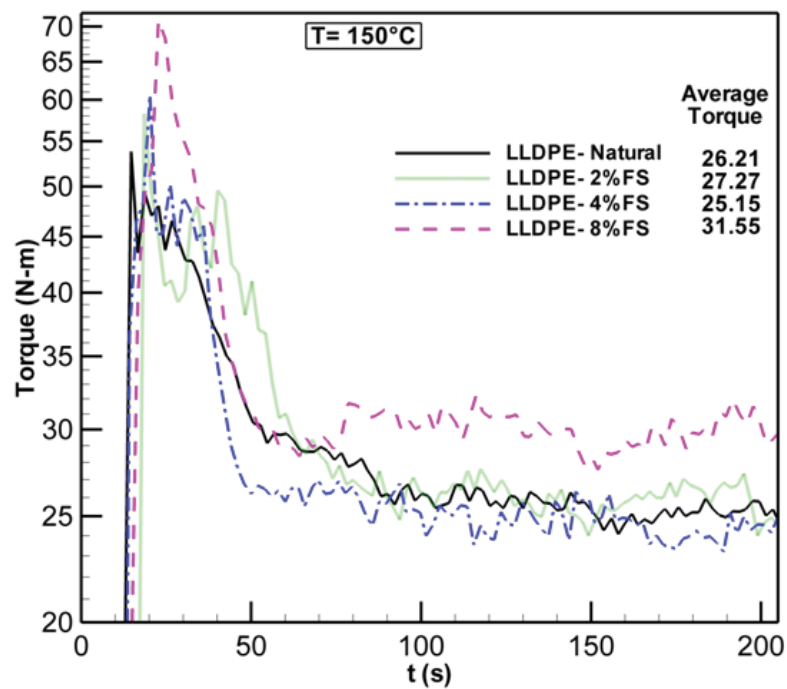
Figure 3.20: Variation of shear rate vs. temperature for natural LLDPE and LLDPE - FS blends. (Y axis in log scale)

52

Figure 3.21: Degraded LLDPE - 8% FS blend during torque rheometry at 210ºC

3.4   Conclusion

This chapter explores the possibility of using nano scale FS for rotationally moldable LLDPE. LLDPE - FS nanocomposites were prepared using dry as well as melt mixing methods. Rheological studies were performed on the LLDPE - FS blends and the important findings are as follows:

1. With the addition of fumed silica in LLDPE increase in dynamic viscosity of melt and higher melt shear resistance were observed. MFI was found to be decreasing with FS content, indicating restricted movements of polymer chains.

2. Parallel plate rheometry showed the zero shear viscosity for natural LLDPE, while LLDPE - FS blends showed an increasing trend of dynamic viscosity at very low shear rates. This is primarily attributed to the entanglement of polymer chains with nano silica and the weak hydrogen bonds formed with polymer chains as no increase in molecular weight is expected.

3. The viscosity calculated using MFI studies showed very close match with the measured viscosity using Anton Paar rheometer at low shear rates. Thus MFI studies can also be used to calculate the dynamic viscosity at a given temperature.

4. Torque rheometry studies indicated thermal stability of LLDPE - FS blends during melt processing and at PIAT during RM. It revealed the increased

torque requirements for blending. To some extent this can be reduced by increasing temperature. As thermal degradation of the material was noticed, with addition of FS, careful process control is necessary.

5. Finally, owing to the optimal MFI requirements, a maximum of 4% FS blend in LLDPE is suggested for RM. This blend was thermally stable and did not affect the processing window of LLDPE.

The viscoelastic and mechanical properties of LLDPE - FS blends after their solidification needs to be further investigated to study the suitability of FS as a nano scale reinforcement for rotationally moldabe LLDPE and are discussed in chapter 4.

Chapter 4

Viscoelastic Properties of LLDPE - FS Nanocomposites

4.1 Introduction

In Chapter 3 rheological studies of LLDPE - FS blends have been carried out. In this chapter, viscoelastic properties of LLDPE - FS blends are studied as the polymeric blends exhibit time dependent characteristics. Polymeric materials when subjected to a uni-axial force or a shear stress, behave differently from perfectly elastic material or a Newtonian fluid. A perfectly elastic material on application of uni-axial force, follow Hook's law which states the induced stress is directly proportional to the resultant strain. The proportionality constant is referred as elastic modulus of the material. A Newtonian fluid on application of shear stress, deform continuously at a strain rate proportional to the applied shear stress. The proportionality constant is referred as viscosity of the fluid. Polymeric materials exhibit mechanical properties which are in between these ideal cases and hence are termed viscoelastic. In a viscoelastic material the stress (σ) is a function of strain and time and is given in Equation 4.1

$$\sigma = f(\varepsilon, t) \tag{4.1}$$

This type of response is referred to as non-linear viscoelastic and is often reduced to the form

$$\sigma = \varepsilon.f(t) \tag{4.2}$$

This type of response is referred to as linear viscoelastic, and indicates that for a fixed value of elapsed time in uniaxial tensile test, the stress will be directly proportional to the strain.

The viscoelastic materials thus exhibit a time dependent strain response to constant stress (creep) and a time dependent stress response to a constant strain (relaxation). Also, when the applied stress is removed the viscoelastic materials recover slowly over a period of time. Even though these effects are observed in

metals at stresses close to yield stress and at high temperatures, polymers normally exhibit this behavior even at low stress and room temperature [141–143].

Mechanically, a harmonic spring is used to represent elastic property and a dash pot is used to represent the viscous property. Although there are no discrete molecular structures which behave like the individual elements of the models, they aid in understanding and analyzing the behavior of viscoelastic materials . Some of the more important mathematical models include Maxwell model and Kelvin or Voigt model [33, 144]. These models were used to represent the variation of stress and strain from mathematical models. The Maxwell model consists of a spring and dash pot in series. The Maxwell equation for linear viscoelasticity is given in Equation 4.3:

$$\frac{d\sigma}{dt} + \frac{\sigma}{t_r} = -\frac{\eta}{t_r}\frac{d\gamma}{dt} \quad \text{with} \quad t_r = \frac{\eta}{E} \tag{4.3}$$

Where t_r is the relaxation time of viscoelastic system, E and η being the modulus of the solid (represented as spring) and viscosity of material (represented as dash pot).

Solving the Equation 4.3 stress relaxation under a constant strain is given by Equation 4.4

$$\sigma(t) = \sigma_0 e^{-t/t_r} \tag{4.4}$$

This indicates that the stress decays exponentially with the time constant, ie relaxation time (t_r).

The Kelvin or Voigt model consists of a spring and dash pot in parallel. The Kelvin or Voigt equation for linear viscoelasticity is represented by Equation 4.5.

$$\frac{d\gamma}{dt} - \frac{\sigma}{\eta} = -\frac{\gamma}{t_r} \quad \text{with} \quad t_r = \frac{\eta}{E} \tag{4.5}$$

Where t_r is the retardation time.

Solving the Equation 4.5 strain recovery once the stress is removed is given by Equation 4.6:

$$\gamma(t) = \gamma_0 e^{-t/t_0}$$
$$\gamma_0 \approx \frac{\sigma_0}{E} \tag{4.6}$$

This represents an exponential recovery of strain which is a reversal of the predicted creep.

The Kelvin or Voigt model gives acceptable first approximation to creep and recovery behavior but does not account for relaxation. Maxwell model can account for relaxation but was poor in relation to creep and recovery. In contrast to the

theoretical models, dynamic mechanical analysis (DMA) is an experimental method used to measure the stress and strain by applying a sinusoidal wave to determine the elastic and loss modulus of viscoelastic material. A brief description of DMA is given below.

4.1.1 Dynamic Mechanical Analysis

DMA can be simply described as applying an oscillating force to a sample and analyzing the material's response to that force as shown in Figure 4.1 [138]. The DMA supplies an oscillatory force, causing a sinusoidal stress to be applied to the sample, which generates a sinusoidal strain [138]. By measuring both the amplitude of the deformation at the peak of the sine wave and the lag between the stress and strain sine waves, quantities like the modulus, the viscosity, and the damping can be calculated.
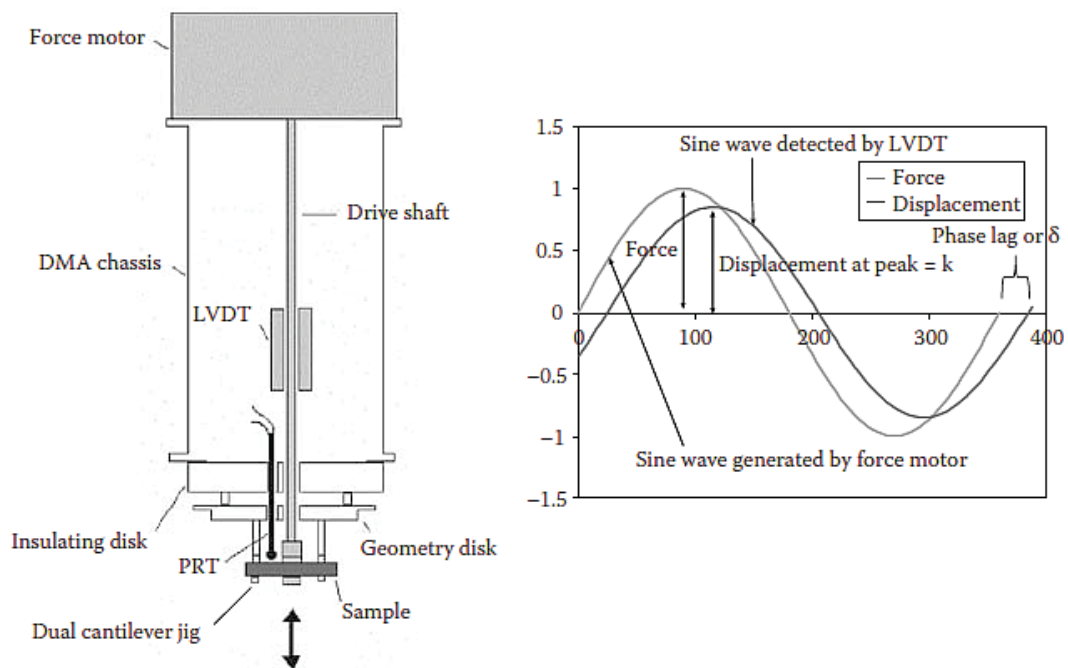
Figure 4.1: Schematic of dynamic mechanical analysis

When a sinusoidal stress is applied to a material it can be represented as given in Equation 4.7.

$$\sigma = \sigma_0 \sin \omega t \tag{4.7}$$

Where ω is the angular frequency and σ_0 the maximum amplitude of stress.

The resultant strain for viscoelastic material will lag behind the stress as shown in Figure 4.1. The strain is thus given by Equation 4.8.

$$\gamma = \gamma_0 \sin(\omega t - \delta) \tag{4.8}$$

Where δ is the phase lag.

These equations are usually represented as stress leading the strain as shown in Figure 4.1. Thus stress can be represented by Equation 4.9 and Equation 4.10.

$$\sigma = \sigma_0 \sin \omega t \cos \delta + \sigma_0 \cos \omega t \sin \delta \tag{4.9}$$

and strain

$$\gamma = \gamma_0 \sin \omega t \tag{4.10}$$

This leads to definition of two dynamic moduli, $E^{'}$ (Storage modulus) and $E^{''}$ (Loss modulus) and can be represented by Equation 4.11

$$
\begin{aligned}
E^{'} &= \frac{\sigma_0}{\gamma_0} \cos \delta \text{ (In phase with strain)} \\
E^{''} &= \frac{\sigma_0}{\gamma_0} \sin \delta \text{ (90}^{\text{o}} \text{ out of phase with strain)}
\end{aligned}
\tag{4.11}
$$

These could be represented on a phasor diagram as shown in Figure 4.2, and from this diagram complex modulus E^* can be defined by Equation 4.12.

$$E^* = \frac{\sigma}{\gamma} = \sqrt{\left(E^{'}\right)^2 + \left(E^{''}\right)^2} = E^{'} + iE^{''} \tag{4.12}$$

Thus storage modulus is known as the real modulus and loss modulus is known as imaginary modulus. Also, storage modulus, loss modulus and phase angle are related as given in Equation 4.13.

$$\tan \delta = \frac{E^{''}}{E^{'}} \tag{4.13}$$

In DMA, a complex modulus, an elastic modulus and loss modulus are calculated from the material response to the sine wave. These different moduli allow better characterization of the material because we can now examine the ability of the material to return energy ($E^{'}$), to lose energy ($E^{''}$), and the ratio of these effects (tan delta), which is called damping. At very low frequencies the polymer show viscous behavior and has very low modulus [145–147]. At high frequencies, the material behaves like a glassy solid with a high modulus as represented in Figure 4.3 [138]. Because of how the complex viscosity (η^*) is calculated in the DMA, we can get this value for a range of temperatures or frequencies in one scan.

$$E^* = E' + iE''$$
$$\text{Tan } \delta = E''/E'$$
$$\eta^* = E^*/\omega$$
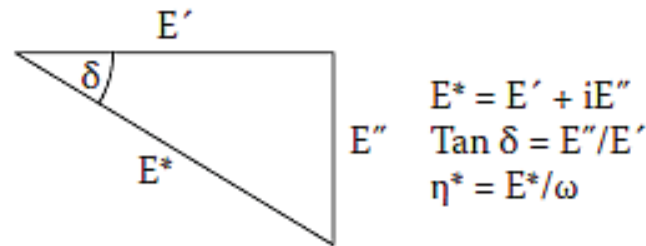
Figure 4.2: Phasor diagram showing complex modulus, storage modulus and loss modulus

The Cox – Merz equation relate the complex viscosity (η^*) to traditional steady shear viscosity (η) for very low shear rates, so that a comparison of the viscosity as measured by DMA and constant shear methods is possible.
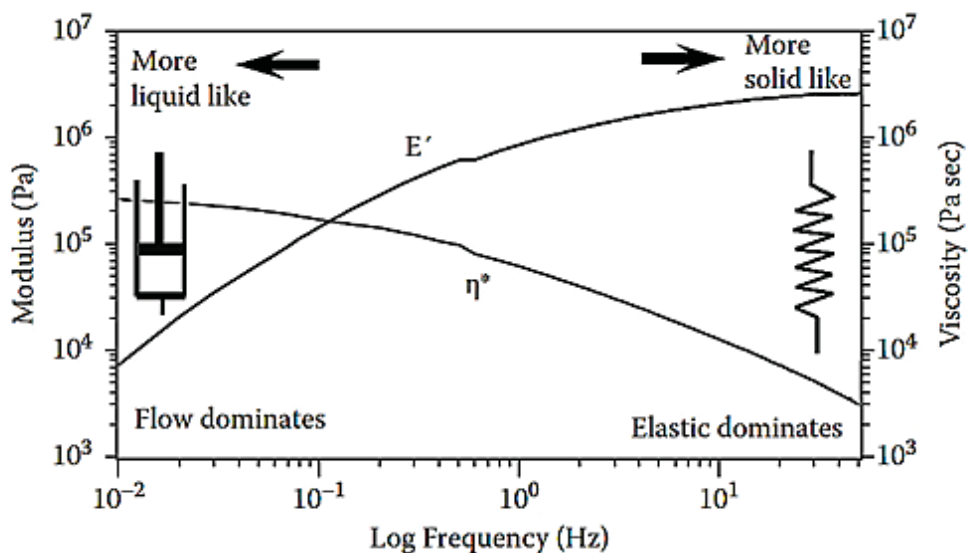
Figure 4.3: Behavior of viscoelastic material with varying frequency

     In this chapter the viscoelastic properties of LLDPE - FS blends are investigated. Based on the rheological studies conducted the blends of LLDPE - FS exhibited melt characteristics suitable for RM. The reinforcement effects of FS in LLDPE matrix at micro level was studied by examining the storage modulus, loss modulus, tan delta and the changes in glass transition temperature. The time dependent creep behavior is also studied to examine the reinforcement effects of FS in LLDPE.

4.2 Materials and Methods

The material used for this study was same as that used for rheological studies. The material used was rotationally moldable grade of LLDPE (R35A042) and FS (Aerosil-200) with important material properties as given in Table 3.1. The samples for DMA were made by compression molding to get a sheet thickness of 3 mm. Dry mixed powder blends were used in compression molding and was air cooled to 60°C before removing the sheets from mold.

4.2.1 DMA Studies

To find the viscoelastic properties viz. storage modulus (E$^{'}$), loss modulus (E$^{''}$) and tan delta, DMA analysis was performed in cantilever configuration using dynamic mechanical analyzer (Q800) supplied by TA Instruments (USA). The DMA Q800 uses a non-contact, direct drive motor to provide the oscillatory or static force required [148]. The motor is constructed of high performance composites that ensure low compliance and is thermostatically controlled to eliminate heat build-up even when using large oscillation amplitudes and high deformation force. The non-contact drive motor transmits force directly to a rectangular air bearing slide. The slide is guided by eight porous carbon air bearings grouped into two sets of four near the top and bottom of the slide. Pressurized air or nitrogen flows to the bearings forming a friction less surface that permits the slide to float. The slide, which connects to the drive shaft and sample clamp, can move vertically 25 mm and its rectangular shape eliminates any twisting of the sample. The schematic view of Q800 showing the details are shown in Figure 4.4b. A high-resolution linear optical encoder is used to measure displacement on the Q800 DMA. Based on diffraction patterns of light through gratings (one movable and one stationary), optical encoders provide exceptional resolution compared to typical LVDT technology. Due to the excellent 1 nm strain resolution, very small amplitudes can be measured precisely. This, combined with the non-contact drive motor and air bearing technology, provides excellent modulus precision and high tan δ sensitivity allowing the Q800 DMA to characterize a broad range of materials.

The specifications of DMA Q800 are given in Appendix A.7. DMA was carried out according to ASTM-D4065[149], ASTM- D4440 [150] and ASTM- D5279 [151].
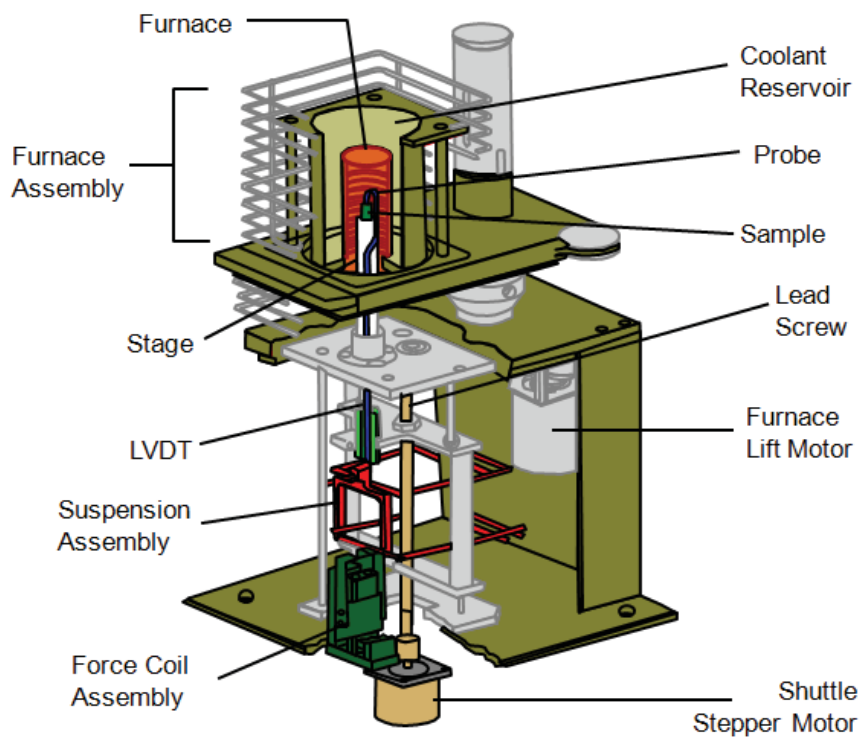
(a) Schematic view of DMA Q800
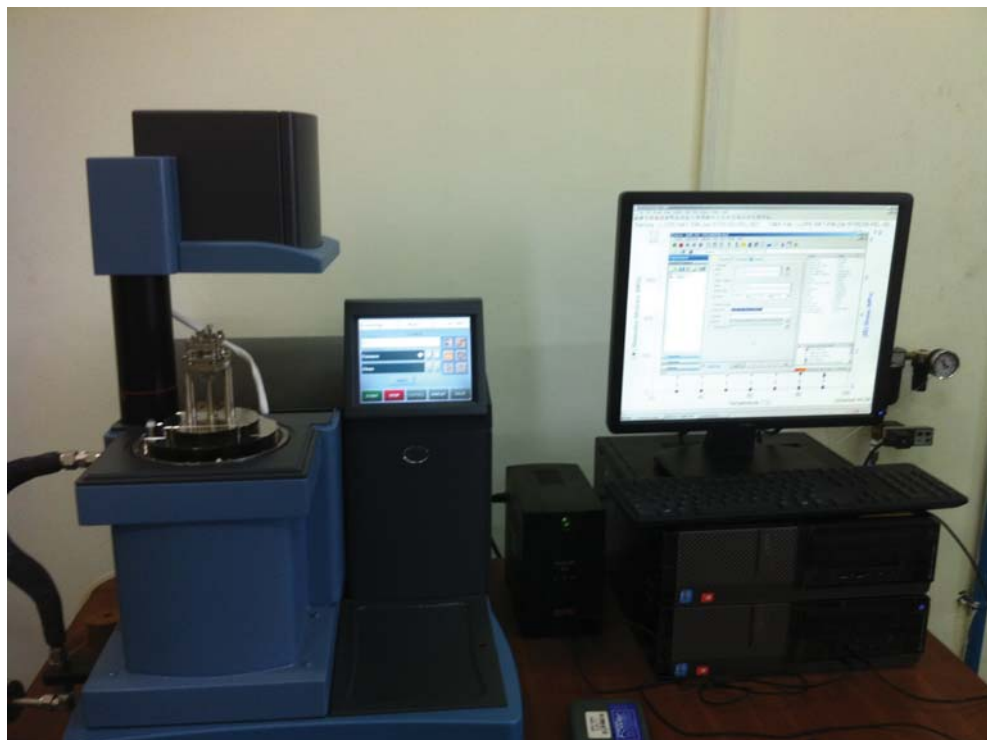
(b) Dynamic mechanical analyser Q800

Figure 4.4: DMA-Q800 and its schematic view

The strain sweep test was performed at a frequency of 1Hz. The temperature was ramped from -150ºC to 100ºC at the rate of 3°C/min at frequency of 1 Hz and amplitude of 20 μm. The frequency sweep test at room temperature (isothermal at 30ºC) ranged from 0.01 Hz to 200 Hz at a set amplitude of 20 μm. The frequency points were equally distributed in log scale with 15 points per decade. The sample size used for the studies was 35 mm long, 12.5 mm wide and 3 mm thick. The experimental set up is shown in Figure 4.4a. All measurements were performed under nitrogen atmosphere.

4.2.2 Viscoelastic Creep

For creep testing, the samples were compression molded and stored for seven months under room temperature (30ºC) before testing. The temperature was ramped from -150ºC to 100ºC at the rate of 3ºC/min at frequency of 1 Hz and amplitude of 20 μm. The stress sweep (0.01 MPa to 10 MPa) was done at a frequency of 1 Hz at room temperature (30ºC). For stepped isothermal creep tests, all the tests were started at 30ºC and temperatures were varied in 10ºC steps up to 100ºC. A soak time of 5 minutes, was given after every temperature step. A constant stress of 0.5 MPa was applied to the samples for 180 minutes at each temperature step (a dwell time of 10,000 s is recommended by ASTM-D6992) for recording the creep strains. The creep tests were done using Creep - TTS mode in single cantilever orientation.

4.3   Results and Discussions

4.3.1   Dynamic Mechanical Characteristics

The dynamic mechanical characteristics ($E^{'}$, $E^{''}$ and tanδ vs. temperature) of LLDPE - FS blends are shown in Figure 4.5. It shows that for a temperature range from -150ºC to 100ºC, there is an increase in storage modulus up to 4% concentration (Figure 4.5b). The storage modulus increased from 1143 MPa to 1408 MPa at 30ºC when the FS was increased from 1 to 4%. Thus a considerable improvement in reversible deformation of the material was seen with incorporation of FS. However, the storage modulus tends to decrease after 4wt% FS composition. The reduction of storage modulus at higher concentrations (FS% > 5%) may be attributed to unavoidable agglomeration leading to the formation of weak grain boundaries. The individual dynamic mechanical characteristics of natural LLDPE and LLDPE - FS blends are given in Appendix B.2.
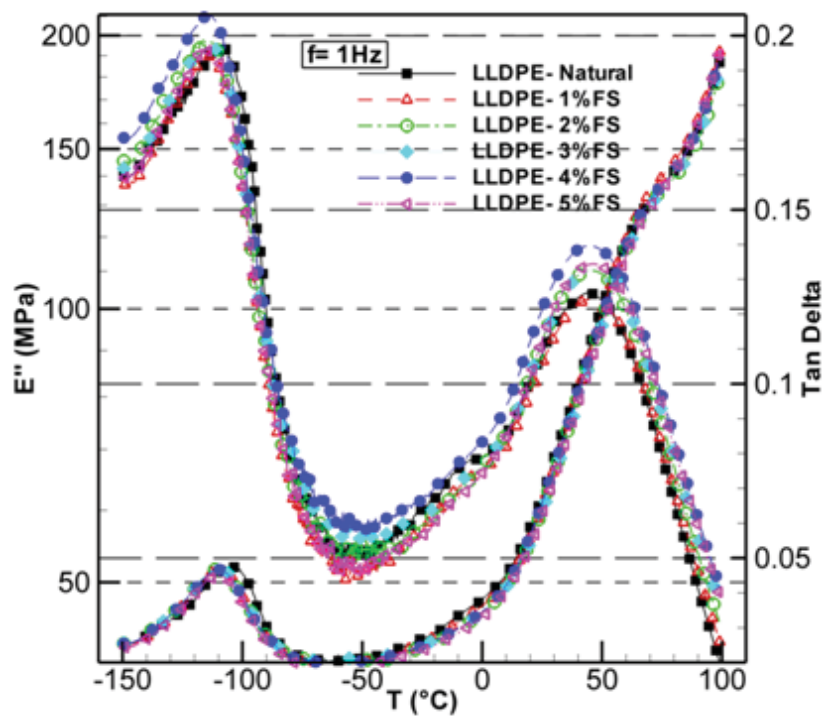
(a) Dynamic mechanical properties vs. temperature for LLDPE - FS nanocomposites; loss modulus (MPa) and tan delta; frequency = 1 Hz; temperature ramp rate =3°C/min.
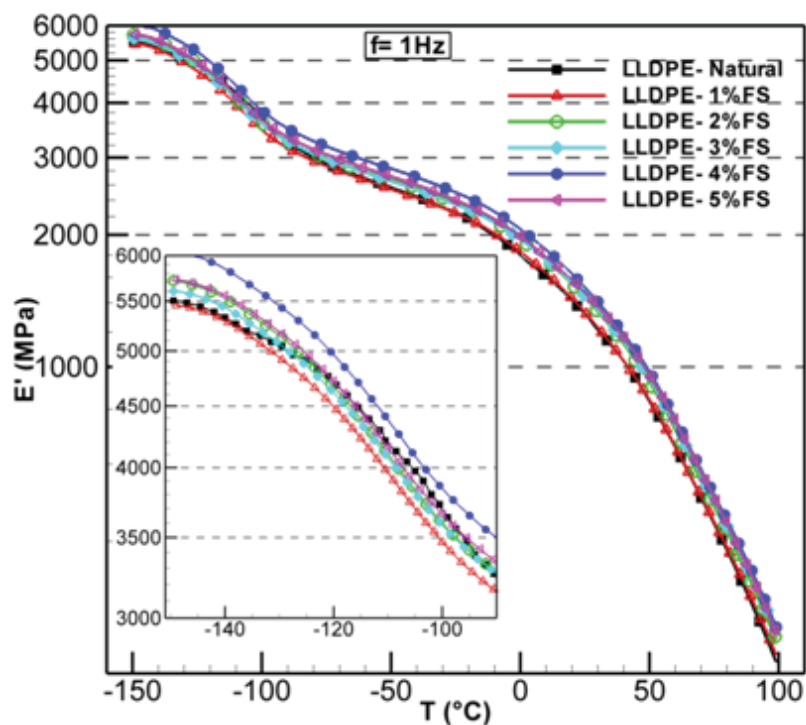
(b) Dynamic mechanical properties vs. temperature for LLDPE - FS nanocomposites; storage modulus (MPa); frequency = 1 Hz; temperature ramp rate =3°C/min.

Figure 4.5: Dynamic mechanical properties - LLDPE - FS blends

Table 4.1: Summary of DMA test results

Composition	Loss Modulus Peaks		Tan Delta Peaks	Storage Modulus Onset		At Room temp 30°C		Max Storage Modulus (Mpa)
	Temp (°C)	Value (MPa)	Temp (°C)	Temp (°C)	Value (MPa)	Storage modulus (MPa)	Loss Modulus (MPa)	
LLDPE - NATURAL	-107.59	196.2	-107.59	-121.38	4771	1143	95.91	5501
				-13.37	2051			
	43.85	102.8		33.85	1143			
LLDPE - 1% FS	-113.12	190.2	-110.88	-129.35	4912	1231	93.05	5454
				-18.24	2147			
	48.84	102		33.21	1166			
LLDPE - 2% FS	-115.39	202.8	-112.86	-129.88	5124	1287	107.6	5710
				-3.37	1966			
	45.23	107.6		36.82	1146			
LLDPE - 3% FS	-112.15	197.7	-109.02	-130.45	5084	1347	98.68	5605
				0.61	1941			
	43.2	110		37.06	1202			
LLDPE - 4% FS	-113.24	212.24	-110.23	-129.13	5415	1408	107	6053
				4.82	1960			
	44.05	7.3		40.24	1186			
LLDPE - 5% FS	-113.25	193.8	-110.54	-123.18	4883	1374	112.1	5734
				3.21	1920			
	46.03	112.1		40.9	1148			
LLDPE - 8% FS	-106.67	202	-105.76	-121.5	4848	1381	103	5615
				-0.72	2005			
	45.74	14.2		42.51	1135			

The details of dynamic mechanical properties along with T_g are summarized in Table 4.1. The T_g may be obtained as the temperature corresponding to the tan delta peaks , loss modulus peaks and change of slope in storage modulus graphs. There exists slight variation in reported T_g based on the method used. T_g is the reversible transition temperature, in amorphous materials or amorphous regions in semi crystalline materials, at which the material transitions from a relatively brittle or glassy state to soft or rubbery state [152, 153]. The glass transition is not a phase transition and therefore, it involves no latent heat. Below this temperature normally rubber like polymers lose flexibility and turn rigid, hard and dimensionally stable and are then considered to be in a glassy state. Above the T_g, all normally rigid, stiff, hard glassy polymers turn soft and flexible, become subject to cold flow or creep and as such turn into a rubbery state. The difference between the rubbery and glassy states lies not really in their geometrical structure, but in the state and degree of molecular motion. Below the T_g the polymer chain segments or groups, as parts of the chain molecular backbone, can undergo limited degrees of vibration. These polymer chain segments do not possess the energy required to rotate about bonds and change positions with respect to segments of the neighboring chains. At or slightly above T_g, rotation sets in, particularly of side groups or branch units, and it is conceivable that only short range molecular segments rather than the entire high polymer molecule would rotate at this point. The much higher coefficient of thermal expansion just beyond T_g is indicative of much greater degree of freedom of rotation [142, 152].

In this study, the T_g recorded as the temperature corresponding to tan delta peaks shifted from -107.59^{o}C to -112.86^{o}C for LLDPE - 2% FS blends. Also, there exists two distinct loss modulus peaks for the natural LLDPE and LLDPE - FS blends as shown in Figure 4.5a representing glass transition. The second peak in loss modulus curve correspond to αT_g, representing the onset of melting of low molecular weight polymer chains, shifted from 44°C (LLDPE natural) to 49°C (LLDPE - 1%FS) and to 46°C (LLDPE - 8% FS) as shown in Figure 4.5a. This implies a slight increase in operating thermal range for the nanocomposites. Below αT_g, reinforcement effects of FS in LLDPE can be seen by the progressive increase in storage and loss moduli. The first peak in loss modulus as well as the tan delta curves (Figure 4.5a) around -120°C, denotes γT_g representing the small scale movements in polymer chains usually associated with inter and intra molecular motions [154]. These transitions are related to either localized movement in the main chain or very large side chain movements [152]. For the LLDPE - FS composites tested, no significant change was observed in γT_g.
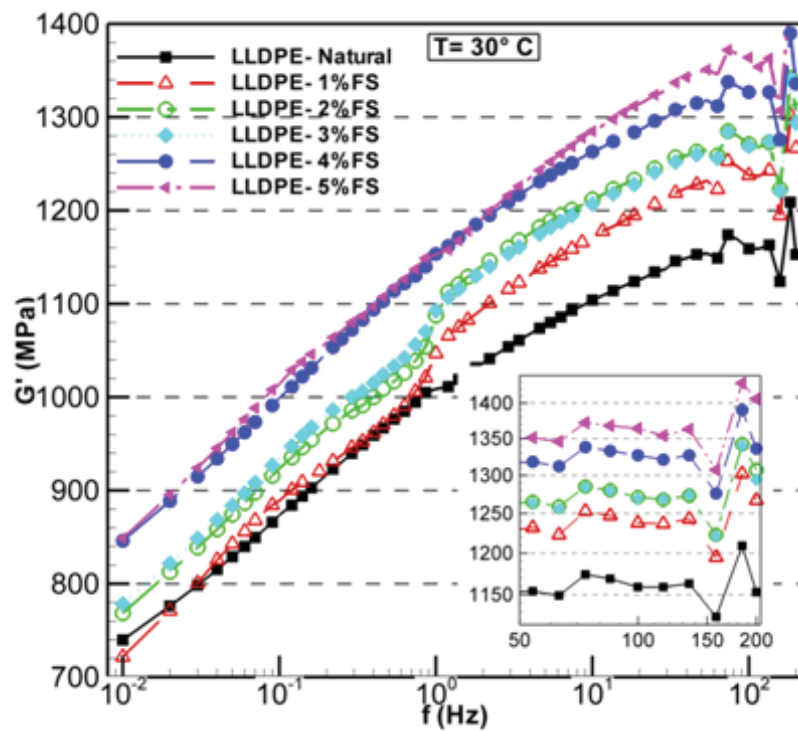
(a) Dynamic mechanical properties vs. frequency (Hz) for LLDPE/FS nanocomposites; shear storage modulus (MPa; temperature = 30°C.
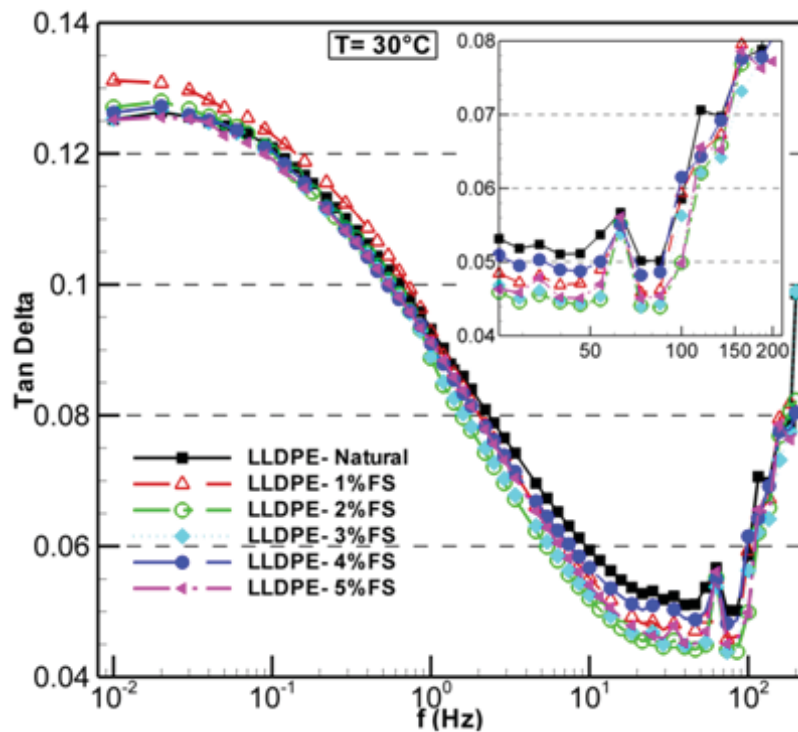
(b) Dynamic mechanical properties vs. frequency (Hz) for LLDPE/FS nanocomposites; Tan δ; temperature = 30°C

Figure 4.6: Dynamic mechanical properties vs. frequency for LLDPE - FS blends

As the rotationally molded products are used in outdoor structural as well as automobile applications, their response to cyclic loading is important. For this purpose, DMA studies were further extended in frequency range from 0.01 Hz to 200 Hz at isothermal conditions (30ºC). At low frequency range, viscous behavior of the material was seen. The shear storage modulus ($G^{'}$) and tan delta values for different frequencies are shown in Figure 4.6. As the frequency increased, the material became stiffer with increased modulus. At any given frequency, it can be seen that the modulus is higher up to 4% of FS. For all compositions, tan delta peaks were observed at 63Hz as shown in the magnified window of Figure 4.6b. This frequency (63Hz) can be regarded as the glass transition frequency for these nanocomposites. At this frequency, $G^{'}$ increased from 1074 MPa for natural LLDPE to 1346 MPa for 4% FS concentration. For practical purpose this frequency (63 Hz) can be regarded as limiting frequency of the material probably due to the breakdown of polymer chains and silica network [155–157]. At higher frequencies, the stress relaxation during each loading cycle is lower. This in turn results into the higher stress which is transferred from LLDPE matrix to the filler. Hence, the energy required to deform LLDPE - FS nanocomposite is much higher and superior to the energy required to break inter particle interactions.

4.3.2   Analysis of Viscoelastic Creep

Since the LLDPE - FS nanocomposite is viscoelastic, the mechanical behavior of polymers strongly depends on time and temperature. The estimation of the long-term deformation under static load often requires conventional creep experiments over a longer period (5 to 10 years) at specific temperatures. TTSP allows generating the master curves at any reference temperature based on short-term creep experiments at various temperatures. The TTSP states that the time response of a material at different temperature can be shifted in the time scale by a shift factor a_T if the underlying molecular motions for the time response at different temperature share the same mechanism and change in temperature only affects the corresponding response speed . The corresponding shift factor a_T was described by Williams, Landel and Ferry (WLF) and is given in Equation 4.14 [136, 137]:

$$\gamma_0(T_0, t) = \gamma\left(T, \frac{t}{a_T}\right) \tag{4.14}$$

Where γ_0 is the strain at reference temperature, (T_0) the reference temperature, (t) the time, and (γ) the strain at the elevated temperature (T). They also defined the WLF equation (Equation 4.15, which enables an empirical description of the shift

factor (a_T) for amorphous polymers above the T_g:

$$\log(a_T) = \frac{-C_1(T - T_0)}{C_2 + (T - T_0)} \tag{4.15}$$

Where C_1 and C_2 are empirical constants.

For many polymers it has been found that C_1 and C_2 are constants and T_0 is taken as T_g. The above relationship holds only in the approximate temperature range above the glass transition temperature [T_g, T_g + 100ºC]. Thus the WLF equation is not valid for semi crystalline polymers below their glass transition temperatures. The shift factors, below T_g, can be defined using an Arrhenius equation (Equation 4.16 [158].

$$\log(a_T) = \frac{\Delta H}{R}\left(\frac{1}{T} - \frac{1}{T_0}\right) \tag{4.16}$$

Where ΔH is the activation energy and R the universal gas constant.
Thus, the independent short term creep tests performed at various temperatures can be shifted horizontally on log time scale axis as shown in Figure 4.7 to generate the creep master curve at any reference temperature.

Stepped isothermal method (SIM) is a further development of TTSP, which was originally introduced for product testing of geosynthetics [68, 72, 73, 159, 160]. Due to the good agreement with conventional long-term creep tests, SIM has become a well-established method for the accelerated product testing of geosynthetics. Standards have been published for both tensile creep (ASTM-D6992)[161] and compressive creep (ASTM-D7361)[162]. The creep analysis was carried out in the elastic region, by identifying the limiting stress using stress sweep as shown in Figure 4.8 It was observed that, for stresses below 0.5MPa, the natural LLDPE shows elastic deformation. Beyond 0.5 MPa, the storage modulus showed decline and loss modulus showed increase, signifying the onset of plastic deformation. Thus in creep analysis, the stress was maintained at 0.5 MPa for all the nanocomposites during experiments.

The creep strain and temperature steps of SIM creep test for various LLDPE - FS blends are shown in Figure 4.9 a-f. From the Figure 4.9 a-f, it can be observed that the creep strains decrease with increased FS content. For example, after 1500 min, the creep strain of 1.2% for natural LLDPE Figure 4.9 a was reduced to 0.8% (20% reduction) for LLDPE - 4 wt% FS nanocomposite (Figure 4.9 e). A similar trend was seen for other compositions.
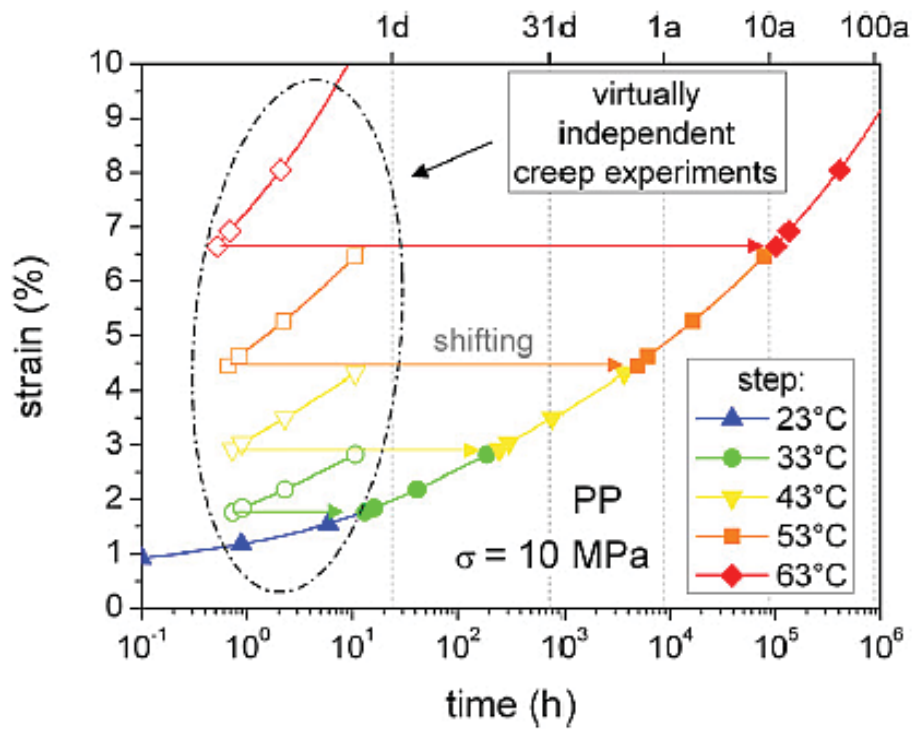
Figure 4.7: Time temperature superposition
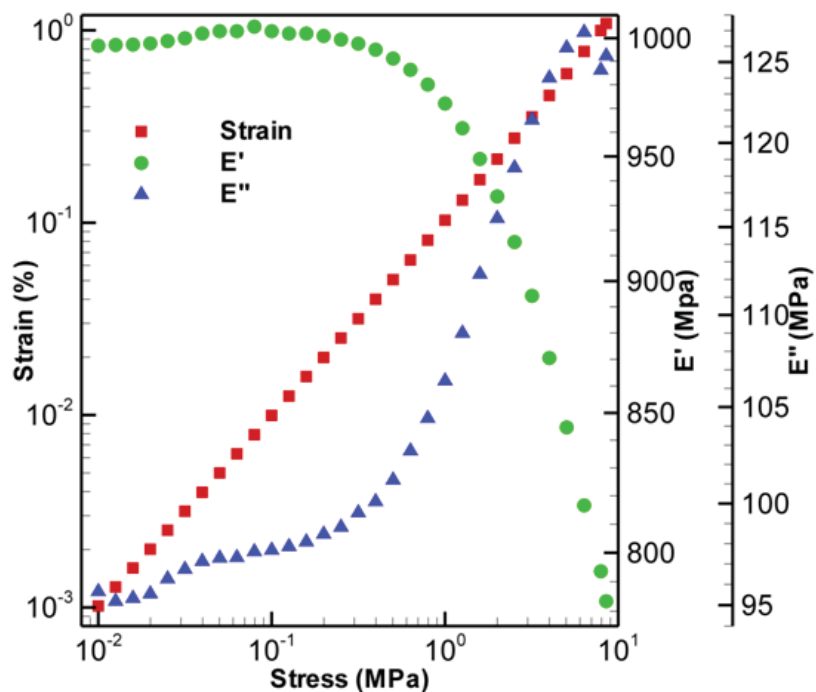
Figure 4.8: Stress sweep: stress (MPa) vs. strain (%), storage modulus (MPa), loss modulus (MPa) for LLDPE/FS nanocomposites; frequency=1Hz.
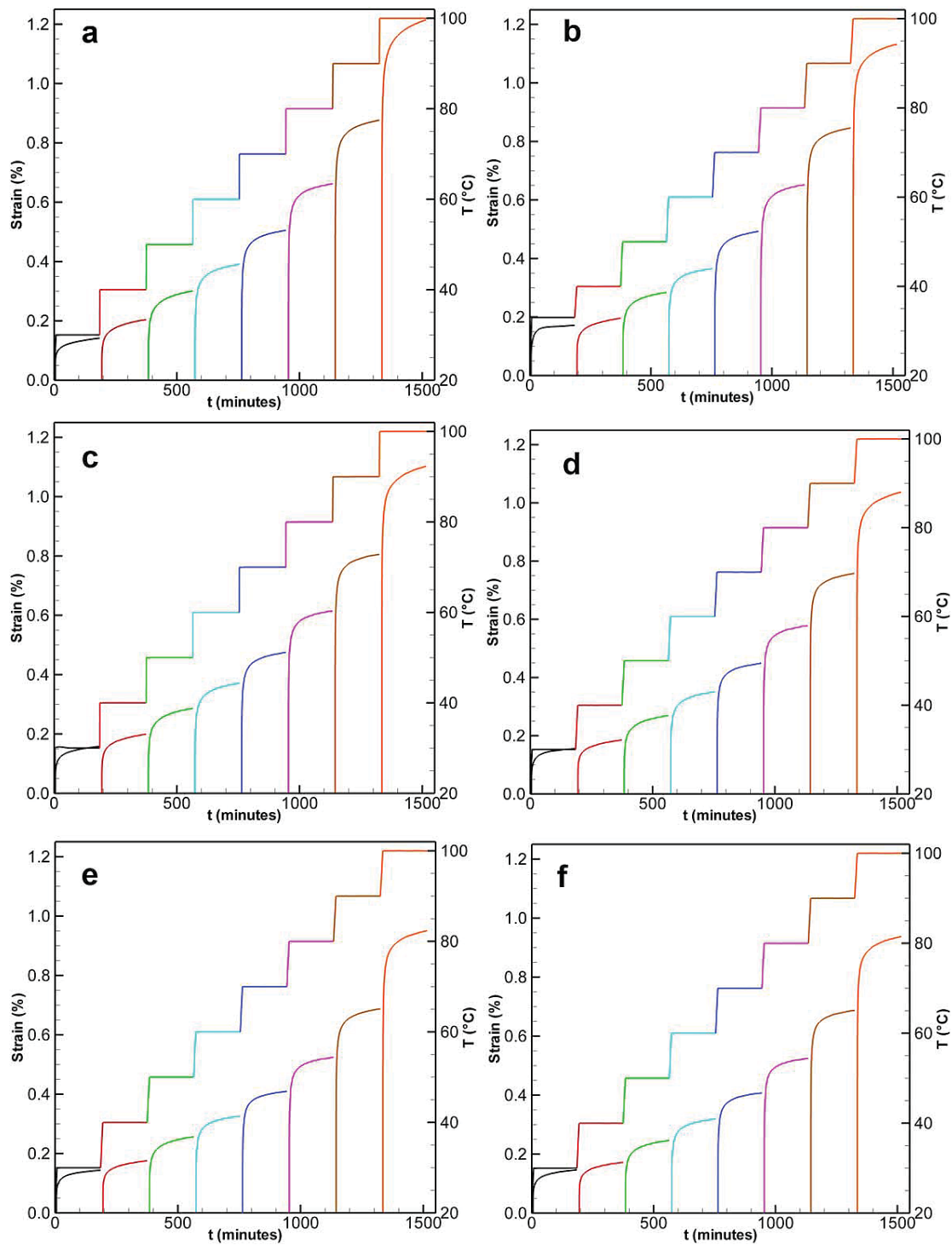
Figure 4.9: Creep SIM data (creep strain vs. time) and temperature
steps for LLDPE/FS nanocomposites: stress = 0.5 MPa
(a) Natural LLDPE; (b) LLDPE - 1% FS; (c) LLDPE - 2% FS; (d) LLDPE
- 3% FS; (e) LLDPE - 4% FS; (f) LLDPE - 5% FS;

70
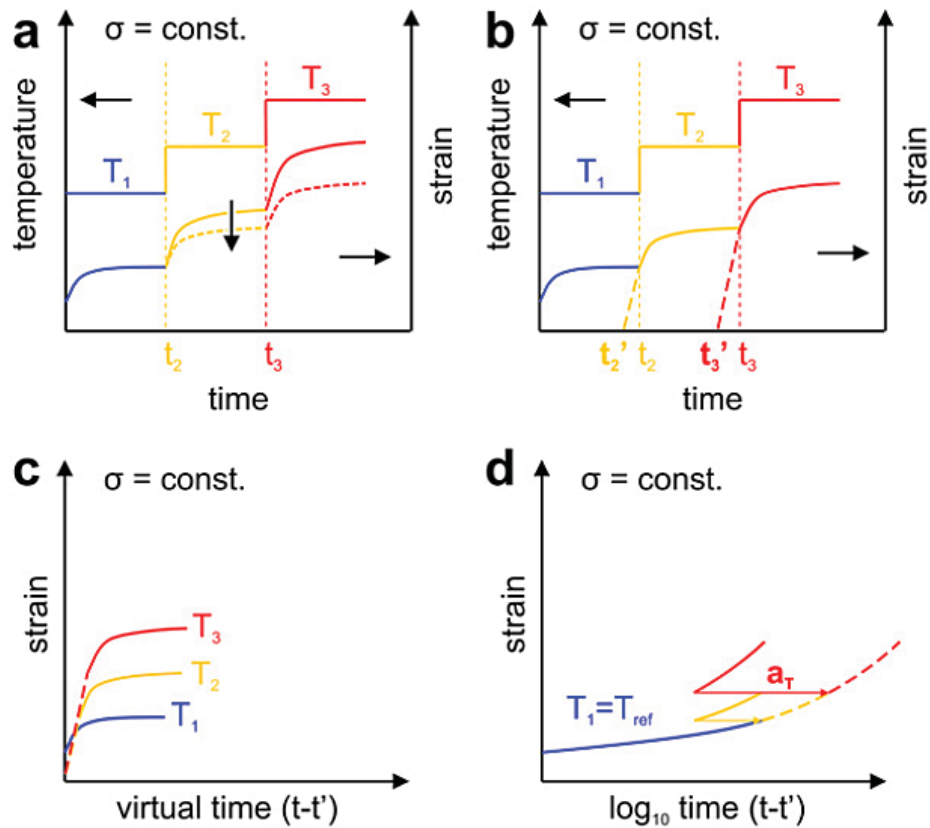
Figure 4.10: Principle of the SIM procedure: (a) correction of measured data due to thermal expansion, (b) determining virtual start time t_0 (c) rescaling d) curve shifting according to TTSP.

The SIM data were adjusted for thermal expansions and previous history of specimen by the change in temperature. The vertical shifting, rescaling and horizontal shifting were carried out to generate the creep master curves [68, 73]. Figure 4.10 describes schematically these adjustments. First of all the temperature is ramped during the creep experiment. This means that the measured deformation does not exclusively account for the creep behavior. Thus, a vertical shift is required to remove the deformation caused by thermal expansion while heating the sample (Figure 4.10a).

According to the Boltzmann superposition principle [163] the creep curves at different temperature steps can be treated as individual tests starting at the virtual start time t_0. When the temperature step T_2 starts at time t_2, some creep has already taken place at the previous temperature T_1. Therefore, a creep experiment corresponding to the behavior measured between t_2 and t_3 would have started at a time $t_2' < t_2$ (Figure 4.10 b). This virtual start time t_0 is empirically determined. The procedure is based on the uniqueness of SIM, using a single

sample; the physical state at the junction between two temperature steps is unique. Assuming that both steps correspond to independent experiments, the creep rate at the end of a temperature step should be identical to the creep rate at the beginning of the next step. Since the heating does not take place instantaneously, there is a small transition region with undefined creep behavior at the beginning of each temperature step. As a result, the data from this transition region should be excluded from the analysis but the time scale is kept in place. However, if the heating is quick enough, the assumption of identical creep rates can still be used. Beginning with an arbitrary value, the starting time t_0 is, therefore, iteratively varied until the slope at the beginning of a temperature step matches the slope at the end of the previous step in the logarithmical time scale $(t - t_0)$, as shown in Figure 4.10 c. This procedure is repeated iteratively for all temperature steps until the SIM data re-scaled in the virtual time scale $(t - t_0)$ is equivalent to a set of independent isothermal creep curves. The rescaling of each temperature step is handled iteratively and the results are all plotted on the virtual time scale $(t - t_0)$ (Figure 4.10 c). The SIM data now correspond to a family of virtually independent creep tests, which can be shifted to a master curve the same way as in conventional TTSP (Figure 4.10 d).

For generating the creep master curves, reference temperatures of 40°C and 50°C were considered and are given in Figure 4.11 and Figure 4.12 respectively. The above temperatures were selected for our study, because the ambient temperature of use for the rotationally molded products exceeds 40°C during summer in Asian countries. The creep master curves were generated using rheology advantage software from TA instruments. As seen from the graphs, the creep strains tend to decrease with the addition of FS. After an estimated loading of sample for one year (5.26×10^5 minutes) at 50°C nanocomposites with 4 wt% FS, exhibited 12% reduction in creep strains compared with natural LLDPE. Further, the creep strains were reduced by as much as 14.5% for 4 wt% FS at 5.26×10^7 minutes (around 100 years). The blends did not show significant variation in percentage of reduction in strains with temperature. It was observed that, blends with 4 wt% FS showed 11% creep strain reduction at 40°C for an estimated loading of 1 year. The increased creep resistance can be attributed to the reinforcement of polymer matrix with FS. Thus, it can be said that addition of FS not only improves the static mechanical properties but also results in significant improvement in their creep behavior.
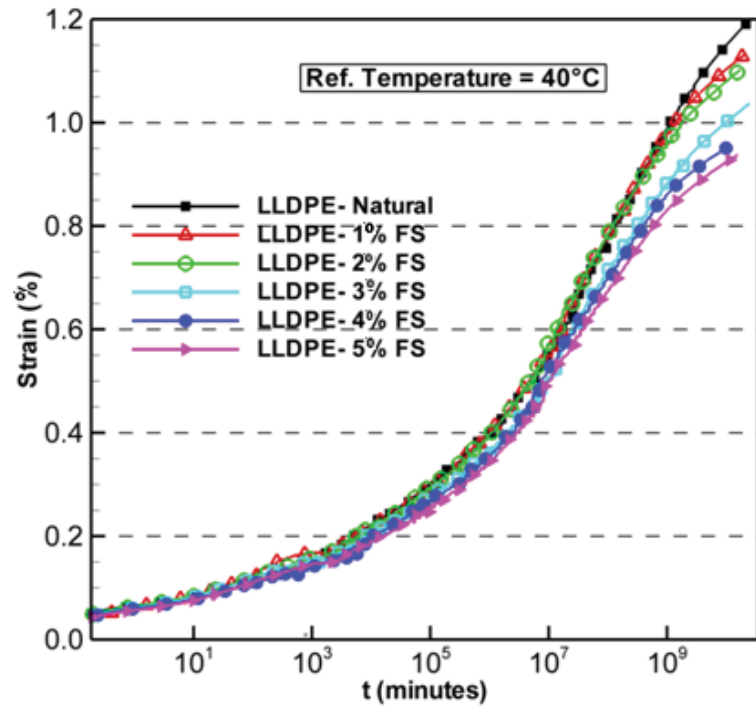
Figure 4.11: Creep master curves for LLDPE - FS nanocomposites at 40ºC
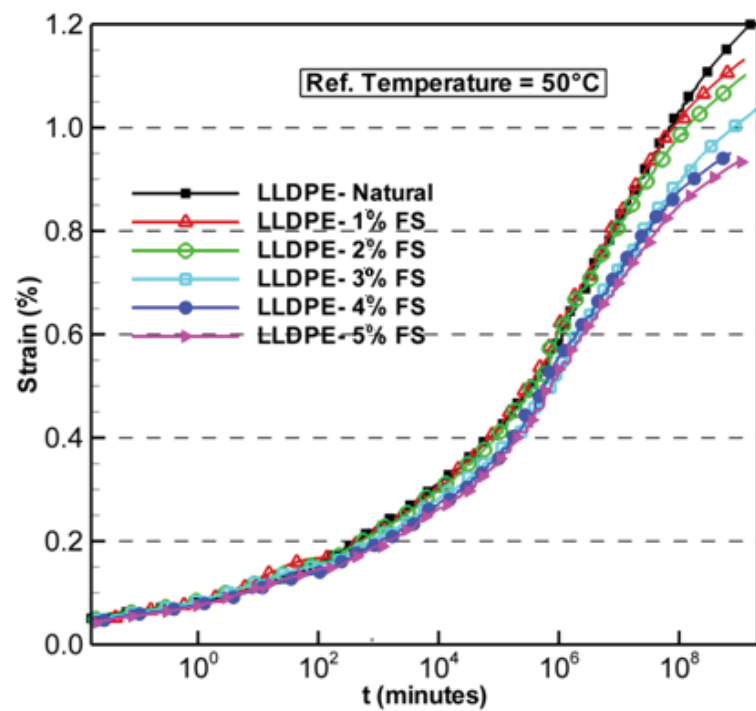
Figure 4.12: Creep master curves for LLDPE - FS nanocomposites at 50ºC

4.4 Conclusion

This chapter explored the possibility of using nano scale FS for rotationally moldable grade of LLDPE. DMA was performed to evaluate the temperature-time dependent material behavior. There was a considerable improvement in storage modulus and loss modulus with the addition of FS till 4% concentration. Creep analysis showed the reduction of creep strains with increased FS content at all temperatures above T_g. Thus FS can be used as a potential nano scale additive for LLDPE. FS contents above 4 wt% are detrimental to the mechanical properties due to agglomeration. This necessitates a careful control over the dispersion of the nanocomposites within the polymer matrix. The dispersion of FS in LLDPE matrix and its effects on mechanical properties needs further investigation.

Chapter 5

Mechanical Properties of LLDPE - FS Nanocomposites

5.1   Introduction

In the previous chapters, the rheological and visco-elastic properties of LLDPE - FS nanocomposites were discussed. Since the rotationally molded products are extensively used for many industrial and domestic outdoor applications, they must possess good mechanical properties. Particulate reinforcements help to enhance the mechanical properties in rotationally moldable polymers. Generally, micro scale additives like fillers, antioxidants, colorants, UV stabilizers, etc. are blended to natural LLDPE to impart the desired properties. These micro scale additives may not reinforce the polymer chains due to its size and may adversely effect the mechanical properties. In this chapter, the mechanical properties of nano scaled fumed silica reinforced LLDPE composites are investigated.

5.2   Materials and Methods

The material used for study of mechanical properties was the same as used in rheological and visco-elastic studies. The material used was rotationally moldable grade of LLDPE (R35A042) hydrophilic FS with the material properties as given in Table 3.1. The melt compounded LLDPE - FS blends were compression molded to obtain the required samples for mechanical testing . From the rheological studies carried out in chapter 3, it can be seen that there is a reduction in MFI of LLDPE with addition of FS. To ensure proper flow of molten polymer in the mold, the samples required for mechanical testing were prepared using compression molding process. The standards like ASTM-D4976 and ASTM-D1928 also specify the sample preparation using pressure processes like injection or compression molding. However, in this study the mechanical performance of purely RM products has been also conducted at industrial scale for comparison and details are given in chapter 7. For compression molding, blends were initially melted at 200ºC before

(a) UTM   (b) Experimental set up- tensile testing

Figure 5.1: Universal testing machine and experimental setup for tensile testing

compressing at 1500 psi for 5 minutes. The compression molded sheets were then air cooled to 60°C before demolding. The samples for tensile testing, flexural testing, impact strength were prepared from these sheets.

5.2.1 Tensile Testing

Tensile testing was conducted as per ASTM-D638[164], to determine the tensile strength, tensile modulus and tensile toughness. The tensile specimen samples were prepared using a die (type 2, ASTM-D638). Five samples were prepared for different FS compositions (1- 8 wt%). The samples were tested at room temperature (30°C) at a cross head speed of 5 mm/min till rupture using a 10 kN load cell in a standard universal testing machine (UTM). Specifications of UTM are given in Appendix A.8. The experimental set up is shown in Figure 5.1.

5.2.2 Flexural Testing

The flexural tests were done in three point bending configuration to determine and compare the flexural modulus at different strain rates according

Figure 5.2: Experimental set up - flexural testing

to ISO 178 [165]. The test specimens were 3mm thick and a nominal span of 50 mm was used for testing at room temperature (30°C). Five samples were prepared for various FS compositions ($1 - 8$ wt%). The flexural tests were conducted in a standard universal tensile testing machine at cross head speeds of 1, 5 and 50 mm/min. The experimental set up of flexural test is shown in Figure 5.2. In flexural testing, the test specimen is supported in three point bending configuration and is deflected at a selected rate (cross head speed) at mid span until the specimen fractures or until the deformation reaches maximum specified deflection. During the procedure the force applied to the specimen is measured. Flexural stress is then defined as the nominal stress of the outer surface of the test specimen at mid span and is given by Equation 5.1 [165].

$$\sigma_{f} = \frac{3FL}{2bh^{2}} \tag{5.1}$$

Where F is the applied force, L is the span, b is the width and h is the thickness of test specimen.

Flexural strain is the fractional change in length of an element of the outer surface of the test specimen at mid span and is usually expressed as dimensional ratio or percentage and is given by Equation 5.2.

$$\varepsilon_{f} = \frac{6dh}{L^{2}} \tag{5.2}$$

Figure 5.3: Izod/Charpy - impact tester

Where d is the deflection at mid span.

The flexural modulus is then defined as the ratio of difference in flexural stress at 0.05% and 0.25% flexural strain to the corresponding difference in flexural strain.

5.2.3 Impact Testing

The izod impact tests were done on a standard izod-charpy impact tester as per ASTM D256 [166] at room temperature (30°C) to determine the impact strength. The samples (5 nos) confirming to the above standard were prepared using a die and notch cutter. The prepared notches were inspected to ensure compliance with ASTM D256 (V notch, 45° included angle, 2.54 mm maximum depth). The test set up is shown in Figure 5.3

5.2.4 Scanning Electron Microscopy

To correlate the tensile behavior of material with the dispersion of nanocomposites, particle size distribution, scanning electron microscopy (SEM) was performed. The morphological studies for studying the FS particle size, dispersion, and its effect on tensile fracture of LLDPE - FS samples were performed by scanning electron microscopy (SEM; EVO 18, Zeiss, Germany) as shown in

Figure 5.4: Scanning electron microscope (Courtesy - Goa University)

Figure 5.4. The specifications of the scanning electron microscope are given in Appendix A.9. The samples were pre-coated with 80% gold and 20% palladium in a vacuum chamber. This is done to prevent the accumulation of static electric fields at the specimen due to the electron irradiation during imaging and to improve contrast. The SEM can produce high resolution images of the sample surface.

In SEM, electrons are thermoionically emitted from a tungsten or lanthanum hexa boride cathode and are accelerated towards an anode; alternatively electrons can be emitted via field emission. The electron beam, which has an energy ranging from a few hundred eV to 100 keV, is focused by one or two condenser lenses in to a beam. Characteristic X - rays are emitted when the primary beam causes the ejection of inner shell electrons from the sample and are used to determine the elemental composition of the sample. The back scattered electrons emitted from the sample can be used alone to form an image or in composition with the characteristic X - rays. These signals are monitored by photo multiplier tubes and magnified. An image of the investigated microscopic region of the specimen is observed in cathode ray tube and is photographed.

5.2.5   X Ray Diffraction Analysis

To study the crystallinity of natural LLDPE and LLDPE - FS blends X-ray diffraction (XRD) analysis was performed. Room temperature (30°C) XRD spectra of the LLDPE - FS nanocomposites were recorded with a wide angle X-ray diffractometer (Mini Flex II, Rigaku, Japan)with Cu Kα radiation (λ=0.15405 nm). The specifications of X-Ray diffractometer is given Appendix A.10. XRD is used to determine the size and shape of the unit cell or degree of crystallinity for any compound using the diffraction of X-rays. X-ray diffraction studies are used for the finger print characterization of crystalline materials and their structure determination. Each crystalline/semi crystalline solid has its unique characteristics.

5.3   Results and Discussions

The yield strength, maximum tensile strength, elastic modulus and toughness for different LLDPE - FS composition are given in Table 5.1. Significant improvements in mechanical properties were observed in LLDPE with the addition of FS. With respect to macroscopic behavior during the tensile tests, all samples showed large plastic deformation along with a typical neck formation; a common characteristics for thermoplastic materials. From Table 5.1, it can be observed that, there is a progressive increase in tensile modulus from 818.2 MPa (for natural LLDPE) to 1180.46 MPa (4% FS). An increase in the yield strength and maximum tensile strength for the nanocomposites with respect to neat LLDPE can also be seen. An increment of almost 9% is observed in the tensile Strength for LLDPE - FS-3% composition. For the extreme compositions like 8 wt% of FS, though the maximum tensile strength and modulus have improved yield strength reduced. Since, nano particles and polymer chains have comparable size, the nano particles can act as temporary crosslinks between the polymer chains, providing localized regions of enhanced strength, which in turn can retard the growth of cracks or cavities [18].

The engineering stress – strain curves of LLDPE - FS nanocomposites are shown in Figure 5.5. From Figure 5.5, it can be seen that the elongation at break significantly increases with augmentation of FS content, thereby increasing the tensile toughness. This can be verified from the fact that, for blends with 2 wt% of FS, more than 300% elongation was observed while for blends with 4 wt% of FS, an elongation of 225% was recorded. However, the trend is subjected to major decrease after 4 wt% of FS composition. The mobility of polymer chains is not

Table 5.1: Tensile testing : LLDPE - FS nanocomposites

Sample Type	Yield strength (MPa)	Max. Tensile strength (MPa)	Tensile Modulus (MPa)	Tensile Toughness mJ/mm^3
LLDPE - Natural	16.04	17.75	818.2	10.72
LLDPE - 1% FS	16.67	18.65	1009.97	38.39
LLDPE - 2% FS	15.34	17.86	1115.09	42.99
LLDPE - 3% FS	16.18	19.36	1147.17	2.48
LLDPE - 4% FS	16.3	18.81	1180.46	29.24
LLDPE - 5% FS	13.51	18.27	956.91	19.21
LLDPE - 8% FS	14.99	19.63	1081.98	1.86

hindered at low concentration of FS and it provide reinforcement to the LLDPE matrix. At higher concentrations (above 5%) of FS in LLDPE, plastic deformation was hindered leading to a brittle fracture. Form Figure 5.5 it can also be observed that, there is an increased ability for dissipation of energy at low FS concentration. Tensile toughness increased by 325% for blends with 3 wt% FS, and no fracture initiation has taken place up to 300% strain (Table 5.1). The tensile toughness was calculated as the area under the stress – strain curve. The increase in tensile toughness can be attributed to the bonding between polymer chains and FS, by forming a network structure [155]. This network structure is formed by hydrogen bonding between LLDPE chains and silica groups.

Table 5.2: Flexural testing: LLDPE - FS nanocomposites

Sample Type	Flexural Modulus at 1 mm/min (MPa)	Flexural Modulus at 5 mm/min (MPa)	Flexural Modulus at 50 mm/min (MPa)
LLDPE - Natural	252.02	271.74	534.71
LLDPE - 1% FS	257.18	278.57	467.05
LLDPE - 2% FS	259.7	300.42	559.16
LLDPE - 3% FS	278.94	300.52	559.29
LLDPE - 4% FS	266.58	296.57	441.34
LLDPE - 5% FS	276.27	327.51	624.18
LLDPE - 8% FS	293.3	303.33	427.36

The flexural modulus was calculated (ISO 178) as the ratio of difference in flexural stress and strains at 0.05% and 0.25%. The averaged values of flexural modulus of the five samples tested at various speeds are given in Table 5.2. The load deflection curves obtained from flexural test are given in Appendix B.3.
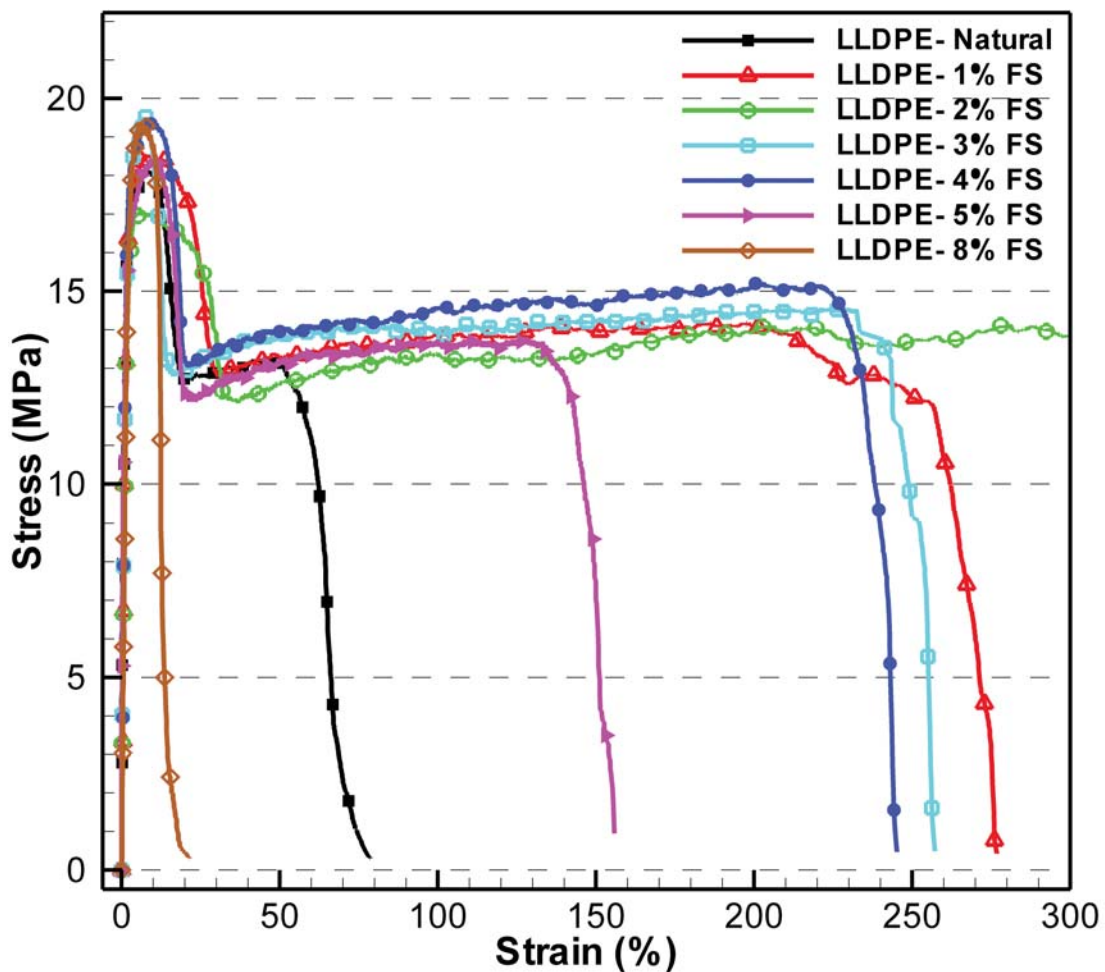
Figure 5.5: Engineering stress vs. strain for LLDPE/FS
nanocomposites:

As seen from the results, the flexural modulus showed progressive increase
with addition of FS till 5 wt% for all cross-head speeds. The flexural modulus
recorded a maximum of 624.18 MPa for 5 wt% FS at a strain rate of 50 mm/min
in comparison to natural polymer at 534.71 MPa. It is noteworthy that the
phenomenon of strain hardening (increase in tensile strength with strain rate) was
also observed during this testing. Increase in flexural modulus and tensile modulus
thus confirms the reinforcement of polymer matrix with the addition of FS.

Along with mechanical strength, resistance to impact is another desired
characteristic for RM products as it is used in many outdoor applications. To
evaluate the shock resistance, Izod impact test for the LLDPE - FS blends were
carried out. The impact strength values are shown in Table 5.3. The impact
strength reported is the average value of five samples tested for each composition.

Even though the impact strength was not significantly affected by the presence of FS, a slight decline can be observed with increasing concentrations of FS. This can be attributed to the polymer chain mobility affected due to the increased polymer chain entanglements caused by the presence of FS [167–169]. The addition of FS in LLDPE provides reinforcement in small concentrations by forming a three dimensional network structure aided silicone-hydrogen bonds and the increased entanglement of polymer chains. This is caused by the polymer chains being partly adsorbed on the filler surface and partly being entangled with neighboring ones.

Table 5.3: Impact testing: LLDPE - FS nanocomposites

Sample Type	Impact Strength (J)
LLDPE - Natural	0.854
LLDPE - 1%FS	0.8647
LLDPE - 2%FS	0.8327
LLDPE - 3%FS	0.822
LLDPE - 4%FS	0.8223
LLDPE - 5%FS	0.822
LLDPE - 8%FS	0.822

To correlate the above observations with the micro structure, a morphological study of LLDPE - FS nanocomposites was performed using SEM to examine the dispersion of FS in LLDPE. The micrograph of natural LLDPE is shown in Figure 5.6. LLDPE matrix was seen as dark color in high magnification.
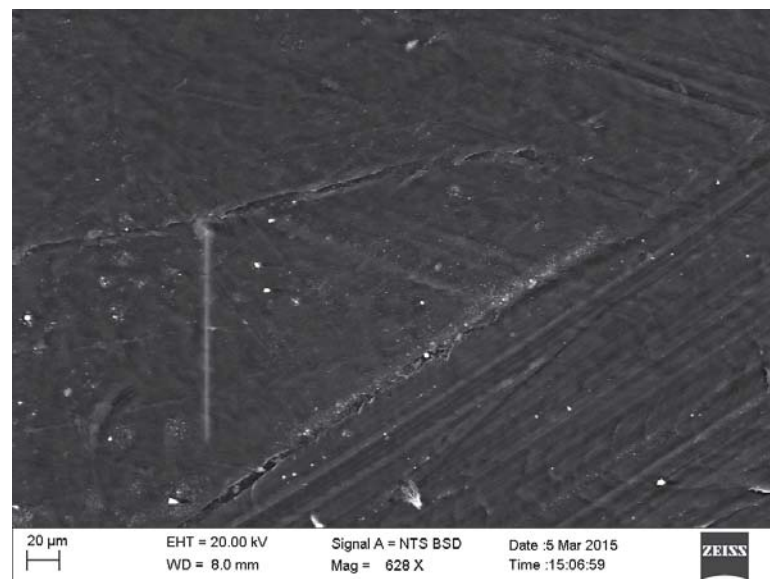
Figure 5.6: Micrograph of natural LLDPE

The micrographs in Figure 5.7 show a fine distribution of 2 wt% FS within LLDPE matrix with a little agglomeration. Average particle size of FS in the range of 50 − 100 nm was evident as shown in Figure 5.7b. Although the dispersion was proper, non-uniformity was observed only at low scale. Proper dispersion of nano particles are necessary to obtain proper particle - polymer chain interactions leading to the reinforcement of polymer chains.
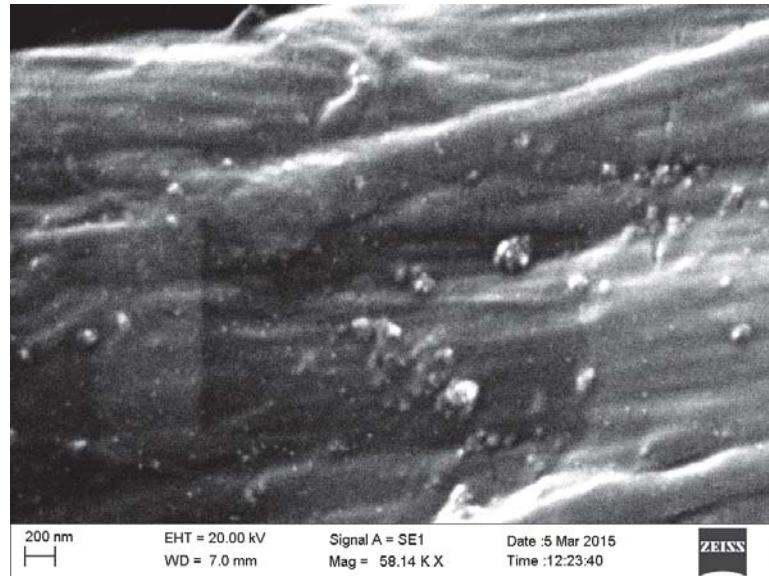
(a) FS dispersion in LLDPE matrix at 2% concentration
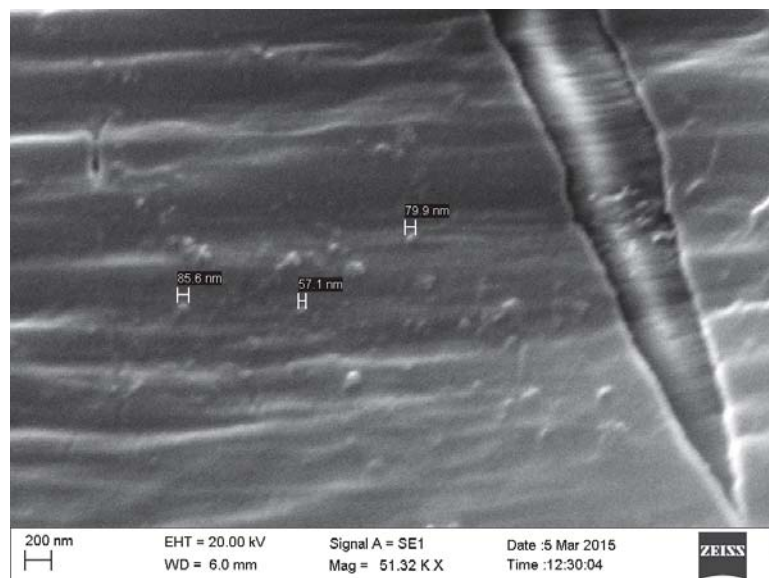
(b) FS particle sizes

Figure 5.7: Micrographs of LLDPE - 2% FS nanocomposites

The micrographs in Figure 5.8 show the distribution of FS in LLDPE at 4 wt% concentration. Figure 5.8a shows uniform distribution of FS, while

agglomerates of FS were occasionally seen at higher resolution, as shown in Figure 5.8b. It was observed that onset of occasional agglomeration of FS in LLDPE oocurs at 4% FS concentration. The nanocomposites were prepared by melt compounding and thus 4% FS can be treated as the maximum FS content in LLDPE for obtaining proper dispersion.
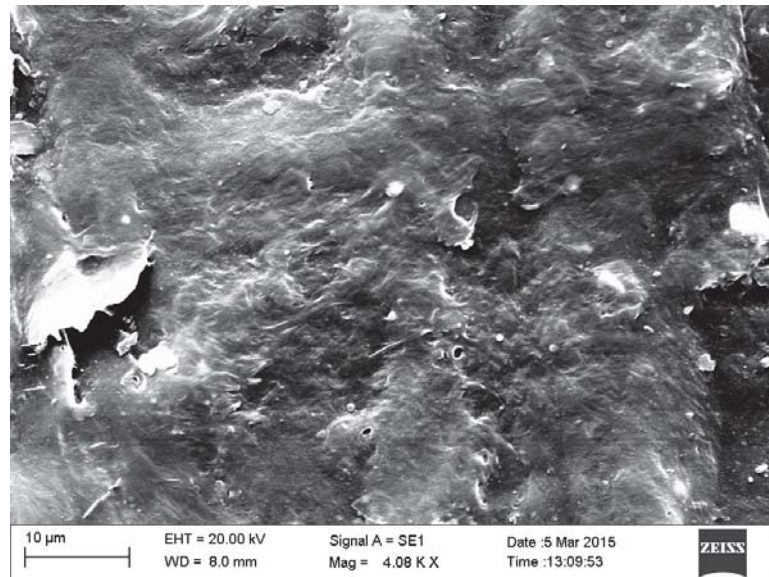
(a) FS dispersion in LLDPE matrix at 4% concentration
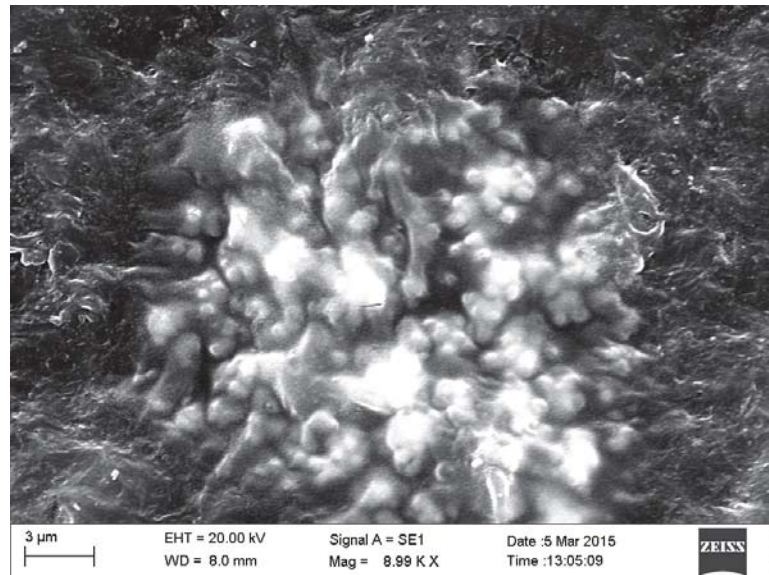
(b) Occasional FS agglomeration in LLDPE - 4% FS nanocomposites

Figure 5.8: Micrographs of LLDPE - 4% FS nanocomposites

The micrographs of 5% FS and 8% FS in LLDPE are shown in Figure 5.9 and Figure 5.10 respectively. At 5 wt% FS composition, agglomeration initiated and agglomerates of different size and shapes ranging from 1 mm to 10 mm were
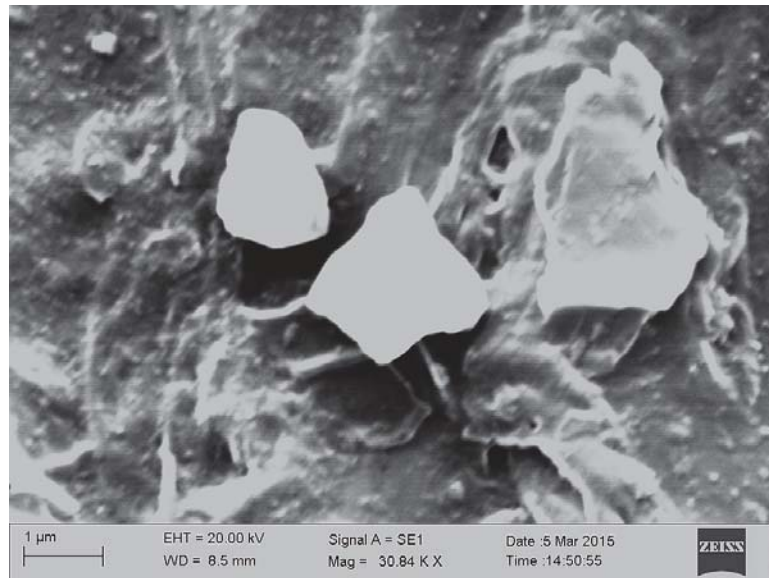
Figure 5.9: Micrograph of LLDPE - 5% FS nanocomposite
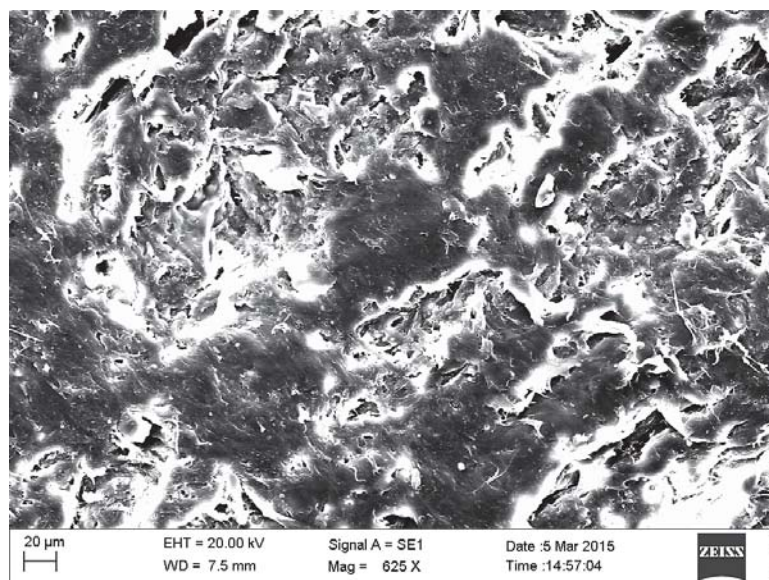
Figure 5.10: Micrograph of LLDPE - 8% FS nanocomposite

observed as shown in Figure 5.9. At higher concentrations, of 8 wt%, FS tend to form structures as seen in Figure 5.10. Surface treatment of LLDPE and addition of proper coupling agents may prevent the possible agglomeration of FS at larger concentrations. The use of coupling agents and surfactants need to be further investigated. The enhancement in mechanical properties was a result of proper dispersion of FS in LLDPE matrix. The use of proper coupling agents and surfactants may help to further increase the mechanical properties.

During the tensile testing, improvement in percentage of elongation was observed at 3 wt% and 4 wt% FS in LLDPE. This can be correlated to the formation of ellipsoid structures in the micrographs of fractured surface as shown in Figure 5.11 and Figure 5.12.It is evident that along with LLDPE, the FS structures are also highly deformed, indicating a ductile fracture. This further proves the reinforcement effects of FS at small concentrations in LLDPE.
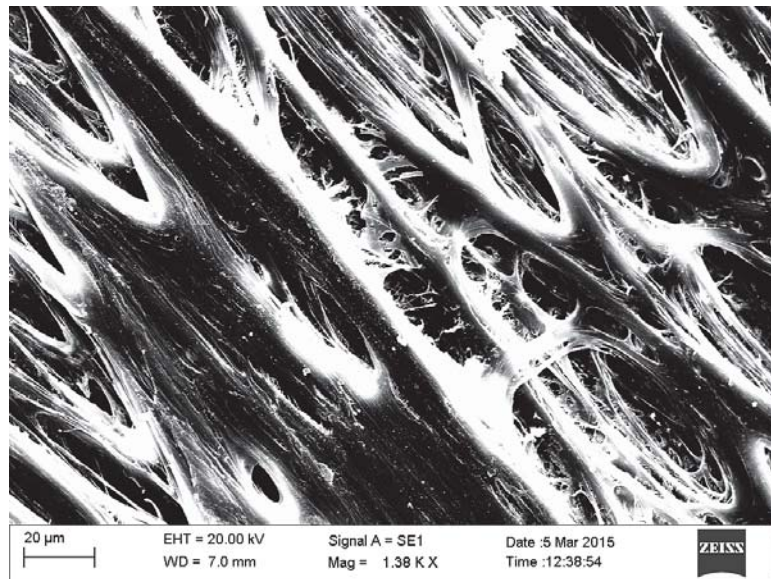
Figure 5.11: Micrograph of fractured surface of LLDPE - 3%FS nanocomposite
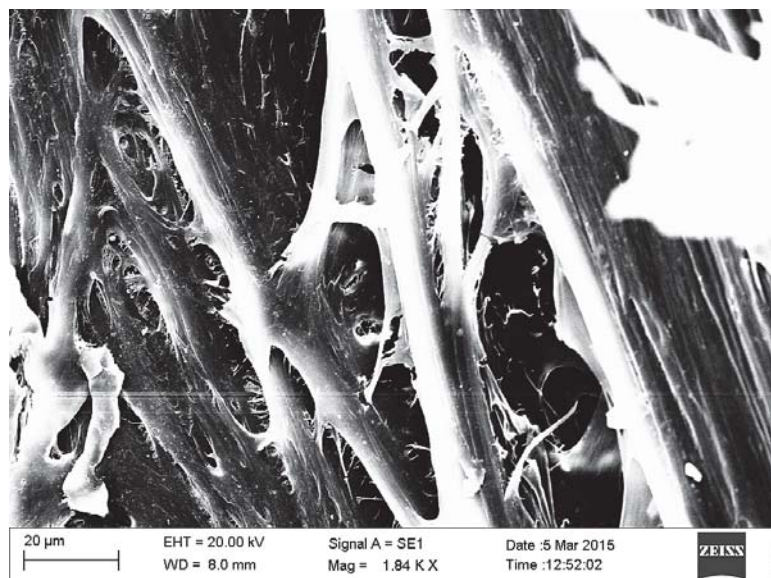
Figure 5.12: Micrograph of fractured surface of LLDPE - 4% FS nanocomposite

The micrograph of fractured surface of LLDPE - 8% FS is shown in Figure 5.13. It can be seen that the elongated ellipsoid structures like in 3% or 4% FS composition was no longer present in the fractured surface. It rather indicates the presence of largely stacked FS structure. From the tensile testing it was observed that the elongation at break was significantly reduced with concentrations of FS above 5%. The micrograph too reveal that there was no elongation in the LLDPE - FS structure. At such concentrations, FS tend to disperse less, creating lesser adhesion to polymer chains. This results in weak and brittle zones in the polymer matrix which can be correlated to the brittle fracture during the tensile testing of the nanocomposite.
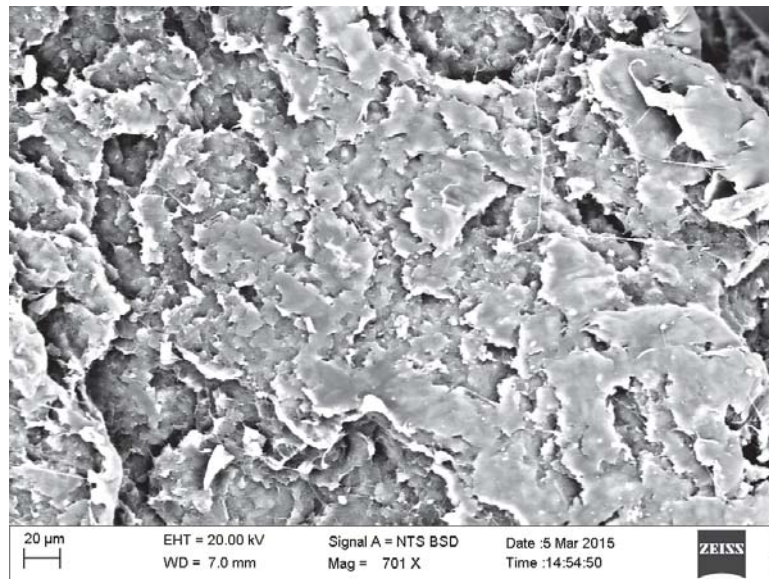
Figure 5.13: Micrograph of fractured surface of LLDPE - 8% FS nanocomposite

With the addition of FS in LLDPE the variation in the semi crystalline structure of LLDPE was examined by using XRD analysis and is shown in Figure 5.14. The two peaks corresponding to the diffraction planes of LLDPE indicated that the semi crystalline structure of LLDPE remained unchanged during compounding. However, the intensity of the crystalline peaks of LLDPE reduced with the addition of FS. The presence of FS in molten matrix, affects the mobility and re-crystallization of polymer chains, and thus reduces the crystallinity of LLDPE. It was established in Poly olefene - FS blends by Kalfus *et al* that the degree of matrix reinforcement gets considerably affected by the extent of matrix crystallinity [31]. FS in LLDPE polymer blend occupies the amorphous regions in the polymer matrix and tends to increase the melt viscosity resulting in reduction of spherulitic growth.
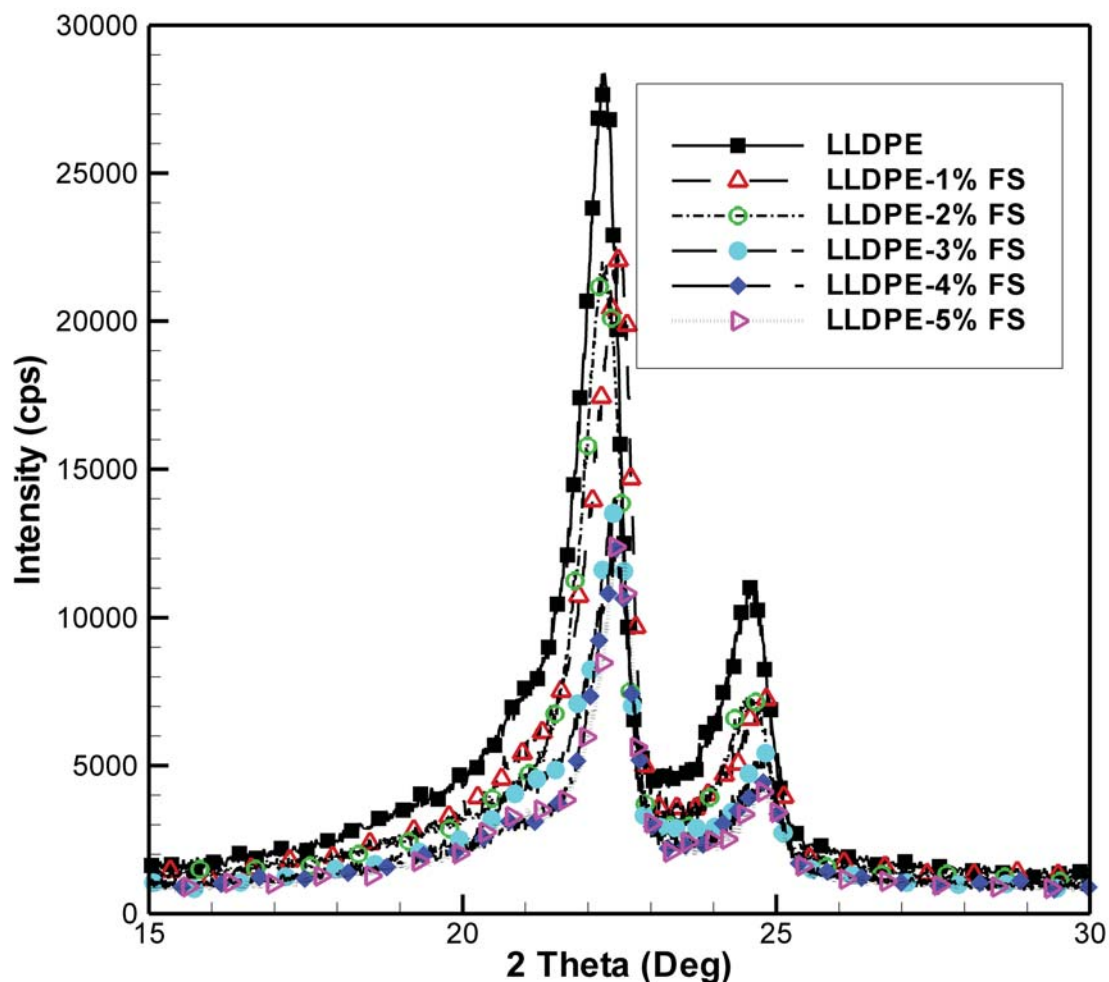
Figure 5.14: XRD plots of natural LLDPE and LLDPE - FS blends

Table 5.4: Reduction in crystallinity of LLDPE - FS blends (XRD analysis)

Description	Reduction in Crystallinity (%)
LLDPE	-
LLDPE - 1% FS	24.23
LLDPE - 2% FS	24.86
LLDPE - 3% FS	46.38
LLDPE - 4% FS	49.66
LLDPE - 5% FS	54.52

The percentage of crystallinity was calculated by comparing the areas under the crystallinity curves with that of pure LLDPE. The results are shown in Table 5.4. It was observed that even with small addition of FS there is a significant reduction in crystallinity of LLDPE (24.23% reduction for 1% FS). The crystallinity

of LLDPE matrix further reduced with addition of FS. At a concentration of 5% FS in LLDPE a 54.5% reduction in crystallinity from that of natural LLDPE was observed.

5.4   Conclusion

The addition of FS in low concentrations provided reinforcement to LLDPE matrix. This can be observed with the increase in static mechanical properties like tensile modulus, tensile strength, toughness and flexural modulus. the findings of mechanical and morphological analysis of LLDPE - FS blends are as follows:

1. The tensile modulus increased by 44% for a concentration of 4% FS in LLDPE. There was also a remarkable increase in tensile toughness with the addition of FS. The mechanical properties were thus significantly improved with the addition of FS in LLDPE.

2. The micro structural studies using SEM also showed FS was well dispersed in LLDPE matrix at low concentrations providing matrix reinforcement.

3. The examination of fractured surfaces of LLDPE - FS nanocomposites showed formation of reinforced ellipsoid structures enhancing the elongation at break at small concentrations of FS. At higher concentrations (>5% FS) the micrographs showed no elongated structures and the samples had a brittle failure during tensile testing.

4. A reduction in crystallinity of natural LLDPE was observed with the addition of FS. The studies using XRD showed a reduction of 50% crystallinity with the addition of 4% FS. This indicates LLDPE - FS blends are more amorphous than natural LLDPE.

From these laboratory scale investigations, it can be concluded that 4% FS in LLDPE provide good reinforcement and melt flow characteristics required for RM. The LLDPE - 4% nanocomposites need to be rotationally molded in industrial scale to further confirm these laboratory scale findings. Further, the effect of nano silica in mold release of LLDPE need to be investigated.

Chapter 6

Cycle Time Reduction in Rotational Molding of LLDPE - FS Nanocomposites

6.1 Introduction

Rotational molding suffers a disadvantage of longer cycle times as compared with the other polymer processing methods like blow molding, injection molding, etc. Since the rotational molding process is time consuming in comparison with polymer processing methods like extrusion, injection molding, blow molding, etc. any decrease in cycle time is considered beneficial. This helps in improving the productivity of the process. The overall cycle time of a rotational molding process involves times required for heating as well as cooling of the part. In case of LLDPE the molders use a typical demolding temperature of 50°C to demold the part. At this temperature LLDPE shrinks and detaches itself from the mold inner wall. Any attempt to demold the part above this temperature (e.g. 80°C, 70°C, etc.) results in damaging the part due to the strong adhesion of the part with the mold. This in turn increases the cooling cycle times. To address this issue, an attempt has been made to demold the part made of LLDPE - FS nanocomposites at temperatures higher than common demolding temperature (50°C). As there is no quantitative method to measure the adhesive force between the mold and LLDPE - FS nanocomposites an innovative method was designed to measure the same. This chapter discusses the effect of LLDPE FS composites on the adhesive forces between the material and the mold.

6.2 Materials and Methods

To study the adhesion of LLDPE and LLDPE - FS nanocomposites to mold surface, a fixture was designed for using with UTM, used to study the static mechanical properties discussed in previous chapter. The fixture was provided with a heating chamber to melt the polymer. One end of the fixture was mounted on the fixed end of UTM while the other end was fixed on the movable jaw of UTM with the load cell. With this arrangement the pulling force required for separating the product could be accurately measured. The fixture along with its installation on standard UTM is shown in Figure 6.1 and Figure 6.2. The detailed drawings of the fixture are given in Appendix B.4. The mold along with the top plate was made of both Aluminum and Steel to study the effect of mold material in demolding LLDPE - FS nanocomposites. Thermocouples were used to measure the temperatures of heating chamber, mold and the polymer melt. The polymer melt temperature was used to control the process of heating, molding, cooling and demolding. A fan was used to cool the mold during cooling cycle. This simulates the condition of forced air circulation during cooling of a typical rotationally molded product.
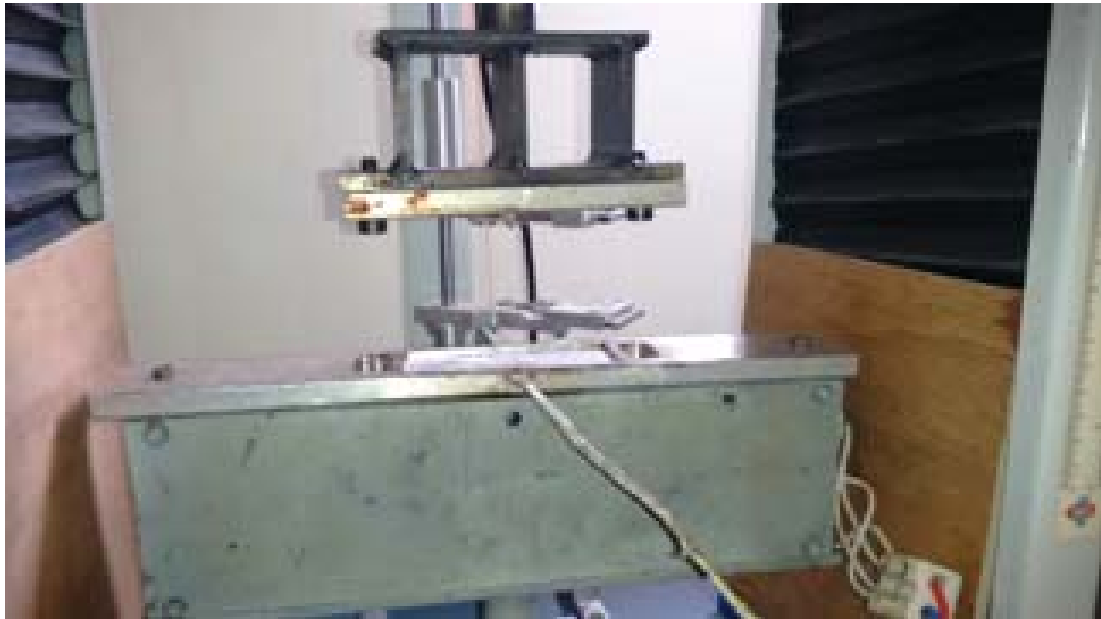
Figure 6.1: Fixture for pulling force measurement

The material used for this study is same as that used for reological and mechanical characterization. The material used was rotationally moldable grade of LLDPE (R35A042)and Hydrophilic FS of grade Aerosil-200 supplied by Evonik industries as given in Table 3.1.

Figure 6.2: Installation of fixture on standard UTM

6.2.1   Pulling Force Measurement

A test specimen of 100 x 40 x 3 mm was made using natural LLDPE and
LLDPE - FS blends. 11 g of LLDPE and LLDPE - FS blends were used to make the
test specimen. The powder was heated in the fixture and was compressed by UTM
by applying a force of 500 N. The powder was heated to 200ºC and was allowed to
cool down. Forced air cooling was done with the help of a pedestal fan. The pulling
force was measured by UTM in tensile mode at temperatures of 80ºC, 65ºC and
50ºC. These temperatures can be regarded as common demolding temperatures in
RM machine. The experiment was done for both aluminum (grade 2024) and steel
(grade S275)which are used as mold materials. The effect of pulling force on cross
head speed was also monitored at 5, 25 and 100 mm/min to study the mold ejection
rates.

6.3   Results and Discussions

During rotational molding the polymer melt coats the mold inner surface
and adheres to it, forming the shape of the mold. During the removal of the product
from the mold, the adhesive forces between part and mold become significant. The
factors affecting the pulling force are the presence of mold release agents, type of
polymer, temperature, pulling rate, mold material along with its surface finish and

the product design. No mold release agents were used during the experiments. The variation of pulling force with changes in temperature and pulling rate on steel and aluminum mold are shown in Figure 6.3. It can be observed that the pulling force needed to remove the product from mold reduces with addition of FS both mild steel and aluminum molds at higher temperatures. The minimum pulling force for LLDPE -FS blends was observed at 80°C and thus it can be considered ideal temperature to remove the product from mold. However, natural LLDPE showed lower pulling force at 50°C than at 80°C. The reduction in pulling force denotes the lower adhesion of polymer to the inner mold surface. This can facilitate easier product removal and possible reduction in cycle time. Along with the reduction in pulling force, there can be a reduction in cycle time if the product is removed at 80°C instead of 50°C. A typical IAT curve for LLDPE - 4% FS from the industrial trials are shown in Figure 6.4. It can be seen that a heating rate of 11°C/min and a cooling rate of 4.5^{o}C/min is observed while molding the product. Thus, if the product is removed at 80°C instead of 50°C, 6.7 minutes can be saved. The application of mold release agents can further reduce the adhesive forces between polymer and mold and needs separate investigations.
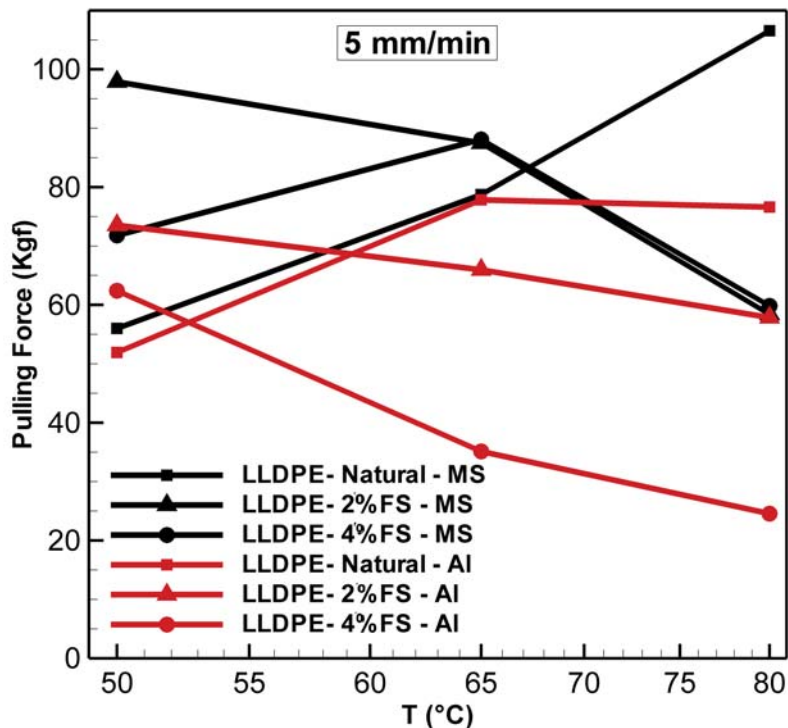
Figure 6.3: Variation in pulling force at cross head speed of 5 mm/min

The rate of pulling, varies with the part ejection method used. Smaller pulling rates were observed during manual product removal while higher pulling rates can be seen with mechanical or pneumatic aids. The variation in pulling force at 80°C for different pulling rates are shown in Figure 6.5. It can be seen that the
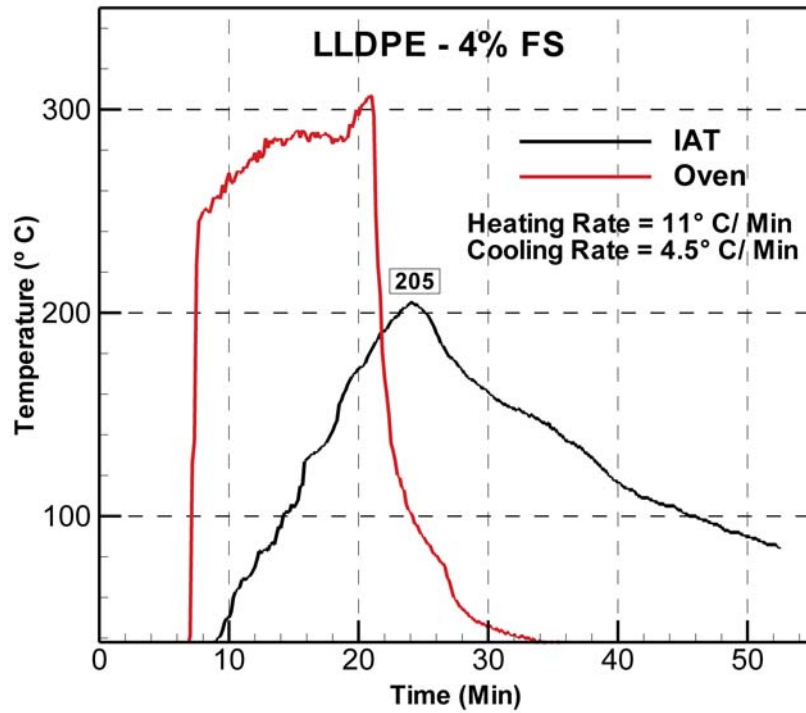
Figure 6.4: Heating and cooling rates in rotational molding - LLDPE - 4% FS: industry trials
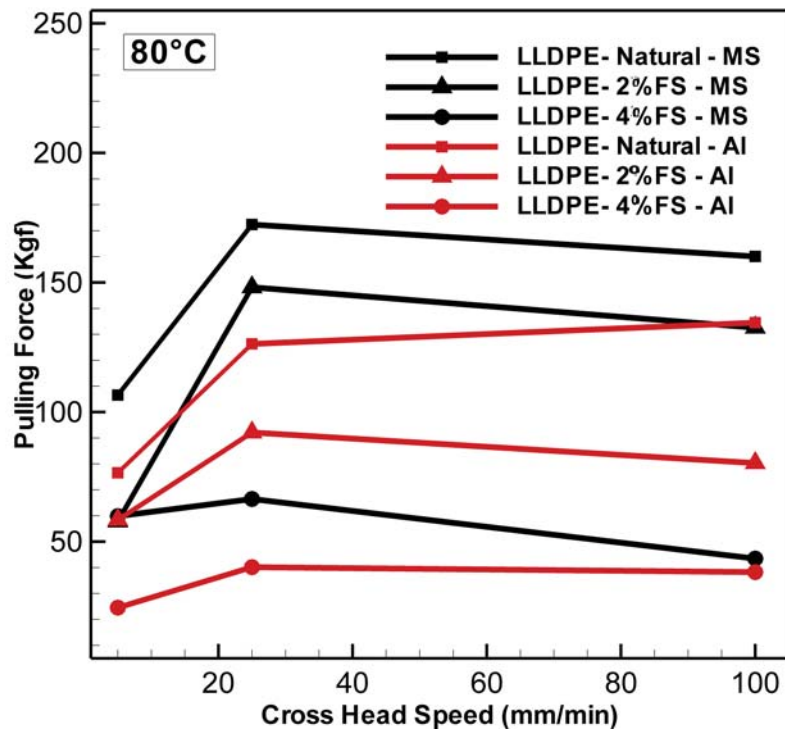
Figure 6.5: Variation in pulling force at temperature of 80°C

pulling force increased with the increase in pulling rate. The increase in pulling force was not significant above cross head speed of 25 mm/min. Both aluminum and steel molds showed the similar trend. It can be observed that the blends with LLDPE - 4%FS showed the lowest pulling force even at higher pull rates. Thus LLDPE - 4% FS blends can be considered to reduce the adhesion with the mold during cooling and facilitates easy and quick part removal. This in turn results in reduction of cycle time during RM.

6.4 Conclusion

Successful part removal is a crucial step in rotational molding. The adhesion of part to mold surface after solidification is highly undesirable as it may damage the part. In industry this problem is avoided by the use of mold release agents. However, additional time is required for applying mold release agents to the mold. Use of non stick coating is expensive and calls for additional care in mold handling. The LLDPE - 4% FS blends used in this study, tend to reduce the pulling force needed for the part removal at higher temperatures. The parts can be demolded at 80ºC with ease which is difficult for LLDPE alone. Also, for a typical cooling rate of 4.5ºC/min a savings of 6.7 min can be obtained by removing the part at 80ºC instead of 50ºC. This can provide possible reduction in cycle time of rotational molding process. Hence it can be noted that LLDPE - FS nanocomposites provide enhanced mechanical properties with good melt characteristics without adversely affecting the cycle time of rotational molding process. These laboratory scale findings were further evaluated in industry scale by compounding and rotationally molding LLDPE - 4% FS blend in industry scale. These findings are given in next chapter.

Chapter 7

Rotational Molding of LLDPE - FS Nanocomposites at Industry Scale

7.1 Introduction

In the previous chapters, rheological characteristics, viscoelastic, mechanical properties and assessment of pulling force requirements to reduce cycle time for LLDPE - FS blends were discussed. The findings in these chapters were based on investigations carried out at laboratory scale.

Though the laboratory scale investigations were carried out in specific conditions (according to the standards), limited quantity of actual materials, customized experimental set-up (that mimic the industrial conditions), scaling up studies are necessary to ascertain the use of LLDPE - FS nanocomposites in real life product. This chapter investigates the scaling up of rotationally molding LLDPE - FS nanocomposites at industrial level and comparing the results with laboratory scale findings. In previous chapters, composition of 4% FS in natural LLDPE has proved to provide the required melt characteristics for RM. Generally, use of nano scale reinforcements for improving the processability as well as mechanical properties of rotationally molded products is not preferred by the molder. It may be due to the fact that control of the process is difficult mainly due to the bi-axial rotation of mold in aggressive heating environment which makes the use of conventional temperature measuring devices very difficult. Apart from this, melt compounding using the extruders poses significant problems like agglomeration, separation, etc. Also, it is speculated that incorporation of such nanocomposites may adversely affect the powder flow characteristics within the mold thus producing a defective part. To overcome the above difficulties and to prove the advantages of LLDPE - FS nanocomposites in an industrial environment , trials were conducted at GMI Zarahak Moulders Ltd. Goa. The Industry produces rotationally molded products for liquid storage, environmental protection and material handling applications. An attempt has been made to reinforce particulate nano scale FS with natural LLDPE

by melt compounding in an industrial single screw extruder at Kenwood Industries, Goa. The pellets were pulverized and rotational molding was carried out using a three arm bi-axial rotational molding machine by carefully monitoring the IAT within the mold. Monitoring the IAT has provided significant improvements in product quality and repeatability [10]. Wireless temperature monitoring system (TEMPLOGGER^{TM}) was used to monitor IAT. The effect of FS on powder flow characteristics, melt flow characteristics, static mechanical properties, dynamic mechanical properties, creep and stress relaxation behavior have been found thus covering an entire regime for a typical rotation molding process. Studies were conducted to correlate the above findings with the morphological structure of the nanocomposites obtained.

7.2 Material and Methods

7.2.1 Materials

The material used for this study was rotationally moldable grade of LLDPE (Relene - LL36RA045) supplied by Reliance India Limited. The industry where the trials were conducted uses this material in bulk for RM. The specifications of Relene - LL36RA045 are given in Appendix A.3. This material is comparable with R35A042 (GAIL Industries) used in our laboratory studies and is summarized in Table 7.1. Hydrophilic FS of grade Aerosil-200 was used for nano reinforcement (Evonik industries) as given in Table 3.1.

Table 7.1: Comparison of LLDPE grades LR35A042 and L36RA045

Specifications	Unit	R35A042	LL36RA045
MFI	g/10min	4.2	4.5
Density @ 23ºC	g/cc	0.935	0.936
Vicat Softening Point	ºC	115	117

To remove the entrapped moisture, FS was dried at 105ºC in a temperature controlled oven for 2 hours. LLDPE and 4wt% FS were melt mixed in an industrial five stage single screw extruder at Kenwood Industries, Goa, India. A screw rpm of 65 was used to obtain the extrudate. The temperature at different sections in the screw barrel of the melt extruder was maintained between 220ºC and 240ºC. Figure 7.1 shows the melt screw extruder used in this study. The extrudate was

cooled in the water bath and cut in the form of pellets. These were pulverized using a disc pulverizer and sieved to 35 mesh (500μm). The pulverizer used for compounding LLDPE - 4%FS blends is shown in Figure 7.2 along with a vibro-screen used for screening the powder particles suitable for RM. The pulverized LLDPE - 4%FS blend was used to make baffles of size 330 x 330 x 1250 mm by RM process. The mold used for this purpose along with the LLDPE - 4% FS powder obtained after compounding and pulverizing is shown in Figure 7.3.

A bi-axial rotational molding machine (RT 2203B- CACCIA Engineering) was used to make the rotationally molded baffles used in underground sewage treatment tanks. The product was selected mainly due to less material requirements, simple product features and no curved surface to facilitate the easy cutting of samples. The specifications of RT 2203B is given in Appendix A.11 and is shown in Figure 7.4. It is a semi automatic carousal type rotational molding machine with three arms, where three distinct operations of mounting the mold, heating of the mold in the furnace and cooling of the mold are simultaneously performed. The IAT of the mold was monitored by using TEMPLOGGER^{TM} supplied by Roto Solutions, SA. The specifications of TEMPLOGGER^{TM} is given in Appendix A.12. The TEMPLOGGER^{TM} was fixed to the rotating arm with thermocouple for monitoring real time IAT and oven temperatures. The set up is shown in Figure 7.5.

Figure 7.1: Industrial melt extruder (Courtesy: Kenwood Industries).

Figure 7.2: Industrial pulverizer and vibro-screen (Courtesy: Kenwood Industries).

Figure 7.3: Mold used for rotational Molding - Baffle (Courtesy: GMI Zarahak Moulders)scale bar 1" shown.

Figure 7.4: Rotational molding machine-CACCIA-RT 2203B (Courtesy: GMI Zarahak Moulders).

Figure 7.5: Experimental set up for IAT measurements using TEMPLOGGER$^{\text{TM}}$ (Courtesy: GMI Zarahak Moulders).

7.2.2 Powder Characteristics and MFI

The bulk density and dry flow time of LLDPE powder was tested in accordance with ASTM D 1895-96 which is redefined for the use in rotational molding by Affiliation of Rotational Moulding Organisations (ARMO). The dry flow time, is measured as the time to fill the 100 cc volume of measuring cup using 100 g of polymer. The MFI was measured at 190°C/2.16 kg, according to ASTM-D1238, method A.

7.2.3 DMA, Creep and Stress Relaxation

The DMA and creep tests were performed as explained in chapter 4. In stress relaxation tests, for a predefined strain of 1%, stress response was noted for 15 min. The tests were repeated at different temperatures ranging from 30°C to 100°C varying in steps of 10°C similar to the one as discussed in isothermal creep tests above. All measurements were performed under nitrogen atmosphere.

7.2.4 Mechanical Testing and SEM

Mechanical testing including tensile testing, flexural testing, impact testing and SEM were conducted as described in chapter 5 (section 5.2).

7.3 Results and Discussions

7.3.1 Powder Analysis

To obtain good quality rotationally molded products, the quality of LLDPE powder is a key factor. Bulk density of the powder and its dry flow time are considered as essential quality parameters for the powder. In our studies, both natural LLDPE and LLDPE - 4% FS were pulverized and sieved to 35 mesh (500 μm). To assess the effect of nanocomposite on the powder flow characteristics bulk density and dry flow of the powder were measured. The bulk density and dry flow tests performed revealed a marginal reduction in bulk density of LLDPE - 4% FS blend in comparison with natural LLDPE. It was observed that the bulk density reduced from 0.3575 g/cc to 0.2977 g/cc. The dry flow time measured was slightly increased from 10 s to 13 s in comparison with natural LLDPE. A microscopic

examination of LLDPE - 4% FS powder as shown in Figure 7.6 revealed presence of feathery structures around particles which might be contributing to slight increase in dry flow time. The natural LLDPE powder exhibited no feathery structures as seen from Figure 7.7 indicating better powder quality.
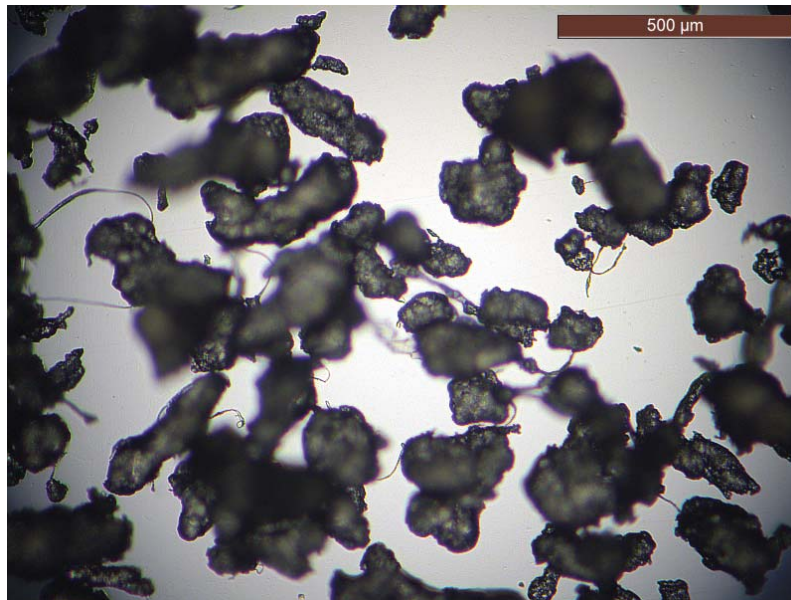

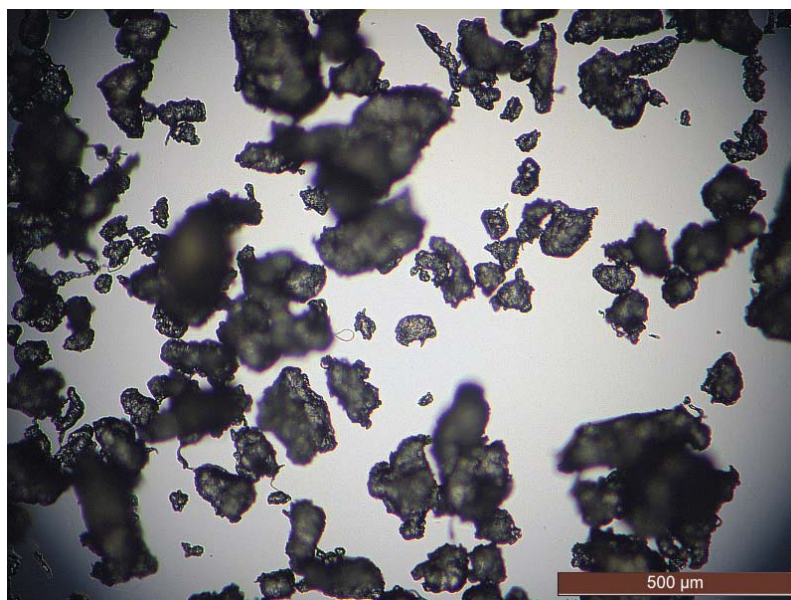Figure 7.6: Magnified powder particle showing feathery structures - LLDPE - 4% FS

Figure 7.7: Magnified powder particle - natural LLDPE

This needs further investigations; however, the small changes in the above parameters did not indicate any major impact on powder flow characteristics within the mold.

103

Along with dry flow time and bulk density MFI is an important indicator of flow of molten polymer within the mold. The variation of MFI for the industrial and laboratory scale findings are shown in Table 7.2. For the industrial grade, the MFI of natural LLDPE reduced from 4.72 g/10 min to 3.5 g/10 min with the addition of 4% FS. This is an indication of chain entanglement or the hindrance created to the movement of polymer chains, thereby showing some increased resistance to melt shear. For rotational molding generally a MFI of 3.5 g/10 min is acceptable. It can be noticed that the results of laboratory scale and those obtained with industrial grade material are quiet closer.

To ensure that a rotationally molded product has highest mechanical properties, the proper curing of the polymer within the mold is of utmost importance. For this purpose, IAT within the mold was monitored and a PIAT of 200$^\text{o}$C was considered as an indicator of optimal curing. The IAT plots of samples molded with natural LLDPE and LLDPE - 4% FS are given in Figure 7.8 and Figure 7.9.

Table 7.2: Comparison of LLDPE grades LR35A042 and L36RA045

Material	Unit	Melt Flow Index 190$^\text{o}$C/2.16 kg
Industry scale		
Natural LLDPE	g/10min	4.72
LLDPE - 4%FS	g/10min	3.5
Laboratory scale		
Natural LLDPE	g/10min	4.49
LLDPE - 4%FS	g/10min	3.65

It was observed that a PIAT of 205$^\text{o}$C was achieved, indicating a proper curing of the product. The samples were then examined for defects and porosity. The microscopic examination of the inner surface of product has shown considerable reduction in pin hole size with the addition of FS in LLDPE. For natural LLDPE pin holes to the size of 220 μm can be seen in Figure 7.10. Also numerous pin holes of sizes ranging from 50 to 100 μm can be seen

With the addition of FS the maximum size of pin holes reduced to 65 μm as seen in Figure 7.11. Most of the pin holes present in the sample were less than 50 μm
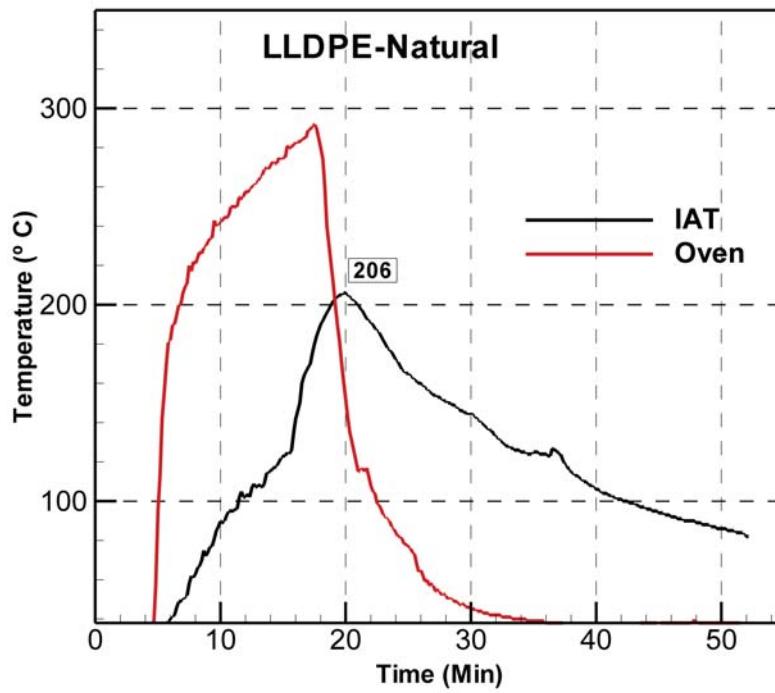
Figure 7.8: Internal air temperature plots for natural LLDPE
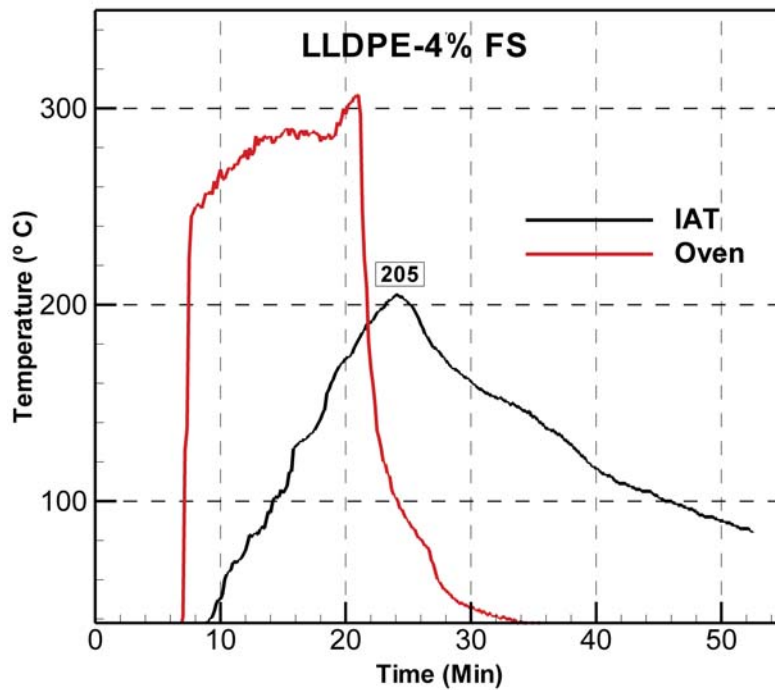
Figure 7.9: Internal air temperature plots for LLDPE - 4% FS blend

in size. This clearly indicate the addition of FS suppresses the bubble formation limiting the size of pin holes.
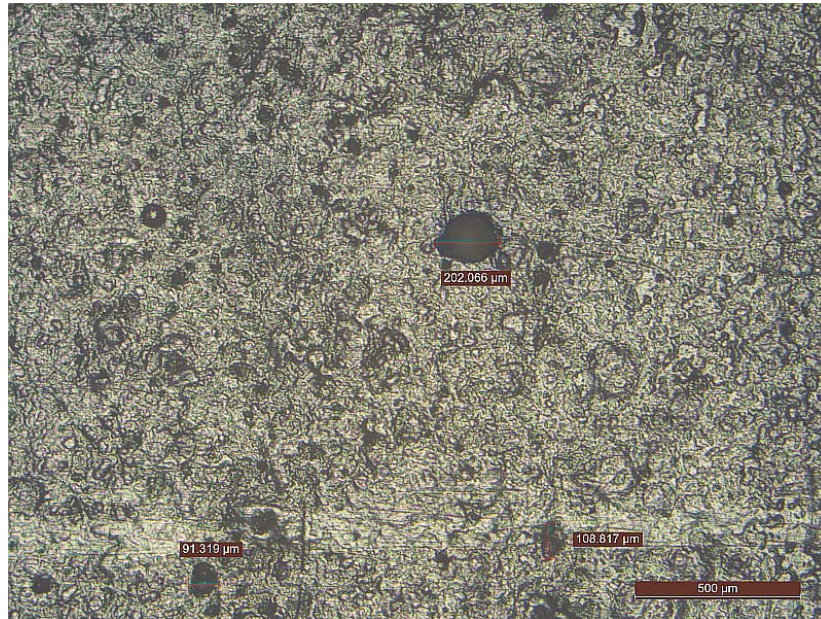
Figure 7.10: Magnified inner surface of natural LLDPE showing pin holes
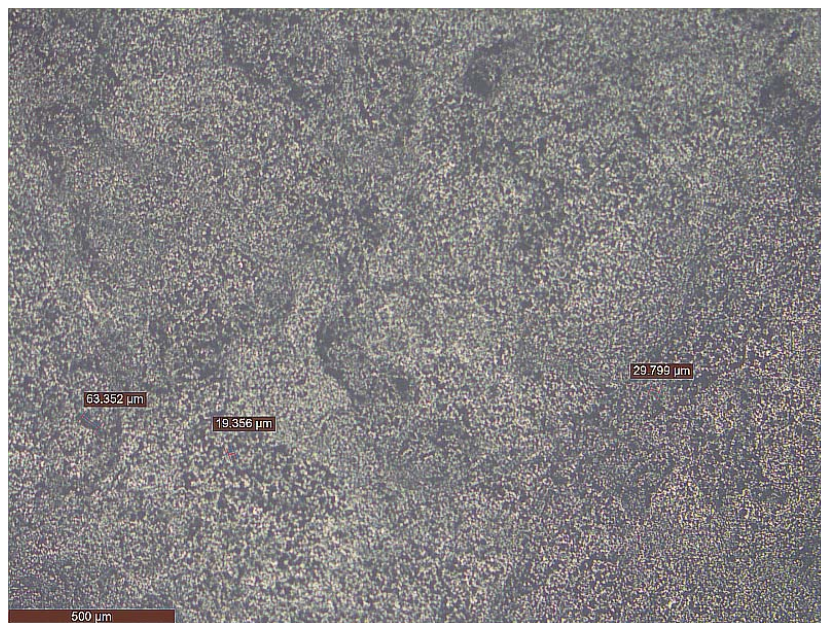
Figure 7.11: Magnified inner surface of LLDPE - 4% blend showing pin holes

7.3.2   Mechanical and Viscoelastic Properties.

The tensile strength, modulus and flexural modulus also shown considerable enhancement for the rotationally molded LLDPE - 4% FS blend. The engineering stress – strain curves are shown in Figure 7.12.
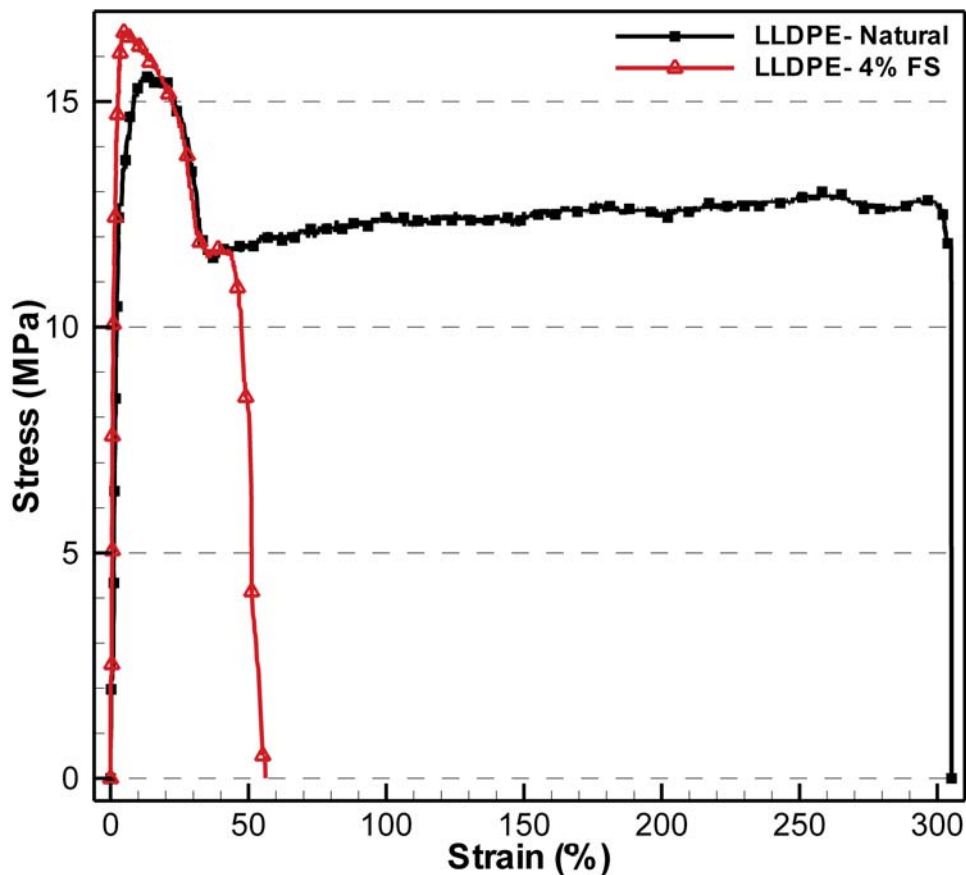
Figure 7.12: Engineering stress strain curves for natural LLDPE and LLDPE - FS blends

The natural LLDPE showed plastic deformations with typical neck formation while LLDPE - 4% FS showed a reduction in plastic deformation with necking. From Figure 7.12, it can be seen that the elongation at break reduced with addition of FS, thereby decreasing the tensile toughness. However, slight increase in mechanical properties like ultimate tensile strength, and tensile modulus were observed. The tensile modulus increased from 750.43 MPa to 1882.52MPa with the addition of FS, while tensile strength showed an increase of 10%. The morphological studies of fractured sample showed tendency to form extended FS-LLDPE structures resulting in ductile fracture. The micro graphs of fractured surface of LLDPE - 4% FS is shown in Figure 7.13. The fractured surface showed the plastic deformation of the moderately agglomerated FS. The FS was found to be dispersed uniformly in LLDPE matrix, even though few local agglomerations are observed at higher magnification as shown in Figure 7.14. The agglomeration of FS in LLDPE is not desired as it leads to lesser adhesion of FS to polymer chains. This results in weak and brittle zones in the polymer matrix and can lead to reduced plastic deformation and brittle fracture.
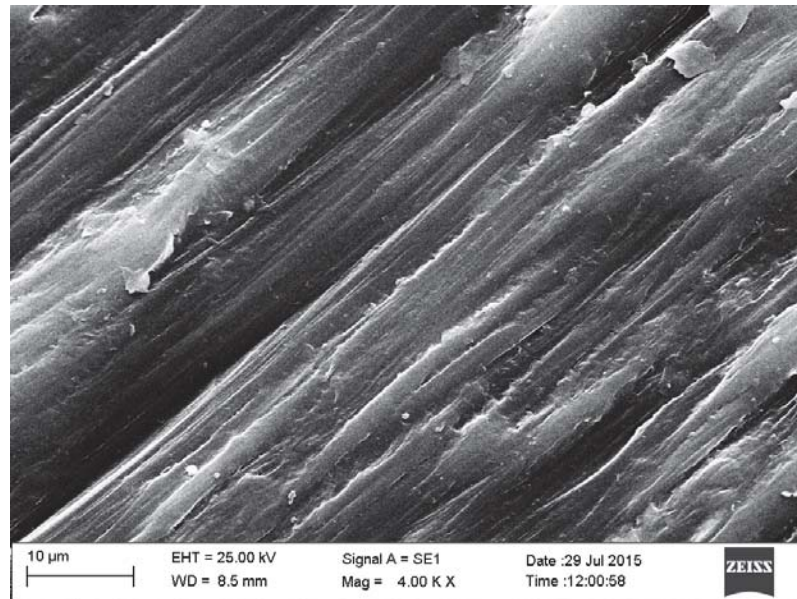
(a) At lower magnification
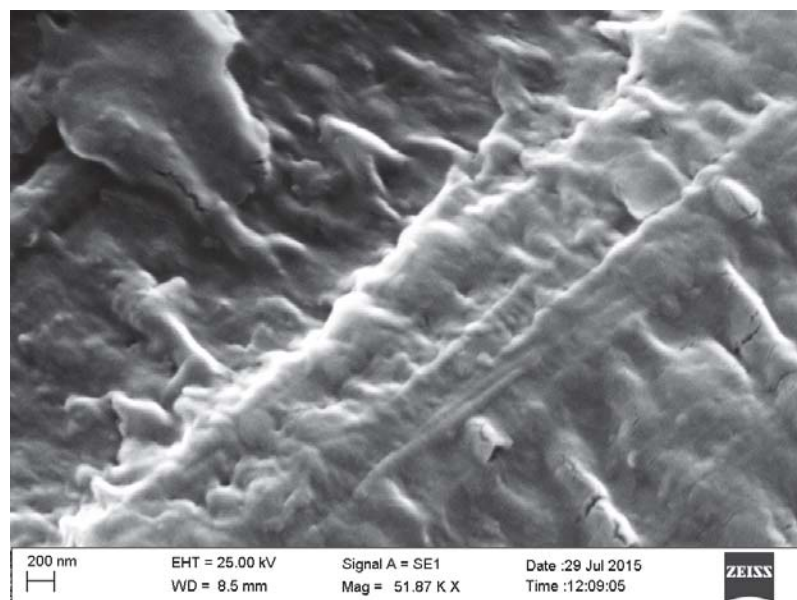
(b) At higher magnification

Figure 7.13: Micrographs of fractured surface of LLDPE - 4% FS blends

The flexural modulus at three different cross head speeds and is given in Table 7.3. As seen from the results, the flexural modulus showed progressive increase with the increase in cross head speed. The flexural modulus recorded a maximum of 637.05 MPa for 4 wt% FS at a cross head speed of 50 mm/min in comparison to natural polymer at 542.11 MPa. It is noteworthy that the phenomenon of strain hardening (increase in tensile strength with strain rate) was also observed during this testing. Increase in flexural modulus and tensile modulus thus confirms the reinforcement of polymer matrix with the addition of FS.
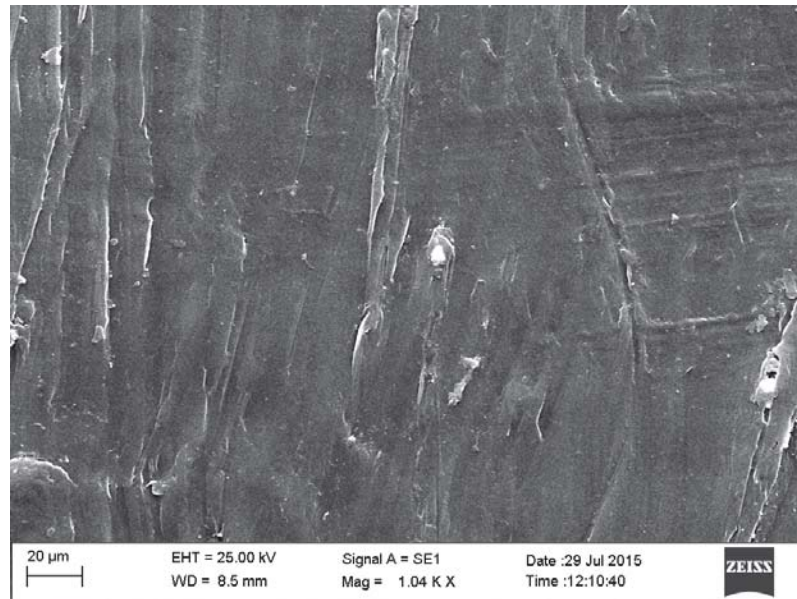
(a) At lower magnification
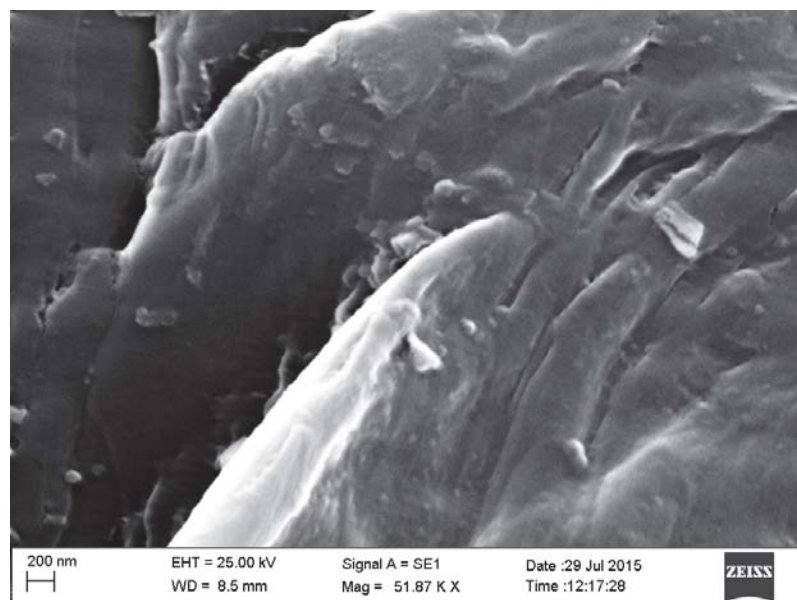
(b) At higher magnification

Figure 7.14: Micrographs of LLDPE - 4%FS blends showing dispersion of FS in LLDPE .

In addition to mechanical strength, resistance to shock loads is important for rotationally molded products as it is used in many outdoor applications. To evaluate the shock resistance, Izod impact test for the LLDPE - FS blends were carried out. The impact strength recorded 0.935 J (74.96 J/m) for natural LLDPE and 0.873 J (69.84 J/m) for LLDPE - 4% FS blends. The reduction in impact strength is due to the reduced energy dissipation caused by restricted polymer chain movement in presence of FS[75].

Table 7.3: Flexural testing: LLDPE - FS nanocomposites

Material	Flexural Modulus at 1 mm/min (MPa)	Flexural Modulus at 5 mm/min (MPa)	Flexural Modulus at 50 mm/min (MPa)
LLDPE - Natural	333.8	379.24	542.11
LLDPE - 4% FS	442.7	470.4	637.05
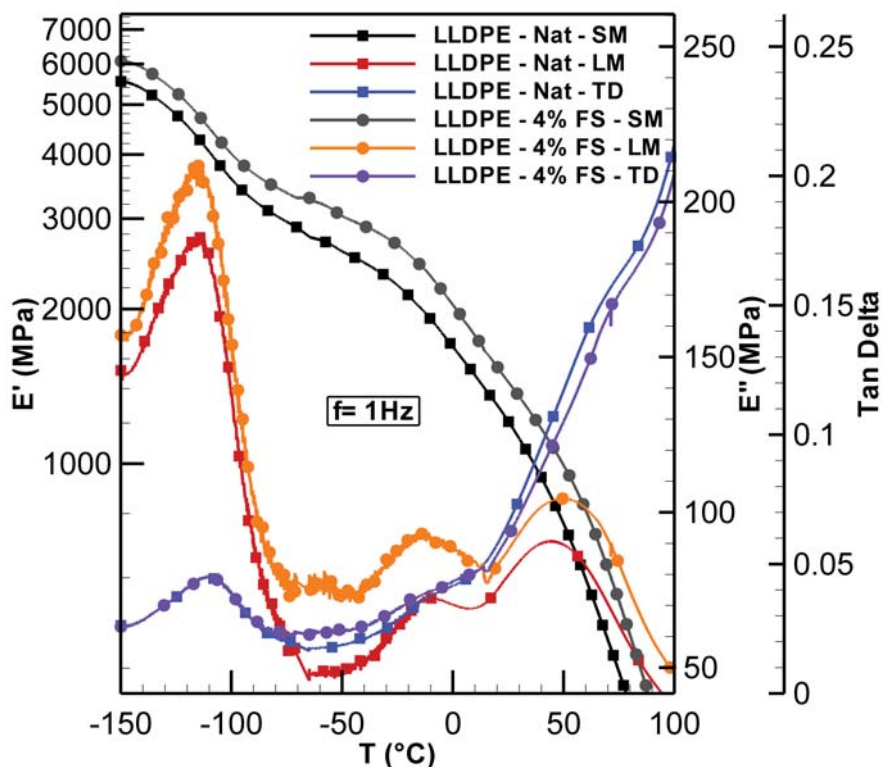
Figure 7.15: Dynamic mechanical properties of natural LLDPE and LLDPE - 4% FS blends showing E', E'' and tan delta.

The dynamic mechanical characteristics (E', E'' and tan delta vs. temperature) of LLDPE and LLDPE - 4 wt% FS blends are shown in Figure 7.15. It shows that for a temperature range from -150°C to 100°C, there is an increase in storage moduli and loss moduli for LLDPE - FS composite as compared with natural LLDPE. At room temperature, an increase in storage modulus by 20% and loss modulus by 15% could be seen for the nanocomposite. Two distinct peaks are observed in loss modulus curve representing the glass transition temperatures (T_g) as shown in Figure 7.15. The first peak at -127°C represents γ T_g representing the small scale movements in polymer chains usually associated with inter and intra molecular motions [154]. The second peak at 46°C represents α T_g representing the onset of melting of low molecular weight polymer chains. At 4% FS concentration

the shift in both α and γ T_g were not significant as compared to natural LLDPE. These findings were in agreement with the laboratory scale findings.

Table 7.4: Comparison of industry scale and laboratory scale test results

Specification	Industry Scale		Laboratory Scale	
	Natural LLDPE	LLDPE - 4% FS	Natural LLDPE	LLDPE - 4% FS
Tensile Modulus (MPa)	750.43	1882.52	818.2	1180.46
Maximum Tensile Strength (MPa)	15.54	16.97	17.75	18.81
Flexurual Modulus @ 5 mm/min (MPa)	379.24	470.4	271.74	296.57
Impact Strength (J)	0.935	0.873	0.854	0.822
Maximum Storage Modulus (MPa)	5547	6078	4771	5415
Storage Modulus @ 30°C (MPa)	1119	1291	1143	1408
Loss Modulus @ 30°C (MPa)	84.08	96.64	95.91	107
γ T_g (°C)	-127.1	128.3	-107.59	-110.23
α T_g (°C)	46.2	47.3	43.85	44.05

A comparison of laboratory scale findings and industrial test results for natural LLDPE and LLDPE - 4% FS are given in Table 7.4. It can be observed that being a stress free process the rotationally molded industry sample exhibited better mechanical properties than the laboratory sample. Also, the rotationally molded sample was properly cooked as a PIAT of 205°C was maintained. The maximum tensile modulus for industry sample recorded 1882.52 MPa in comparison to 1180.46 MPa for LLDPE - 4% FS blend. The storage modulus also showed increased values for industrially molded samples. Similar increase in flexural modulus and impact strength can be noted for rotationally molded industry sample. The flexural modulus increased from 296.57 MPa to 470.4 MPa, while impact strength increased from 0.8222 J to 0.873 J for LLDPE - 4% FS blend. γ T_g showed

a reduction from -107.59^{o}C to -127.1^{o}C for rotational molded sample. This can be attributed to the slight variation in the material used in industry. The α T$_g$ showed no significant variation for the industrial and laboratory scale sample. The results showed improved mechanical properties in industrial scale in line with the laboratory scale studies. Hence, it can be concluded that FS provide reinforcement to LLDPE matrix enhancing the mechanical properties.

7.3.3 Viscoelastic Creep and Stress Relaxation Studies.

The master curves generated using SIM in the elastic region of polymer composite is shown in Figure 7.16. It can be noticed that, the creep strains reduced with the addition of FS. After an estimated loading of sample for one year (5.26 x 10^5 minutes) at 50°C nanocomposites with 4 wt% FS, exhibited 13% reduction in creep strains compared with natural LLDPE. The blends did not show significant variation in percentage of reduction in strains with temperature. It was observed that, blends with 4 wt% FS showed 14% creep strain reduction at 40°C for an estimated loading of 1 year in comparison with natural LLDPE. The increased creep resistance can be attributed to the reinforcement of polymer matrix with FS. Further, the stress relaxation characteristics of LLDPE and LLDPE - 4 wt% FS at predefined strain of 1% at different temperatures are shown in Figure 7.17. Detailed stress relaxation behavior of LLDPE - 4% FS for a temperature range of 30 to 100°C is shown in Figure 7.18. It shows the stress relaxation curves at successive accumulated steps of temperature increments 10°C followed by 15 min stress relaxation. There is no significant variation in the maximum resultant stress before relaxation (un-relaxed stress) for LLDPE and LLDPE - 4% FS nanocomposite at any temperature. However, the un-relaxed stress decreased continuously from a maximum of 6.57 MPa at 30°C to 0.66 MPa at 100°C for LLDPE - 4% FS.Similarly for natural LLDPE, the un-relaxed stress decreased continuously from a maximum of 6.56 MPa at 30°C to 0.64 MPa at 100°C. The reduction of un-relaxed stress at higher temperature corresponds to a reduction of storage modulus.

Figure 7.19 shows the variation of relaxation modulus of natural LLDPE and LLDPE - 4% FS with time. It can be observed that the relaxation modulus decrease with time. The relaxation modulus decreased from 621 MPa to 56 MPa for natural after being strained at 1% over a period of one year for LLDPE at 40°C. Similar decrease in relaxation modulus was observed for LLDPE - 4% FS blends. During an isothermal relaxation process, at high strain levels and higher temperatures of relaxation, the polymer chains uncoil. This results in disentangling and aligning of polymer chains causing the material to soften leading to a reduction in relaxation modulus at elevated temperatures for both LLDPE and LLDPE - 4% FS blends.
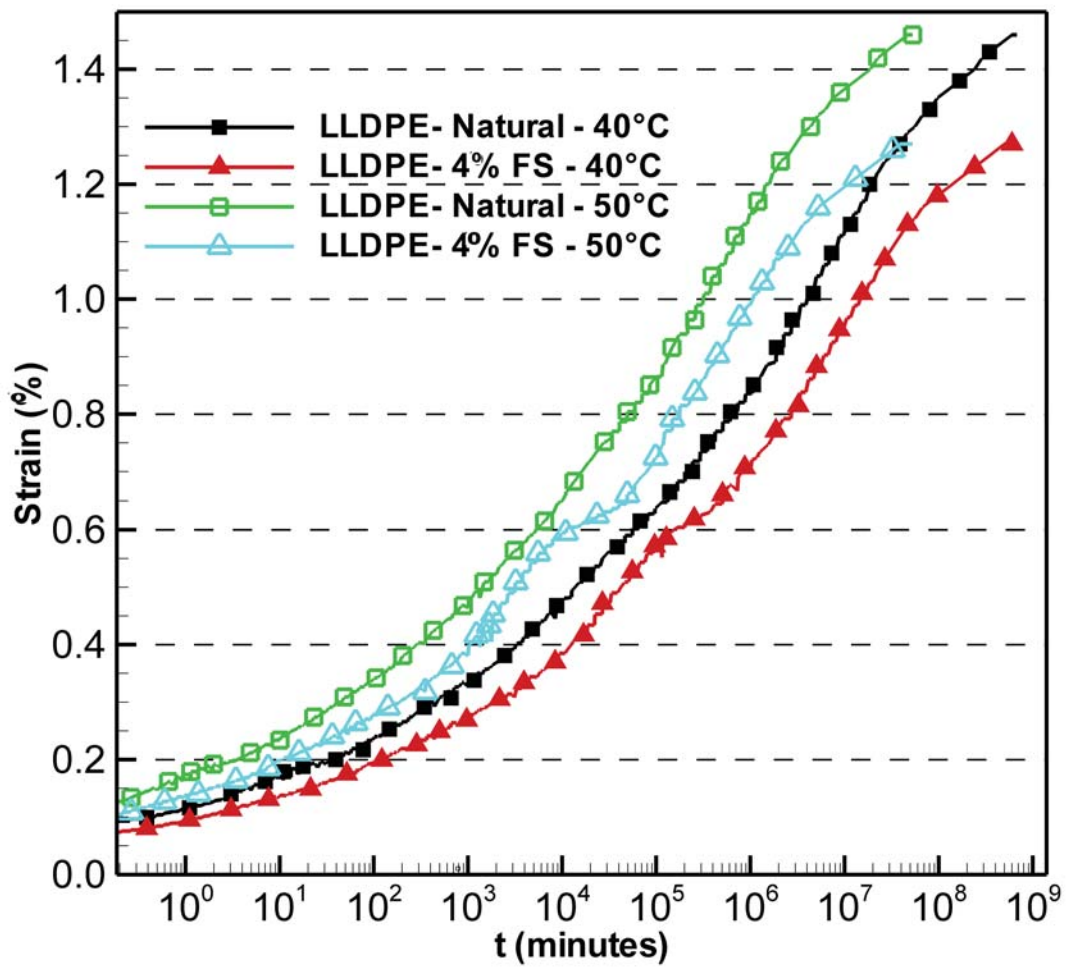
Figure 7.16: Creep master curves for natural LLDPE -4%FS FS
nanocomposites at 40ºC and 50ºC

At any temperature, the addition of FS in natural LLDPE, has not affected the
relaxation modulus and it remained almost constant.
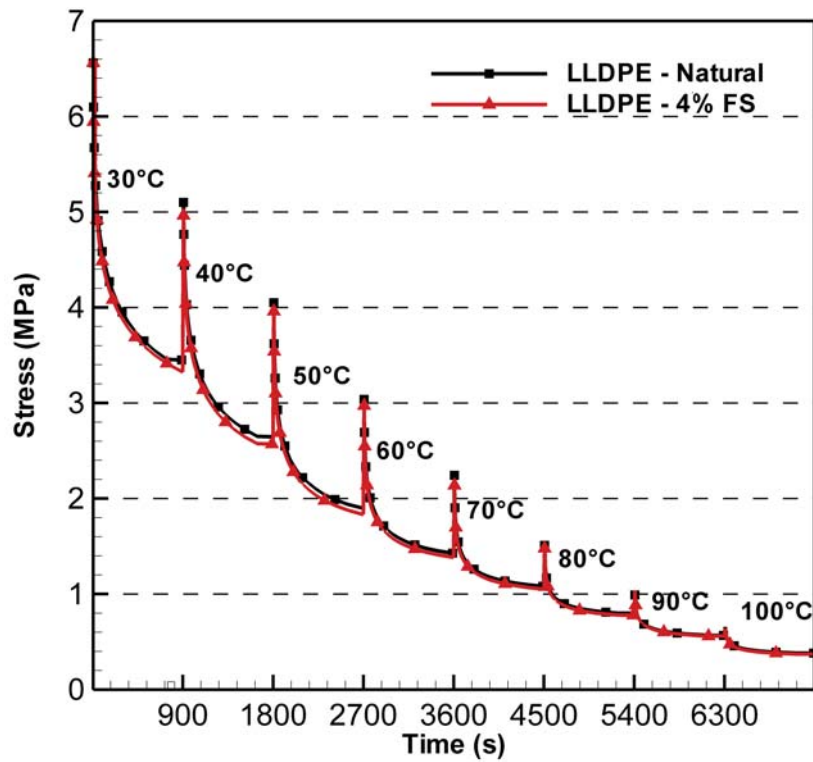
Figure 7.17: Stress relaxation curves at 1% strain at various temperatures for natural LLDPE and LLDPE - FS
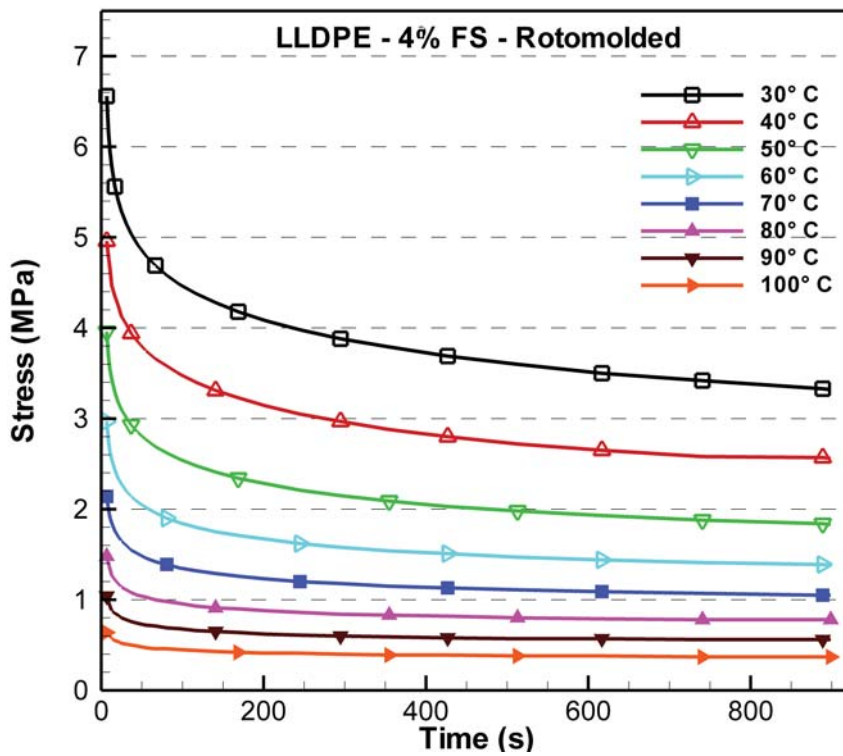
Figure 7.18: Stress relaxation curves for LLDPE - 4% FS at 1% strain
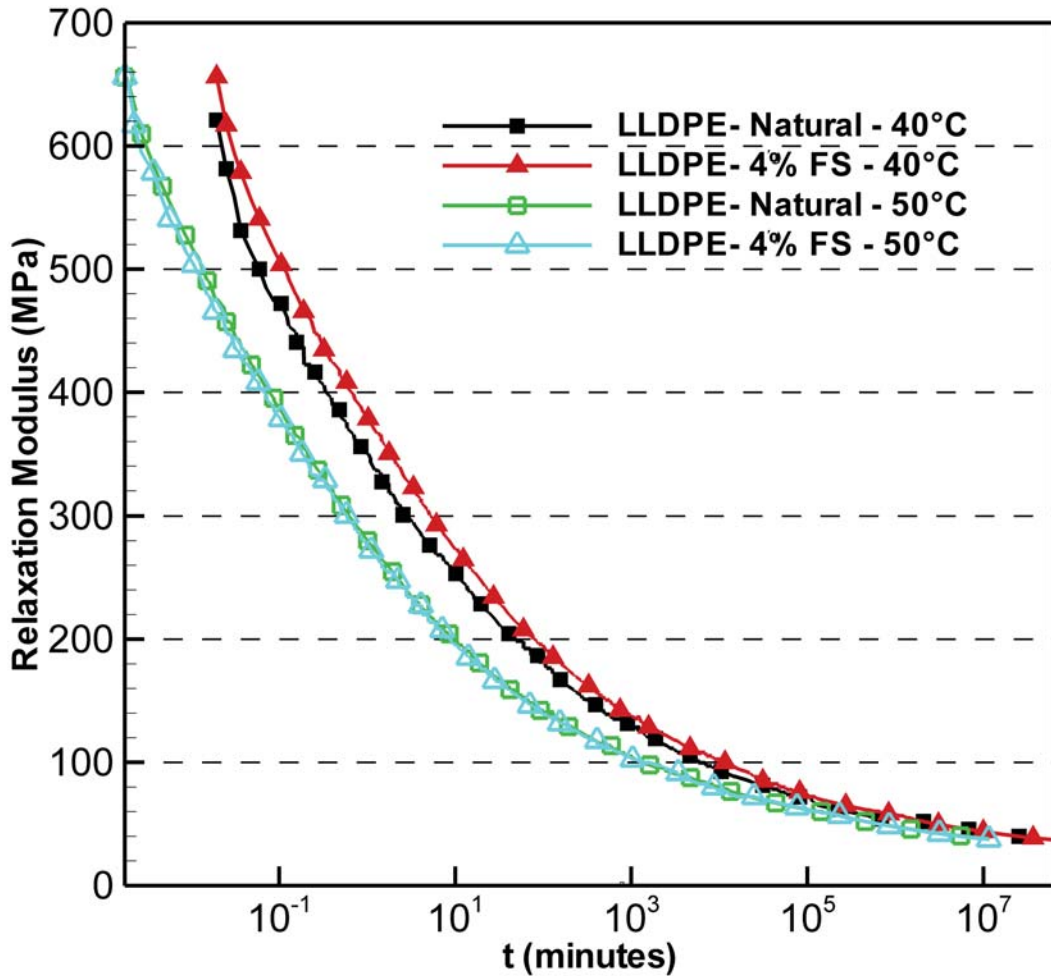
Figure 7.19: Stress relaxation master curves for natural LLDPE - 4%FS
FS nanocomposites at 40°C and 50°C

7.4 Conclusion

This chapter explores the industry scaling of nano scale FS as a reinforcement for rotationally moldable LLDPE. Melt compounding of LLDPE with 4% FS was carried out in industry to obtain fine powder suitable for rotational molding. It was found that the dry flow time was increased slightly from 10 s to 13 s while the bulk density was reduced from 0.3575 g/cc to 0.2977 g/cc with the addition of 4% FS in LLDPE. This did not affect the powder flow characteristics within the mold during molding. LLDPE - 4% FS nanocomposites were then rotationally molded in a bi-axial rotational molding machine at industrial scale. The process was carefully monitored and controlled using wireless temperature sensing device. This ensured proper curing of the rotational molded products. The products were

tested for static and dynamic mechanical properties and it was found that:

1. The LLDPE - 4% FS blends provided better product with reduced pin hole size and improved mechanical and viscoelastic properties.

2. Static Mechanical properties like tensile modulus increased from 750.43 MPa to 1882.52 MPa for LLDPE - 4% FS blends.

3. Creep properties showed a reduction of creep strains by 13% at all temperatures with the addition of 4% FS in LLDPE.

4. Stress relaxation of natural LLDPE remained constant with the addition of FS nano particles.

5. The mechanical and viscoelastic properties observed in industry trials was in comparison with the laboratory scale findings

Hence, it can be noted that nano scale FS provides good reinforcement to LLDPE matrix and can be considered as a potential additive for rotational molding. The changes in cycle time reduction in rotational molding need to studied with the addition of FS in LLDPE. It can be seen that with addition of FS, the PIAT of 200°C provided good curing and hence maintained the same cycle time during heating. Thus, it can be concluded that with addition of 4% FS in LLDPE, enhanced mechanical properties was observed without affecting the cycle time in industrial trials.

Chapter 8

Conclusions and Recommendations for Future Work

This research work focuses on developing and analyzing the effect of FS nano particle for rotational molding of LLDPE. Extensive experimentation were carried out to study the rheological and melt flow characteristics of the LLDPE FS nano-composites. The effect of FS on mechanical as well as viscoelastic properties including creep behavior and stress relaxation were investigated. The morphological and X ray diffraction studies showed the dispersion of FS and its effects on crystallinity in LLDPE. An amount of 4% by weight of FS was found suitable to improve the melt flow as well as static and dynamic mechanical properties of rotational moldable LLDPE. Finally, the LLDPE - 4% FS blends were tested at industrial scale for a rotationally molded product and the results were compared with the laboratory scale findings. The important conclusions of this study are as follows:

1. LLDPE - FS nano composites were prepared in laboratory using dry mixing and melt mixing methods. MFI studies and dynamic rheological studies were carried out to study the melt and rheological characteristics of polymer blends. The MFI for natural LLDPE reduced from 4.49 g/10 min to 3.14 g/10 min with the addition of 8% FS. At 4% FS composition MFI recorded 3.65% making it suitable for rotational molding. The melt viscosity observed at lower frequencies (shear rates) during dynamic rheological studies, showed very close match with the viscosity calculated using MFI studies. For LLDPE - 4% FS blends at 0.1 - 10 rad/s, the calculated viscosity of 1418.4 Pa.s using MFI studies is close to 1494.7 Pa.s using rheometry studies. Similar observation was made for natural LLDPE and LLDPE - 2% FS blends at low shear rates. Zero shear viscosity of 3430 Pa.s was observed for natural LLDPE at low angular frequency of 0.01 rad/sec indicating the plateauing of viscosity plots at low frequency. For LLDPE - FS blends plateauing of viscosity plots were not observed and an increasing trend of viscosity at low

frequency was observed. This behavior was predominantly due to the nano filler polymer chain interactions indicating higher melt shear resistance. The torque rheometry studies carried out revealed the increased initial torque requirements for blending. To some extent, this can be reduced by increasing temperature. As thermal degradation of the material was noticed, with addition of FS, careful process control is necessary. Finally, owing to the optimal MFI requirements, a maximum of 4% FS blend in LLDPE can be recommended for rotational molding. This blend was found to be thermally stable and did not affect the processing window of LLDPE.

2. To study the reinforcement effects of FS in LLDPE matrix, dynamic mechanical analysis was carried out. It was observed that the storage modulus improved from 1143 MPa to 1408 MPa for LLDPE - 4% FS blends at 30°C. Similarly loss modulus also improved from 96 MPa to 107 MPa for LLDPE - 4% FS blends at 30°C. Above 4% FS concentration, reduction in storage modulus was observed and was attributed to the agglomeration of FS at higher concentrations. Shift in the α T_g towards higher values was noticed. α T_g increased from 43.5°C to 49°C indicating increased operating temperature range for LLDPE - FS blends. The γT_g at -120°C was not significantly affected with the addition of FS in LLDPE.

3. The frequency studies conducted in range of 0.01 Hz to 200 Hz at 30°C showed a tan delta peak at 63 Hz for natural LLDPE and LLDPE - FS blends representing a glass transition frequency. At this frequency, $G^{'}$ increased from 1074 MPa for natural LLDPE to 1346 MPa for 4% FS concentration. For practical purpose this frequency (63 Hz) can be regarded as the limiting frequency of the material due to the breakdown of polymer chain and silica network. The time dependent creep behavior of LLDPE also showed a reduction of 11% creep strains over a span of 1 year at 40°C with the addition of 4% FS. The viscoelastic studies thus proves the suitability of FS in LLDPE making it a potential nano composite for use in rotational molding.

4. The static mechanical properties of LLDPE - FS blends were found to be superior than natural LLDPE. Tensile testing, flexural tests and impact tests were carried out to evaluate the static mechanical properties. The tensile modulus improved from 818 MPa to 1180.46 MPa for LLDPE - 4% FS blends. Further, a reduction in crystallinity along with an increase in tensile toughness of the material was observed. Tensile toughness improved by 300% and 200% for LLDPE - 2% FS and for LLDPE - 4% FS blends. The flexural

modulus for natural LLDPE showed an increase from 534.71 MPa to 624.18 MPa for 5% FS composition at a cross head speed of 50 mm/min. The Izod impact test showed comparable impact strength for LLDPE and LLDPE - FS blends, showcasing the occupancy of FS in amorphous regions of LLDPE, did not affect the shock absorption ability of LLDPE. The micro structural studies using SEM showed FS was well dispersed in LLDPE matrix at low concentrations, providing matrix reinforcement and enhancing the mechanical properties. At higher concentrations of FS in LLDPE, agglomeration was observed in tensile fractured surface leading to brittle fractures and reduced toughness. FS contents above 4 wt% are detrimental to the mechanical properties due to agglomeration. This necessitates a careful control over the dispersion of the nano composites within the polymer matrix.

5. Along with improvement in melt flow characteristics, static and dynamic mechanical properties , the effect on processibility of the LLDPE - FS composites was studied. Since cycle time reduction is a crucial aspects of processibility , attempts were made to reduce the cycle time during cooling stage of the process. For this purpose, an alternative approach was followed in which an innovative fixture was developed to study the adhesion force by measuring the pulling force required to demold the product. It was found out, that the addition of FS in LLDPE reduced the pulling force needed to eject the part from the mold made of aluminum and steel at higher temperatures. The minimum pulling force (for LLDPE - FS blends) needed to remove the part from its mold was observed at 80°C. Hence, it can be recommended as an ideal temperature to demold the product from its mold. Also, for a typical cooling rate of 4.5°C/min a savings of 6.7 min can be obtained by removing the part at 80°C instead of 50°C. This indicate easy removal and reduced cycle times for LLDPE - 4% FS parts and thus can be considered as ideal for their use in rotational molding.

6. To check the feasibility of the nano composites at industrial scale trials using LLDPE - 4% FS were conducted. LLDPE - 4% FS blend was compounded in an industrial melt extruder and pulverizer at Kenwood Industries, Goa. The baffles for underground septic tanks were rotationally molded using a three arm bi-axial rotational molding machine at GMI Zarahak Industries, Goa. Throughout the process IAT was monitored for proper curing of samples. The inner surface of LLDPE - 4% FS rotationally molded part exhibited lower sized pin holes in comparison with natural LLDPE part. A maximum pin hole size of 65 μm was observed in LLDPE - 4% FS part, in lieu of 220 μm for natural LLDPE. Improved mechanical properties were also observed for

LLDPE - 4% FS nano composites. The ultimate tensile modulus for industry sample recorded 1882.52 MPa in comparison to 1180.46 MPa for LLDPE - 4% blend. The flexural modulus increased from 296.57 MPa to 470.4 MPa, while impact strength increased from 0.8222 J to 0.873 J for LLDPE - 4% FS blend. Similarly, viscoelastic creep studies showed a reduction of creep strains by 13% at all temperatures with the addition of 4% FS in LLDPE. Hence, it can be concluded that with the LLDPE - 4% FS nano composite provides better mechanical properties with acceptable melt characteristics and can be thus be considered as an improved material for rotational molding.

7. As the rotational molding industry is currently looking for alternative materials that can be used to produce products with improved mechanical properties, the recommendations developed in this study, (being tested in industry) can be readily applied to industrial products. Thus the thesis can be regarded as a significant contribution to the rotational molding industry.

8.1 Recommendations for Future Work

This research work demonstrated the possibility of using nano composites for rotational molding. As there is a need to develop better materials and composites for rotational molding, the current research work can be further extended to study the following promising areas in rotational molding:

1. The usage of FS can be extended to polypropylene for the use in RM. Currently rotationally moldable PP is developed and is gaining popularity due to its improved mechanical properties. FS nano particles may provide reinforcement to the polymer chains thereby providing good melt shear strength and enhanced mechanical properties.

2. The demonstrated improved properties of LLDPE - FS nano composites make it suitable for rotolining. The usage of LLDPE - FS nano composites in rotolining need to be investigated. This study will further enhance the suitability and acceptance of FS in rotationally moldable LLDPE.

3. Warpage of parts is a major concern for the rotational molder, particularly when the thickness of the part is large. Hence studies can be undertaken to

investigate warpage of LLDPE - FS nano composites.

4. Finally the simulations studies can be undertaken to study the flow of molten polymer within the mold by taking into account the changes in material properties reported in this work.

References

[1] R J Crawford and Throne J.L. *Rotational molding Technology*. Plastics Design Library William Andrew Publishing, 2002.

[2] A Shah. New grades expand the horizon of rotomoulding. *Reliance Industries, ARMO 2013, Rotomoulding conference*, Goa, India, 2013.

[3] R J Crawford and J A Scott. The formation and removal of gas bubbles in a rotational molding grade of pe. *Plast. Rubber Proc. Appl*, 7(2):85–99, 1987.

[4] A G Spence and R J Crawford. Removal of pin-holes and bubbles from rotationally moulded products. *Proc. Instn. Mech. Engrs., Part B, J.Eng. Man*, 210:521–533, 1996.

[5] R J Crawford. Causes and cures of rotomolding problems. *Rotation*, 3:10–14, 1994.

[6] K O Walls R J Crawford. Shrinkage and warpage of rotationally molded parts. *paper presented at Society of Plastics Engineers (SPE) Topical Conference on Rotational Molding, Cleveland,OH*, 1999.

[7] A G Spence and R J Crawford. The effect of processing variables on the formation and removal of bubbles in rotationally molded products. *Polymer Engineering & Science*, 36(7):993–1009, 1996.

[8] R J Crawford and S Gibson. Rotational moulding, the basics for designers. *Rotation*, July/August, 2000.

[9] G Gogos. Bubble Removal in Rotational Molding. *Polymer Engineering and Science*, 44(2):388–394, 2004.

[10] R J Crawford and P J Nugent. A new process control system for rotational moulding. *Plastics Rubber and Composites Processing and Applications*, 17(1):22–31, 1992.

[11] O Wandres. Contemporary mold developments. *ARMO 2013, Rotomoulding conference*, Goa, India, 2013.

[12] A Bazargan and G McKay. A review - Synthesis of carbon nanotubes from plastic wastes. *Chemical Engineering Journal*, 195-196:377–391, 2012.

[13] G Chang, Ling He, W Zheng, A Pan, J Liu, Y Li, and R Cao. Well-defined inorganic/organic nanocomposite by nano silica core-poly(methyl methacrylate/butylacrylate/trifluoroethyl methacrylate) shell. *Journal of Colloid and Interface Science*, 396:129–137, 2013.

[14] A Dorigato and A Pegoretti. (Re)processing effects on linear low-density polyethylene/silica nanocomposites. *Journal of Polymer Research*, 20(3), 2013.

[15] S Sahebian, S M Zebarjad, J Vahdati Khaki, and S A Sajjadi. The effect of nano-sized calcium carbonate on thermodynamic parameters of HDPE. *Journal of Materials Processing Technology*, 209(3):1310–1317, 2009.

[16] E Bafekrpour, G P Simon, Minoo N, J Habsuda, C Yang, and B Fox. Preparation and properties of composition-controlled carbon nanofiber/phenolic nanocomposites. *Composites Part B: Engineering*, 52(0):120–126, 2013.

[17] C Garzón and H Palza. Electrical behavior of polypropylene composites melt mixed with carbon-based particles: Effect of the kind of particle and annealing process. *Composites Science and Technology*, 99(0):117–123, 2014.

[18] E Kontou and M Niaounakis. Thermo-mechanical properties of LLDPE/SiO2 nanocomposites. *Polymer*, 47(4):1267–1280, 2006.

[19] O Jacobs and B Schädel. Chapter 9 - Wear behavior of carbon nanotube-reinforced polyethylene and epoxy composites. In Klaus Friedrich and Alois K Schlarb, editors, *Tribology of Polymeric Nanocomposites (Second Edition)*, pages 307–352. Butterworth-Heinemann, Oxford, 2013.

[20] Y Wang, R Cheng, L Liang, and Y Wang. Study on the preparation and characterization of ultra-high molecular weight polyethylene–carbon nanotubes composite fiber. *Composites Science and Technology*, 65(5):793–797, 2005.

[21] R M Guedes, C M C Pereira, A Fonseca, and Mónica S A Oliveira. The effect of carbon nanotubes on viscoelastic behaviour of biomedical grade ultra-high molecular weight polyethylene. *Composite Structures*, 105(0):263–268, 2013.

[22] T T Dang, M Nikkhah, A Memic, and A Khademhosseini. Chapter 19 - Polymeric Biomaterials for Implantable Prostheses. In Sangamesh G Kumbar, Cato T Laurencin, and Meng Deng, editors, *Natural and Synthetic Biomedical Polymers*, pages 309–331. Elsevier, Oxford, 2014.

[23] M Naffakh, A M. Díez-Pascual, C Marco, G J. Ellis, and M Gómez-Fatou. Opportunities and challenges in the use of inorganic fullerene-like nanoparticles to produce advanced polymer nanocomposites. *Progress in Polymer Science*, 38(8):1163–1231, 2013.

[24] J Jancar, J F Douglas, F W Starr, S K Kumar, P Cassagnau, A J Lesser, S S Sternstein, and M J Buehler. Current issues in research on structure-property relationships in polymer nanocomposites. *Polymer*, 51(15):3321–3343, 2010.

[25] R J Kane, G L Converse, and R K Roeder. Effects of the reinforcement morphology on the fatigue properties of hydroxyapatite reinforced polymers. *Journal of the Mechanical Behavior of Biomedical Materials*, 1(3):261–268, 2008.

[26] R Ou, H Zhao, S Sui, Y Song, and Q Wang. Reinforcing effects of Kevlar fiber on the mechanical properties of wood-flour/high-density-polyethylene composites. *Composites Part A: Applied Science and Manufacturing*, 41(9):1272–1278, 2010.

[27] S Siengchin and J Karger-Kocsis. Binary and ternary composites of polystyrene , styrene − butadiene rubber and boehmite produced by water-mediated melt compounding : Morphology and mechanical properties. *Composites Part B*.

[28] J A Molefi, A S Luyt, and I Krupa. Comparison of the influence of copper micro and nano particles on the mechanical properties of polyethylene/copper composites. *Journal of Materials Science*, 45(1):82–88, 2009.

[29] S K Esthappan, S K Kuttappan, and R Joseph. Thermal and mechanical properties of polypropylene/titanium dioxide nanocomposite fibers. *Materials and Design*, 37:537–542, 2012.

[30] E Yilgor, T Eynur, C Kosak, S Bilgin, I Yilgor, O Malay, Y Menceloglu, and G L. Wilkes. Fumed silica filled poly(dimethylsiloxane-urea) segmented copolymers: Preparation and properties. *Polymer (United Kingdom)*, 52(19):4189–4198, 2011.

[31] J Kalfus, J Jancar, and J Kucera. Effect of weakly interacting nanofiller on the morphology and viscoelastic response of polyolefins. *Polymer Engineering & Science*, 48(5):889–894, 2008.

[32] S Karamipour, H Ebadi-Dehaghani, D Ashouri, and S Mousavian. Effect of nano-CaCO3 on rheological and dynamic mechanical properties of polypropylene: Experiments and models. *Polymer Testing*, 30(1):110–117, 2011.

[33] Y Lin. *Polymer Viscoelasticity Basics,Molecular Theories,Experiments and Simulations*. World Scientific Publishing Co. Pte. Ltd, 2nd edition edition, 2011.

[34] S W Shang, J W Williams, and K J M Soderholm. No Title. *Journal of Material Science*, 30(17):4323–4334, 1995.

[35] P Cassagnau. Linear viscoelasticity and dynamics of suspensions and molten polymers filled with nanoparticles of different aspect ratios. *Polymer (United Kingdom)*, 54(18):4762–4775, 2013.

[36] H Gao, Y Xie, R Ou, and Q Wang. Grafting effects of polypropylene/polyethylene blends with maleic anhydride on the properties of the resulting wood–plastic composites. *Composites Part A: Applied Science and Manufacturing*, 43(1):150–157, 2012.

[37] M Bailly and M Kontopoulou. No Title. *Polymer*, 50(11):2472–2480, 2009.

[38] M Bailly, M Kontopoulou, and K El Mabrouk. Effect of polymer/filler interactions on the structure and rheological properties of ethylene-octene copolymer/nanosilica composites. *Polymer*, 51(23):5506–5515, 2010.

[39] H Barthel, M Heinemann, M Stintz, and B Wessely. Particle sizes of fumed silica. *Particle & Particle Systems Characterization*, 16(4):169–176, 1999.

[40] M I Aranguren. Effect of reinforcing fillers on the rheology of polymer melts. *Journal of Rheology*, 36(6):1165, 1992.

[41] S Barus, M Zanetti, M Lazzari, and L Costa. Preparation of polymeric hybrid nanocomposites based on PE and nanosilica. *Polymer*, 50(12):2595–2600, 2009.

[42] J Tarrio-Saavedra. Controversial effects of fumed silica on the curing and thermomechanical properties of epoxy composites. *eXPRESS Polymer Letters*, 4(6):382–395, 2010.

[43] A Dorigato, Y Dzenis, and A Pegoretti. Filler aggregation as a reinforcement mechanism in polymer nanocomposites. *Mechanics of Materials*, 61:79–90, 2013.

[44] D M Panaitescu, A Nicoleta Frone, and I C Spataru. Effect of nanosilica on the morphology of polyethylene investigated by AFM. *Composites Science and Technology*, 74:131–138, 2013.

[45] M I Sarwar, S Zulfiqar, and Z Ahmad. Polyamide-silica nanocomposites: mechanical, morphological and thermomechanical investigations. *Polymer International*, 57(2):292–296, 2007.

[46] F Yang, Y Ou, and Z Yu. Polyamide 6/silica nanocomposites prepared by in situ polymerization. *Journal of Applied Polymer Science*, 69(2):355–361, 1998.

[47] W G Hahm, H S Myung, and S S Im. Preparation and properties of in situ polymerized Poly(ethylene terephthalate)/fumed silica nanocomposites. *Macromolecular Research*, 12(1):85–93, 2004.

[48] Christmann, A, Ienny, P, Quantin, J C , Caro-Bretelle, A S , and J M Lopez-Cuesta. Mechanical behaviour at large strain of polycarbonate nanocomposites during uniaxial tensile test. *Polymer*, 52(18):4033–4044, 2011.

[49] T Jiang, T Kuila, N H Kim, B C Ku, and J H Lee. Enhanced mechanical properties of silanized silica nanoparticle attached graphene oxide/epoxy composites. *Composites Science and Technology*, 79:115–125, 2013.

[50] M Preghenella, A Pegoretti, and C Migliaresi. Thermo-mechanical characterization of fumed silica-epoxy nanocomposites. *Polymer*, 46(26):12065–12072, 2005.

[51] P Cassagnau and F. Mélis. Non-linear viscoelastic behaviour and modulus recovery in silica filled polymers. *Polymer*, 44(21):6607–6615, 2003.

[52] K Chrissafis, K M Paraskevopoulos, E Pavlidou, and D Bikiaris. Thermal degradation mechanism of HDPE nanocomposites containing fumed silica nanoparticles. *Thermochimica Acta*, 485(1-2):65–71, 2009.

[53] A Vasileiou, G Z. Papageorgiou, M Kontopoulou, A Docoslis, and D Bikiaris. Covalently bonded poly(ethylene succinate)/SiO2 nanocomposites prepared by in situ polymerisation. *Polymer (United Kingdom)*, 54(3):1018–1032, 2013.

[54] J Raghavan and M Meshii. Creep rupture of polymer composites. *Composites Science and Technology*, 57(4):375–388, 1997.

[55] B A Acha, María M R, and N E Marcovich. Creep and dynamic mechanical behavior of PP-jute composites: Effect of the interfacial adhesion. *Composites Part A: Applied Science and Manufacturing*, 38(6):1507–1516, 2007.

[56] B H Amir and M Iskander. Predicting Compressive Creep Behavior of virgin HDPE using Thermal Acceleration. *Journal of Materials in Civil Engineering*, 23(8):1154–1162, 2011.

[57] J Lai and A Bakker. Non-linear creep and recovery behaviour of high-density polyethylene. *Scripta Metallurgica et Materialia*, 28(11):1447–1452, 1993.

[58] J Lai and A Bakker. Analysis of the non-linear creep of high-density polyethylene. *Polymer*, 36(1):93–99, 1995.

[59] D W Hadley and I M Ward. Non-linear creep and recovery behaviour of polypropylene fibres. *Journal of the Mechanics and Physics of Solids*, 13(6):397–411, 1965.

[60] L J Zapas and J M Crissman. Creep and recovery behaviour of ultra-high molecular weight polyethylene in the region of small uniaxial deformations. *Polymer*, 25(1):57–62, 1984.

[61] G J Osanaiye and K P Adewale. Creep and recovery of EPDM elastomer using a modified sandwich rheometer. *Polymer Testing*, 20(4):363–370, 2001.

[62] J F Mano, V Sencadas, A. Mello Costa, and S Lanceros-Méndez. Dynamic mechanical analysis and creep behaviour of β-PVDF films. *Materials Science and Engineering A*, 370(1-2):336–340, 2004.

[63] K Nitta and H Maeda. Creep behavior of high density polyethylene under a constant true stress. *Polymer Testing*, 29(1):60–65, 2010.

[64] Yu Jia, Ke Peng, X L Gong, and Z Zhang. Creep and recovery of polypropylene/carbon nanotube composites. *International Journal of Plasticity*, 27(8):1239–1251, 2011.

[65] M Abu-Abdeen. The unusual effect of temperature on stress relaxation and mechanical creep of polycarbonate at low strain and stress levels. *Materials and Design*, 34:469–473, 2012.

[66] S Siengchin and József Karger-Kocsis. Creep behavior of polystyrene/fluorohectorite micro- And nanocomposites. *Macromolecular Rapid Communications*, 27(24):2090–2094, 2006.

[67] R Seltzer, Y W Mai, and P M. Frontini. Creep behaviour of injection moulded polyamide 6/organoclay nanocomposites by nanoindentation and cantilever-bending. *Composites Part B: Engineering*, 43(1):83–89, 2012.

[68] F Achereiner, K Engelsing, M Bastian, and P Heidemeyer. Accelerated creep testing of polymers using the stepped isothermal method. *Polymer Testing*, 32(3):447–454, 2013.

[69] D Gamby, M C Lafarie-Frenot, A Vinet, and D Guedra-Degeorge. The prediction of the long-term mechanical behaviour of aeronautical laminates. *Composites Science and Technology*, 61(3):439–443, 2001.

[70] G Yang, H Liu, Peng Lv, and B Zhang. Geogrid-reinforced lime-treated cohesive soil retaining wall: Case study and implications. *Geotextiles and Geomembranes*, 35(0):112–118, 2012.

[71] G Q Yang, H Liu, Yi-Tao Zhou, and B L Xiong. Post-construction performance of a two-tiered geogrid reinforced soil wall backfilled with soil-rock mixture. *Geotextiles and Geomembranes*, 42(2):91–97, 2014.

[72] S.-S. Yeo and Y G Hsuan. Evaluation of creep behavior of high density polyethylene and polyethylene-terephthalate geogrids. *Geotextiles and Geomembranes*, 28(5):409–421, 2010.

[73] K. G N C Alwis and C. J. Burgoyne. Accelerated creep testing for aramid fibres using the stepped isothermal method. *Journal of Materials Science*, 43(14):4789–4800, 2008.

[74] A Pegoretti. Creep and Fatigue Behavior of Polymer Nanocomposites. In József Karger-Kocsis and Stoyko Fakirov, editors, *Nano- and Mircro- Mechanics of Polymer Blends and Composites*, pages 301–339. Hanser, 2009.

[75] P Cassagnau. Melt rheology of organoclay and fumed silica nanocomposites. *Polymer*, 49(9):2183–2196, 2008.

[76] A D Drozdov, A L Høg Lejre, and C J Christiansen. Viscoelasticity, viscoplasticity, and creep failure of polypropylene/clay nanocomposites. *Composites Science and Technology*, 69(15-16):2596–2603, 2009.

[77] K Hayashida, H Tanaka, and O Watanabe. Miscible blends of poly(butyl methacrylate) densely grafted on fumed silica with poly(vinyl chloride). *Polymer*, 50(26):6228–6234, 2009.

[78] E Voldner. Crosslinked Polyethylene Scrap Can Be Recycled, 1999.

[79] S X Zhou, L M Wu, J Sun, and W D Shen. Effect of nanosilica on the properties of polyester-based polyurethane. *Journal of Applied Polymer Science*, 88(1):189–193, 2003.

[80] H S Vaziri, I A Omaraei, M Abadyan, M Mortezaei, and N Yousefi. Thermophysical and rheological behavior of polystyrene/silica nanocomposites: Investigation of nanoparticle content. *Materials and Design*, 32(8-9):4537–4542, 2011.

[81] M Gahleitner. Melt Rheology of Polyolefines. *Progress in Polymer Science*, 26:895–944, 2001.

[82] S H Kim, S H Ahn, and T Hirai. Crystallization kinetics and nucleation activity of silica nanoparticle-filled poly(ethylene 2,6-naphthalate). *Polymer*, 44(19):5625–5634, 2003.

[83] Oh Seong-Geun. Poly(ethylene terephthalate)(PET) Nanocomposites Filled with Fumed Silicas by melt compounding. *Macromolecular Research*, 10(4):221–229, 2002.

[84] L C Wu, P Chen, J Chen, J Zhang, and J S He. Noticeable viscosity reduction of polycarbonate melts caused jointly by nano-silica filling and TLCP fibrillation. *Polymer Engineering and Science*, 47(6):757–764, 2007.

[85] Martinez, J M, Augullo, T G, Juan, C M, Fernandez, G A, Barcelo, C O, and A T Palau. Properties of solvent based polyurethane adhesives containing fumed silicas. *Macromolecular Symposia*, 108(1):269–272, 1996.

[86] J M Dealy and R G Larson. *Structure and Rheology of Molten Polymers - From structure to flow behavior and back again*. Hanser Gardner Publications, 2006.

[87] A A Askadskii. *Computational Material Science of Polymers*. Cambridge International Science publishing Viva Books, 1st indian edition edition, 2009.

[88] M Yousfi, S Alix, M Lebeau, J Soulestin, M F Lacrampe, and P Krawczak. Evaluation of rheological properties of non-Newtonian fluids in micro rheology compounder: Experimental procedures for a reliable polymer melt viscosity measurement. *Polymer Testing*, 40(0):207–217, 2014.

[89] M H Wagner, H Bastian, P Ehrecke, M Kraft, P Hachmann, and J Meissner. Nonlinear viscoelastic characterization of a linear polyethylene (HDPE) melt in rotational and irrotational flows. *Journal of Non-Newtonian Fluid Mechanics*, 79(2–3):283–296, 1998.

[90] F J Stadler and H Münstedt. Numerical description of shear viscosity functions of long-chain branched metallocene-catalyzed polyethylenes. *Journal of Non-Newtonian Fluid Mechanics*, 151(1–3):129–135, 2008.

[91] A Mejía, N García, Julio Guzmán, and P Tiemblo. Extrusion Processed Polymer Electrolytes based on Poly(ethylene oxide) and Modified Sepiolite Nanofibers: Effect of Composition and Filler Nature on Rheology and Conductivity. *Electrochimica Acta*, 137(0):526–534, 2014.

[92] J H Zhou, R X. Zhu, J M Zhou, and M B. Chen. Molecular dynamics simulation of diffusion of gases in pure and silica-filled poly(1-trimethylsilyl-1-propyne) [PTMSP]. *Polymer*, 47(14):5206–5212, 2006.

[93] J Zhang, J Lou, S Ilias, P Krishnamachari, and J Yan. Thermal properties of poly(lactic acid) fumed silica nanocomposites: Experiments and molecular dynamics simulations. *Polymer*, 49(9):2381–2386, 2008.

[94] K Lee and M R Mackley. The significance of slip in matching polyethylene processing data with numerical simulation. *Journal of Non-Newtonian Fluid Mechanics*, 94(2–3):159–177, 2000.

[95] Y Rémond. Constitutive modelling of viscoelastic unloading of short glass fibre-reinforced polyethylene. *Composites Science and Technology*, 65(3–4):421–428, 2005.

[96] C S Wu and H T Liao. Modification of polyethylene–octene elastomer by silica through a sol–gel process. *Journal of Applied Polymer Science*, 88:966–972, 2003.

[97] N Vu-Bac, T Lahmer, H Keitel, J Zhao, X Zhuang, and T Rabczuk. Stochastic predictions of bulk properties of amorphous polyethylene based on molecular dynamics simulations. *Mechanics of Materials*, 68(0):70–84, 2014.

[98] A Dorigato, A Pegoretti, and A Penati. Linear low-density polyethylene/silica micro- and nanocomposites: Dynamic rheological measurements and modelling. *Express Polymer Letters*, 4(2):115–129, 2010.

[99] E F Voronin, V M Gun'ko, N V Guzenko, E M Pakhlov, L. V Nosach, R Leboda, J Skubiszewska-Zięba, M L Malysheva, M V Borysenko, and A A Chuiko. Interaction of poly(ethylene oxide) with fumed silica. *Journal of Colloid and Interface Science*, 279(2):326–340, 2004.

[100] L R Bocayuvaa, A S Gomesa, C M F Oliveiraa, and M C V Amorimb. Rheological properties of blends of polycarbonate with poly(ethylene oxide). *Polymer Testing*, 19:321–327, 2000.

[101] Rosales, J A, Arias, G, Rodrõ Âguez, O.S, and N S Allen. Viscosity changes associated with the chemically induced cross linking of plasticized poly(vinyl chloride) measured by parallel plate and torque rheometry: influence of magnesium and barium mercaptide. *Polymer Degradation and Stability*, 68:253–259, 2000.

[102] G A Ari. Using torque rheometer to characterise flow in PVC composites. *Plastics research online*, (10.1002 / spepro.003287.):2, 2010.

[103] L Einar, H Hinrichsen, and S Sintef. Effects of Processing and Degree of Fusion on the Rheology of PVC. *Journal of Vinyl and Additive Technology*, 2(1):18–29, 1996.

[104] W Hale, H Keskkula, and D R Paul. Effect of cross linking reactions on blends of pbt/abs blends. *Polymer*, 40:3665–3676, 1999.

[105] A M Robinson, B Haworth, and A W Birley. Elongational Rheometry of Polyethylene terephthalate / Bisphenol-A Polycarbonate blends. *European Polymer Journal*, 32(9):1061–1066, 1996.

[106] B Muller, J Lowe, D Braeunig, and E McClellan. The ABC of Rotational Molding PVC, 1996.

[107] W Q Wang and M Kontopoulou. Rotational molding of polypropylene/ultra-low-density ethylene-??-olefin copolymer blends. *Polymer Engineering and Science*, 44(9):1662–1669, 2004.

[108] K B Kinghorn. Developing ABS Materials for Rotational Molding. *ARM Fall Conference, Clevland, USA*, 1999.

[109] B Mansure and A B Strong. Optimization of Rotational Molding of Acrylic Filled with Ethylene Methyl Acrylate. *Rotation*, 6(3):21–28, 1997.

[110] E Rabinovitz and Z Rigbi. Rotational Reaction Molding of Polyurethane. *Plastics and Rubber Processing and Applications*, 5:365–368, 1985.

[111] W Yan, R J T Lin, and D Bhattacharyya. Mechanical Properties of Rotational Moulded Polyethylene Composites - Experiments and Theories. In L Ye, Y W Mai, and Z Su, editors, *Composite Technologies for 2020*, pages 154–162. Woodhead Publishing, 2004.

[112] J Olinek, C Anand, and C T Bellehumeur. Experimental study on the flow and deposition of powder particles in rotational molding. *Polymer Engineering and Science*, 45(1):62–73, 2005.

[113] L Therese and E Harkin-Jones. An Investigation Into the Relationship Between the Impact Performance of Rotationally Molded Polyethylene Products and Their Dynamic Mechanical Properties. *Polymer Engineering and Science*, 43(4):905–918, 2003.

[114] A Greco, G Romano, and A Maffezzoli. Selective reinforcement of lldpe components produced by rotational molding with thermoplastic matrix pultruded profiles. *Composites Part B: Engineering*, 56:157–162, 2014.

[115] W. Yan, R. J. T. Lin, and D. Bhattacharyya. Particulate reinforced rotationally moulded polyethylene composites – mixing methods and mechanical properties. *Composites Science and Technology*, 66(13):2080–2088, 2006.

[116] O Kulikov, K. Hornung, and M. Wagner. Novel processing additives for rotational molding of polyethylene. *International Polymer Processing*, 24(5):452–462, 2009.

[117] L T Pick and E H Jones. An investigation into the relationship between the impact performance of rotationally molded polyethylene products and their dynamic mechanical properties. *Polymer Engineering & Science*, 43(4):905–918, 2003.

[118] O Kulikov, K Hornung, and M Wagner. Control of nano-scale structuring and reinforcement in rotational molding of polyethylene. *Macromolecular Symposia*, 296(1):324–335, 2010.

[119] X Yin, L Hong, and Z Liu. A study on the fundamental ceramic–polymer interactions in the high CeO2-loading polyethylene glycol blend. *Journal of the European Ceramic Society*, 25(13):3097–3107, 2005.

[120] C I Rogers, J B Oxborrow, R R Anderson, L F Tsai, G P Nordin, and A T Woolley. Microfluidic valves made from polymerized polyethylene glycol diacrylate. *Sensors and Actuators B: Chemical*, 191(0):438–444, 2014.

[121] M Salarian, M Solati-Hashjin, S S Shafiei, R Salarian, and Z A Nemati. Template-directed hydrothermal synthesis of dandelion-like hydroxyapatite in the presence of cetyltrimethylammonium bromide and polyethylene glycol. *Ceramics International*, 35(7):2563–2569, 2009.

[122] S B Tan, P R Hornsby, M B McAfee, M P Kearns, and M P McCourt. Internal cooling in rotational molding-A review. *Polymer Engineering & Science*, 51(9):1683–1692, 2011.

[123] E Maziers. Rotomolded articles prepared with polyethylene. *Patent Appliction Number 20050255264, USA*, (20050255264), 2005.

[124] Swain R.D. Resin pallets for rotational molding. *Patent Application Number: 6682685*, (6682685), 2004.

[125] M W Sowa. Compound for pinhole-free rotational casting. (3974114), 1976.

[126] D G Needham. Polymers and rotationally molding same. *Patent Application Number: 4668461, USA*, (4668461), 1987.

[127] E Maziers. Use of fluropolymers for rotational molding. *Patent Application Number: 20080018019, USA*, (20080018019), 2008.

[128] J M Dealy and R G Larson. *Structure and Rheology of Molten Polymers. From Structure to Flow Behavior and Back again*. Hanser, Munich, 2006.

[129] S Mould, J Barbas, A V MacHado, J M Nóbrega, and J A Covas. Measuring the rheological properties of polymer melts with on-line rotational rheometry. *Polymer Testing*, 30(6):602–610, 2011.

[130] Department of Polymer Engineering. Mfi testing - viscosity measurements of thermoplastic polymers. *Budapest University of technolog and economics*, 2007.

[131] ASTMD 1238. Standard test method for melt flow rates of thermoplastics by extrusion plastometer. 2004.

[132] J M Dealy and K F Wissbrun. *Melt Rheology and Its Role in Plastics Processing,*. Van Nostrand Reinhold, New York, 1990.

[133] S Kullawadee. *Rheological and Mechanical Behaviour of Poly(Lactic Acid)/Polyethylene Glycol Blends*. PhD Thesis, RMIT University, 2011.

[134] W P Cox and E H Merz. Correlation of dynamic and steady flow viscosities. *Journal of polymer Science*, 28:619–621, 1958.

[135] L Shan, Y Tan, and Y R Kim. Applicability of the cox-merz relationships for asphalt binder. *Construction and Building Materials*, 37:716–722, 2012.

[136] A V Tobolsky and R D Andrews. Systems manifesting superposed elastic and viscous behavior. *The Journal of Chemical Physics*, 13(1):3–27, 1945.

[137] H Leaderman. Creep and creep recovery in plasticized polyvinyl chloride. *Industrial and Engineering Chemistry*, 35(3):374–378, 1943.

[138] K P Menard. *Dynamic Mechanical Analysis A Practical Introduction*. CRC Press, Taylor & Francis Group, 2008.

[139] J L S Wales and Den Otter. Relations between steady flow and oscillatory shear measurements. *Rheological Acta*, 9:115–119, 1970.

[140] S Gebhard. *A Practical Approach to Rheology and Rheometry - 2nd Edition*. HAAKE Instruments Inc, USA, 2000.

[141] Y Song and Q Zheng. Linear viscoelasticity of polymer melts filled with nano-sized fillers. *Polymer*, 51(14):3262–3268, 2010.

[142] A D Drozdov and C J Christiansen. Thermo-viscoelastic and viscoplastic behavior of high-density polyethylene. *International Journal of Solids and Structures*, 45(14–15):4274–4288, 2008.

[143] A D Drozdov, J D E C Christiansen, R Klitkou, and C G Potarniche. Viscoelasticity and viscoplasticity of polypropylene/polyethylene blends. *International Journal of Solids and Structures*, 47(18-19):2498–2507, 2010.

[144] R J Crawford. *Plastics Engineering*. Butterworth Heinemann, Woburn, MA, 3 edition edition, 1981.

[145] R Y Li, J Z Liang, and S C Tjong. Morphology and dynamic mechanical properties of glass beads filled low density polyethylene composites. *Journal of Materials Processing Technology*, 79(1–3):59–65, 1998.

[146] A C Comer, A L Heilman, and D S Kalika. Dynamic relaxation characteristics of polymer nanocomposites based on poly(ether imide) and poly(methyl methacrylate). *Polymer*, 51(22):5245–5254, 2010.

[147] A Krairi and I Doghri. A thermodynamically-based constitutive model for thermoplastic polymers coupling viscoelasticity, viscoplasticity and ductile damage. *International Journal of Plasticity*, 60(0):163–181, 2014.

[148] TA instruments. Dynamic mechanical analysis and thermal analysis. *TA instruments, Year = 2005*.

[149] ASTM D4065. Standard practice for plastics: Dynamic mechanical properties: Determination and report of procedures. 2012.

[150] ASTM D4440. Standard test method for plastics: Dynamic mechanical properties: Melt rheology. 2015.

[151] ASTM D5279. Standard test method for plastics: Dynamic mechanical properties: In torsion. 2001.

[152] J Heijboer. Secondary Loss Peaks in Glassy Amorphous Polymers, 1977.

[153] F C Stehling and L Mandelkern. The Glass Temperature of Linear Polyethylene. *Macromolecules*, 3(2):242–252, 1970.

[154] B Schartel and J H Wendorff. Dielectric investigations on secondary relaxation of polyarylates: comparison of low molecular models and polymeric compounds. *Polymer*, 36(5):899–904, 1995.

[155] A Dorigato. Linear low density polyethylene/cycloolefin copolymer blends. *eXPRESS Polymer Letters*, 5(1):23–37, 2010.

[156] Y Huang, C R Gentle, and J B Hull. A comprehensive 3-D analysis of polymer melt flow in slit extrusion dies. *Advances in Polymer Technology*, 23(2):111–124, 2004.

[157] S Nandi, S Bose, S Mitra, and A K Ghosh. Dynamic rheology and morphology of HDPE-fumed silica composites: Effect of interface modification. *Polymer Engineering and Science*, 53(3):644–650, 2013.

[158] J T Seitz and C F Balazs. Application of time-temperature superposition principle to long term engineering properties of plastic materials. *Polymer Engineering and Science*, 8(2):151–160, 1968.

[159] B S Bueno, M A Costanzi, and J G Zornberg. Conventional and acceleratedcreep tests on nonwoven needle-punched geotextiles. *Geosynthetics International*, 12(6):276–287, 2005.

[160] J G Zornberg, B R Byler, and J W Knudsen. Creep of geotextiles using time–temperature superposition methods. *Journal of Geotechnical and Geoenvironmental Engineering*, 130(1):1158–1168, 2004.

[161] ASTM 6992. Standard test method for accelerated tensile creep and creep-rupture of geosynthetic materials based on time-temperature superposition using the stepped isothermal method. 2003.

[162] ASTM D7361. Standard test method for accelerated compressive creep of geosynthetic materials based on time-temperature superposition using the stepped isothermal method. 2012.

[163] J D Ferry. *Viscoelastic Properties of Polymers*. John Wiley & Sons„ 1980.

[164] ASTM D638. Standard test method for tensile properties of plastics. 2001.

[165] ISO 178. Plastics - determination of flexural properties. 2003.

[166] ASTM D256. Standard test methods for determining the izod pendulum impact resistance of plastics. 2004.

[167] K Karthikeyan, B P Russell, N A Fleck, M O'Masta, H N G Wadley, and V S Deshpande. The soft impact response of composite laminate beams. *International Journal of Impact Engineering*, 60(0):24–36, 2013.

[168] J Niglia, A Cisilino, R Seltzer, and P Frontini. Determination of impact fracture toughness of polyethylene using arc-shaped specimens. *Engineering Fracture Mechanics*, 69(12):1391–1399, 2002.

[169] G Weir. A simple conceptual model for the behaviour of an impacting rigid-plastic, spherical, nano-scale particle. *Current Applied Physics*, 8(3-4):355–358, 2008.

Appendix A

Specifications of Materials and Equipments

A.1 Specification of LLDPE (G-Lene R35A042)

Supplier: GAIL India Limited:
http://www.gailonline.com/final_site/lldpe.html

Specifications	Standard Ref	Unit	Value
Melt Flow Index	ASTM 1238	g/10min	4.2
Density @ 23°C	ASTM D1505	g/cc	0.935
Tensile @ Yield	ASTM D638	Kg/cm^2	185
Elongation @ Yield	ASTM D638	%	16
Flexural Modulus	ASTM D790	Kg/cm^2	6000
Izod Impact strength	ASTM D256A	J/m	-
ESCR (F50)-10% Igepal	ASTM D1693	Hrs	> 48
Vicat Softening Point	ASTM D1525	^{o}C	115

A.2   Specification of Fumed Silica (Aerosil-200)

Supplier: Evonik Industries
https://www.aerosil.com

Properties	Standard Ref	Unit	Value
Specific Surface Area	BET	m^2/g	200± 25
Tapped Density	EN ISO 787	g/l	≈ 50
Moisture	2 hrs @ 105ºC	wt.%	≤ 1.5
Ignition Loss	2 hrs @ 1000ºC	wt.%	≤ 1.0
pH	in 4% dispersion	-	3.7 - 4.5
SiO_2 Content	based on ignited material	wt.%	> 99.8

A.3 Specification of LLDPE (Relene - LL36RA045)

Supplier: Reliance India Limited:

//http://www.ril.com/DownloadFiles/Polymers/pe_
LL36RA045.pdf

Specifications	Standard Ref	Unit	Value
Melt Flow Index	ASTM 1238	g/10min	4.5
Density @ 23ºC	ASTM D1505	g/cc	0.936
Tensile @ Yield	ASTM D638	MPa	18
Elongation @ Yeild	ASTM D638	%	20
Flexural Modulus	ASTM D790	Kg/cm^2	6000
Izod Impact strength	D256	kg.cm/cm	25
Hardness	ASTM D2240	Shore D	55
Vicat Softening Point	ASTM D1525	ºC	117

A.4   Specification of Melt Screw Extruder

Supplier: Deepak Poly Plast pvt ltd:

Specifications	Standard Ref	Unit	Value
Overall Dimensions	LxWxH	mm	1780x580x1721
Main Motor	-	ph, V, rpm	3 ph, 415, 1390
No of Stages	-	No	3
Screw Dimensions	DIA, L, L/DIA	mm	19.3, 572, 24:1
Barrel Dimensions	ID, OD	mm	20, 50
Hopper Dimensions	Conical, Height	mm	95, 170
Screw, Barrel,Hopper Material	-	-	SS

A.5   Specification of Melt Flow Indexer (LMI 4000)

Supplier: Dynisco, USA:
http://dynisco.com.mx/pdf/LMI4000.pdf

Specifications	Standard Ref	Unit	Value
Overall dimensions	LxWxH	mm	300x350x570
Operating Temperature	-	ºC	20-425
Temperature Control	-	ºC	± 0.1ºC
Timer Accuracy	-	s	0.001
Displacement Accuracy	-	mm	± 0.025

A.6   Specification of Parallel Plate Rheometer (MCR 102)

Supplier: Anton Paar, USA:

http://http://http://www.anton-paar.com/in-en/

Specifications	Standard Ref	Unit	Value
Maximum Torque	-	mNm	200
Min. Torque, rotation	-	nNm	5
Min. Torque, Oscillation	-	nNm	7.5
Min. Angular frequency	-	rad/sce	10^{-7}
Max. Angular frequency	-	rad/sce	628
Normal Force range	-	N	0.01 to 50
Temperature range	-	^{o}C	-150 to 1000
Dimensions	-	mm	678 x 444 x 586

A.7   Specification of DMA (Q800)

Supplier: TA Instruments, USA:

http://http://www.tainstruments.com
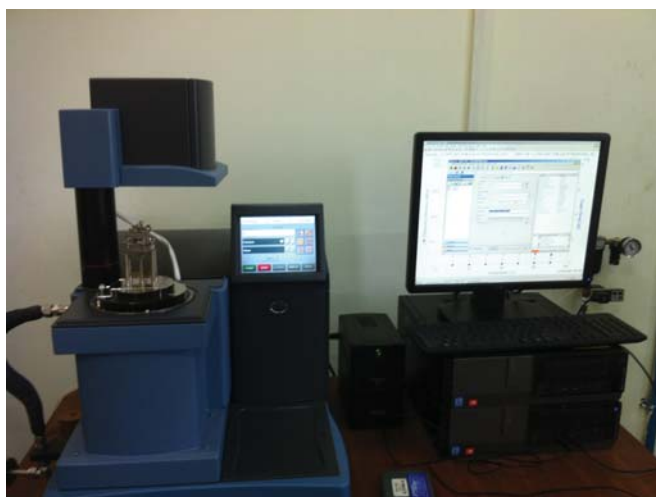
Specifications	Standard Ref	Unit	Value
Maximum Force	-	N	18
Minimum Force	-	N	0.0001
Force Resolution	-	N	0.00001
Strain Resolution	-	nm	1
Modulus Range	-	Pa	10^3 to $3x10^{12}$
Tan Delta Sensitivity	-	-	0.0001
Frequency Range	-	Hz	0.01 to 200
Temperature Range	-	ºC	-150 to 600
Heating rate	-	ºC/min	0.1 to 20
Cooling rate	-	ºC/min	0.1 to 10
Isothermal stability	-	ºC	±0.1

A.8   Specification UTM

Supplier: Deepak Poly Plast Pvt. Ltd. India:

Specifications	Standard Ref	Unit	Value
Maximum Load	-	Kg	950
Maximum Travel	-	mm	600
Load cell Input range	-	Kgf	0 - 9999.9
Accuracy	-	%	0.5
Screw Pitch	-	mm	6.35
Pulse/revolution	-	-	120

A.9   Specification of SEM - EVO18

Supplier: Zeiss, Germany:
http://www.zeiss.com

Specifications	Standard Ref	Unit	Value
Min. resolution	-	nm	3 @ 30kV SE
Acceleration Voltage	-	kV	0.2 to 30
Magnification	-	x	<5 to 1,000,000
Field of View	-	mm	6 at AWD
Chamber Dimensions	-	mm	365ϕ x 275
Pressure range	-	Pa	10-400
X-ray Geometry	-	-	8.5 mm AWD and 35º take off angle

A.10 Specification of XRD

Supplier: Rigaku, Japan:

http://www.rigaku.com/en/products/xrd/miniflex

Specifications	Standard Ref	Unit	Value
X ray tube	-	-	Cu
Data Analysis SW	-	-	PDXL
Optics Filter	-	-	Kβ foil
Goniometer Type	-	-	Vertical
Goniometer Radius	-	mm	150
Scanning Range	-	degree	3 to 145 (2θ)
Scanning Speed	-	degree/min	0.01 to 100(2θ)
Max step width	-	degree	.005(2θ)
Accuracy	-	degree	0.02

A.11   Specification of CACCIA RT 2203B)

Supplier: CACCIA Engineering, Italy :

Specifications	Standard Ref	Unit	Value
Number of arms	-	No	3
Max plate diameter- straight arm	-	mm	2000
Max plate diameter- offset arm	-	mm	1800
Max rpm - Major axis	-	rpm	12.8
Max rpm - Minor axis	-	rpm	12.5
Fuel used	-	-	LPG
Burner Power	-	KW	320
Maximum working temperature	-	ºC	370
Max air consumption	-	l/hr	12000

A.12   Specification of Templogger

Supplier: Roto solutions, SA:

Specifications	Standard Ref	Unit	Value
Temperature range	-	ºC	-20 to 550
Accuracy	-	ºC	±2
Resolution	-	ºC	±0.5
Number of channels	-	No	4
Dimensions	L x W x H	mm	280 x 185 x 185
Operating time	-	min	3x60 min @ 300ºC
Weight	-	Kg	7.5

Appendix B

Graphs and Drawings

B.1   Torque Rheometry Graphs
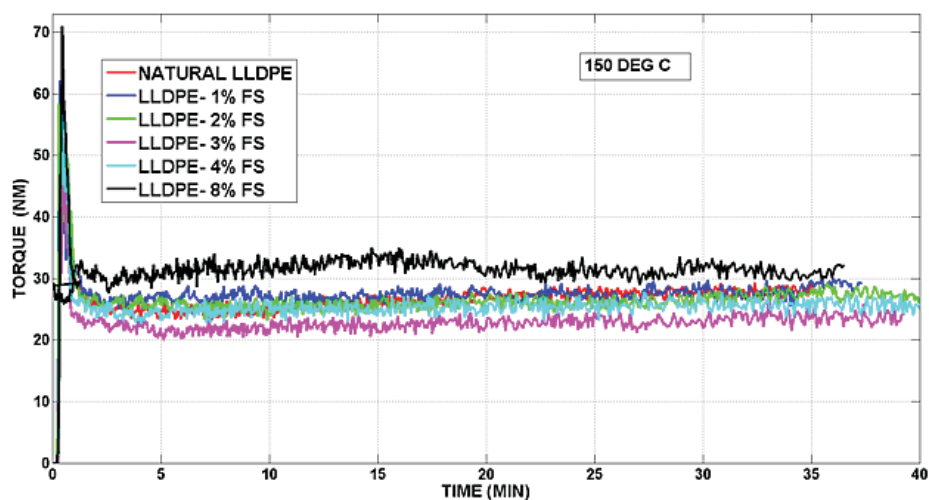
Figure B.1: Torque rheometry graphs for LLDPE-FS blends at 150ºC
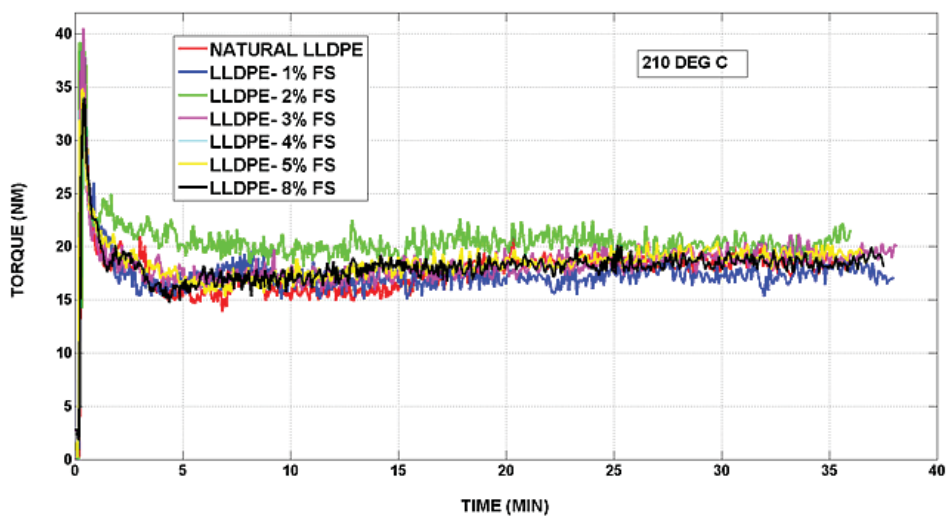
Figure B.2: Torque rheometry graphs for LLDPE-FS blends at 210ºC

B.2 DMA Temperature Ramp Graphs
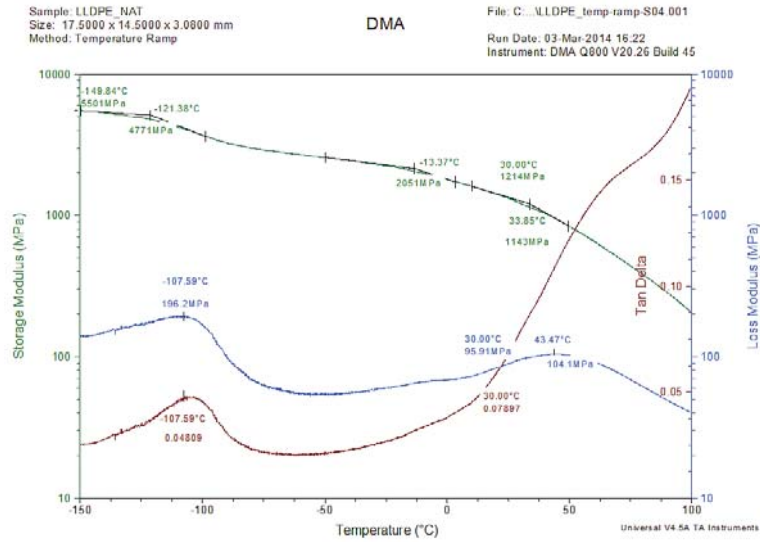
Figure B.3: Natural LLDPE - dynamic mechanical properties
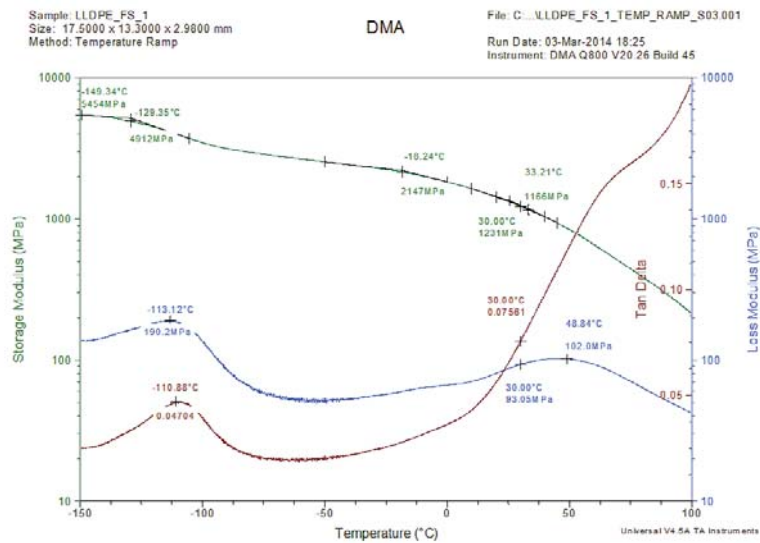
Figure B.4: LLDPE-1%FS - dynamic mechanical properties
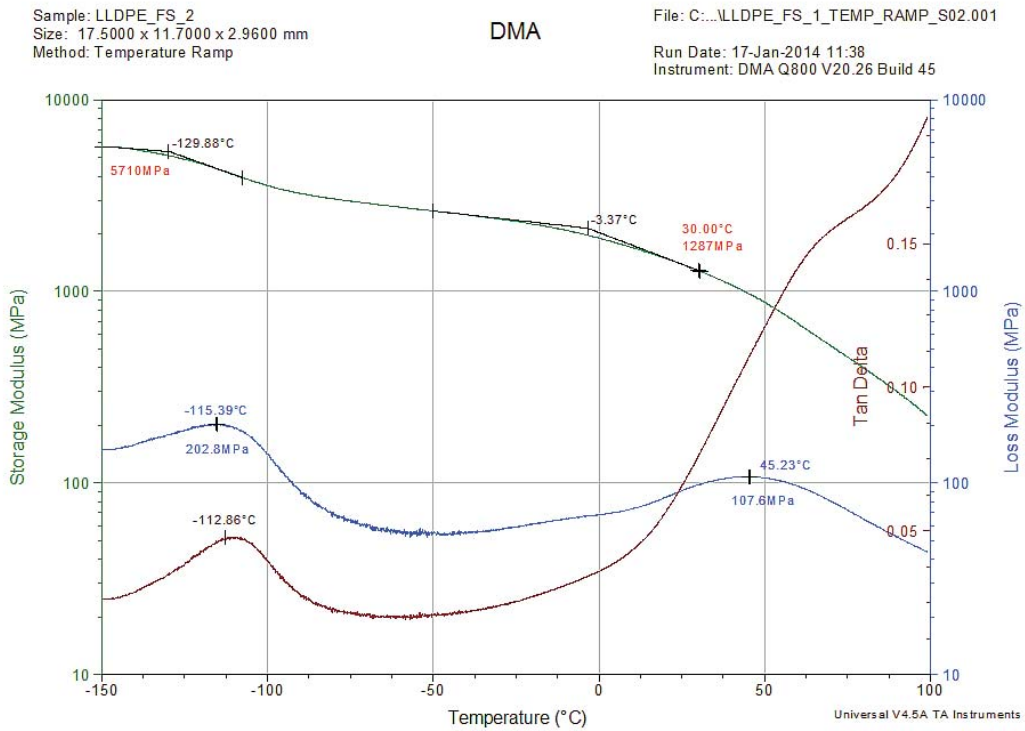
Figure B.5: LLDPE-2%FS - dynamic mechanical properties
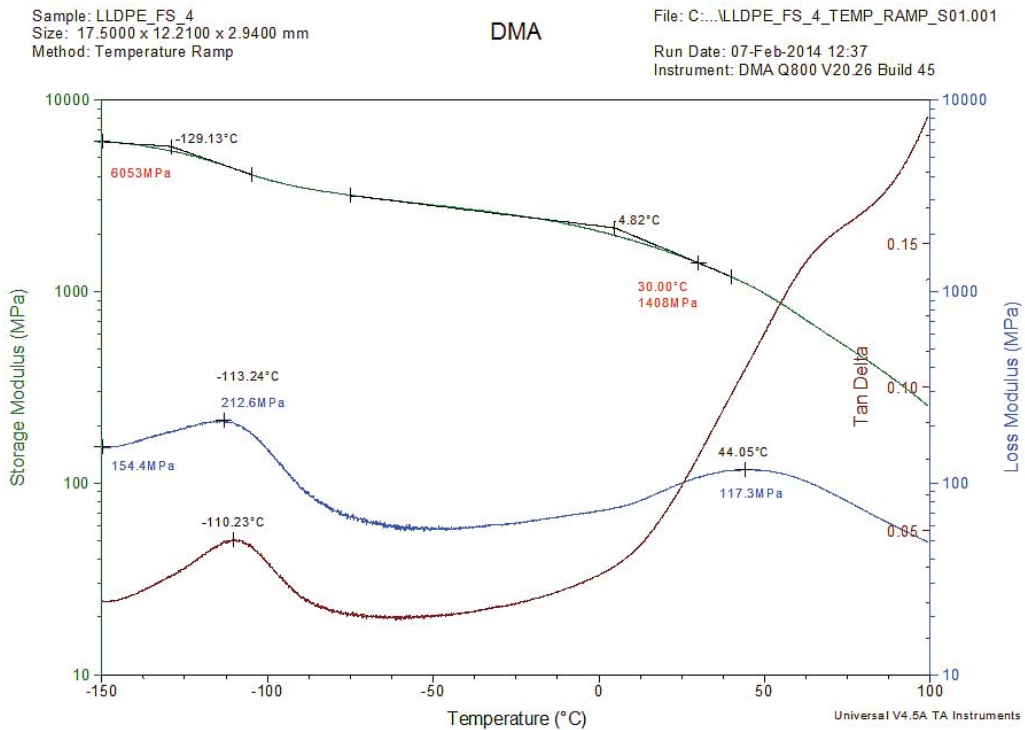
Figure B.6: LLDPE-4%FS - dynamic mechanical properties

148
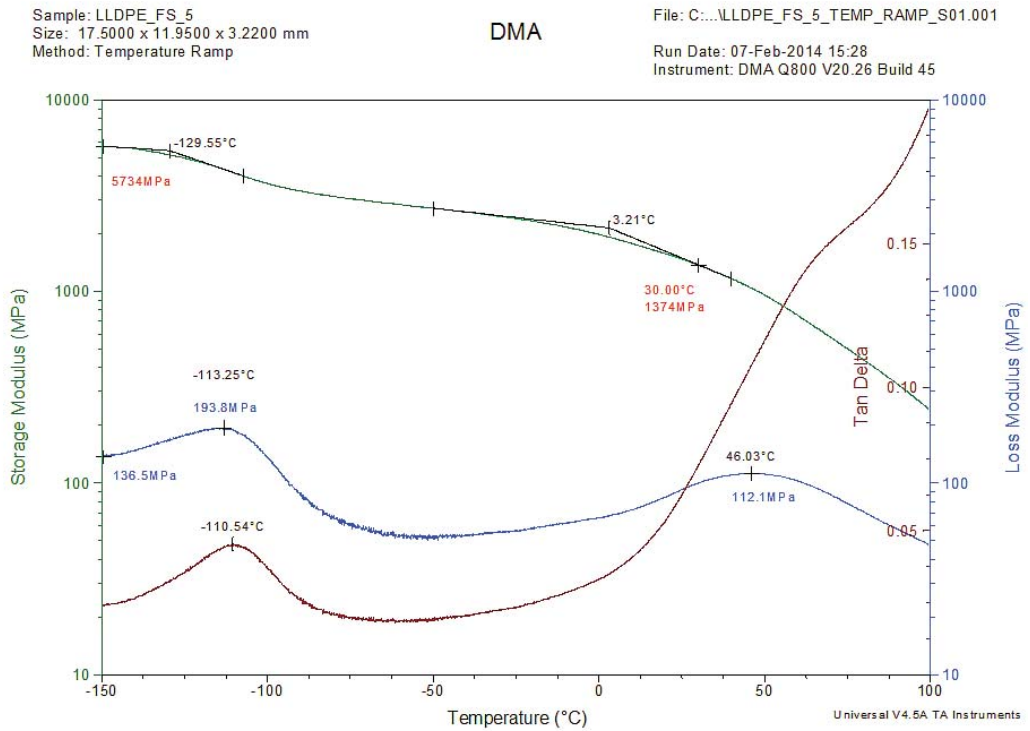
Figure B.7: LLDPE-5%FS - dynamic mechanical properties
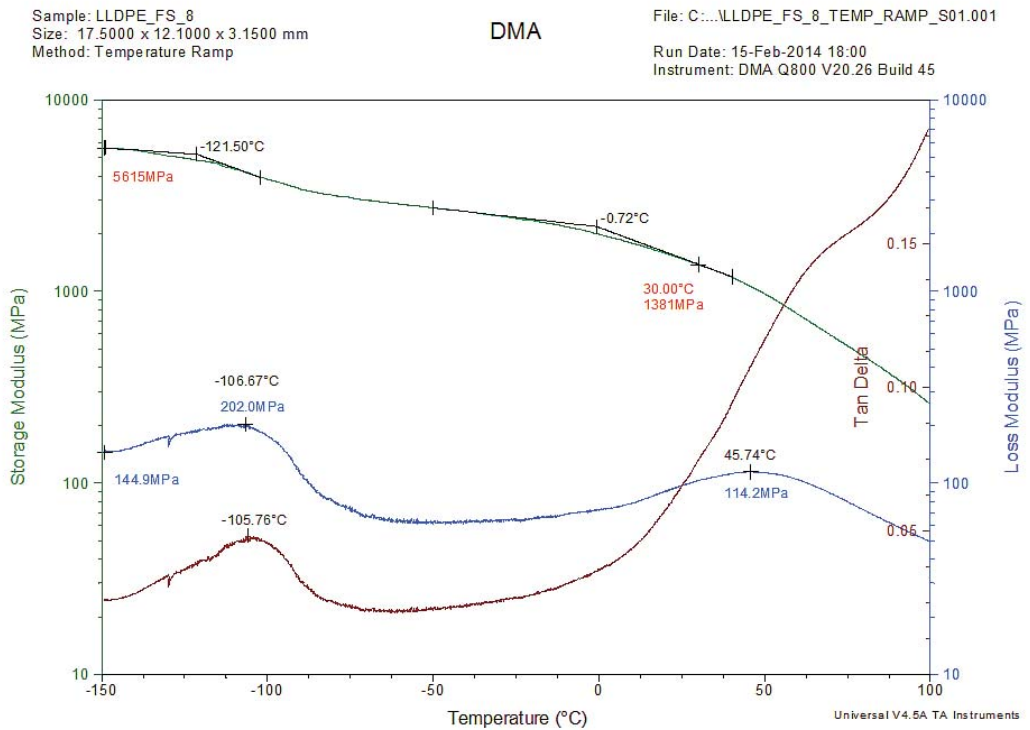
Figure B.8: LLDPE-8%FS - dynamic mechanical properties

B.3 Flexural Testing Graphs
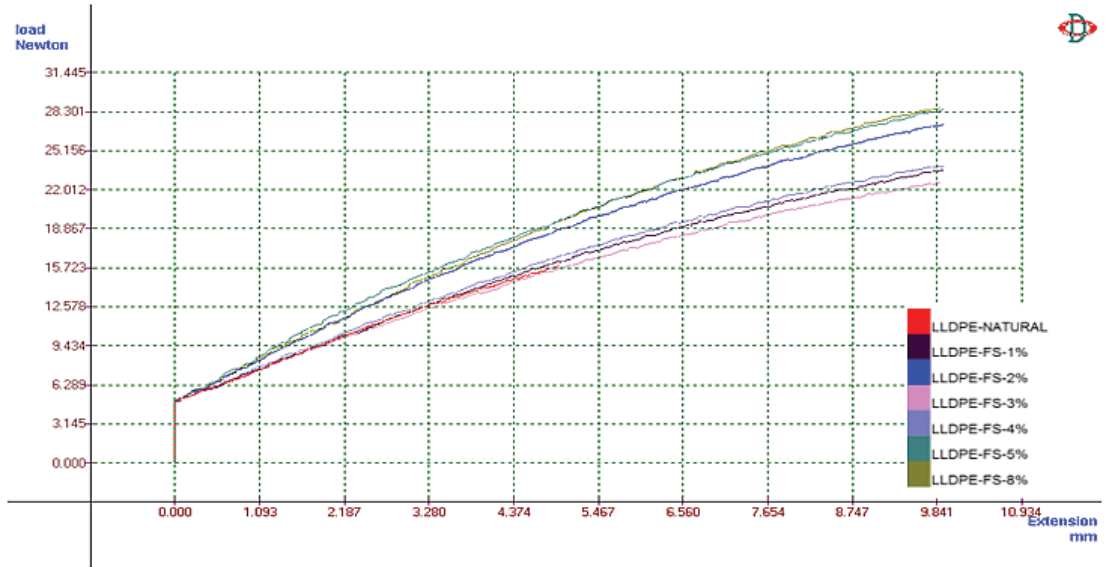
Figure B.9: Flexural testing graphs of natural LLDPE and LLDPE-FS blends at 1.5 mm/min cross head speed
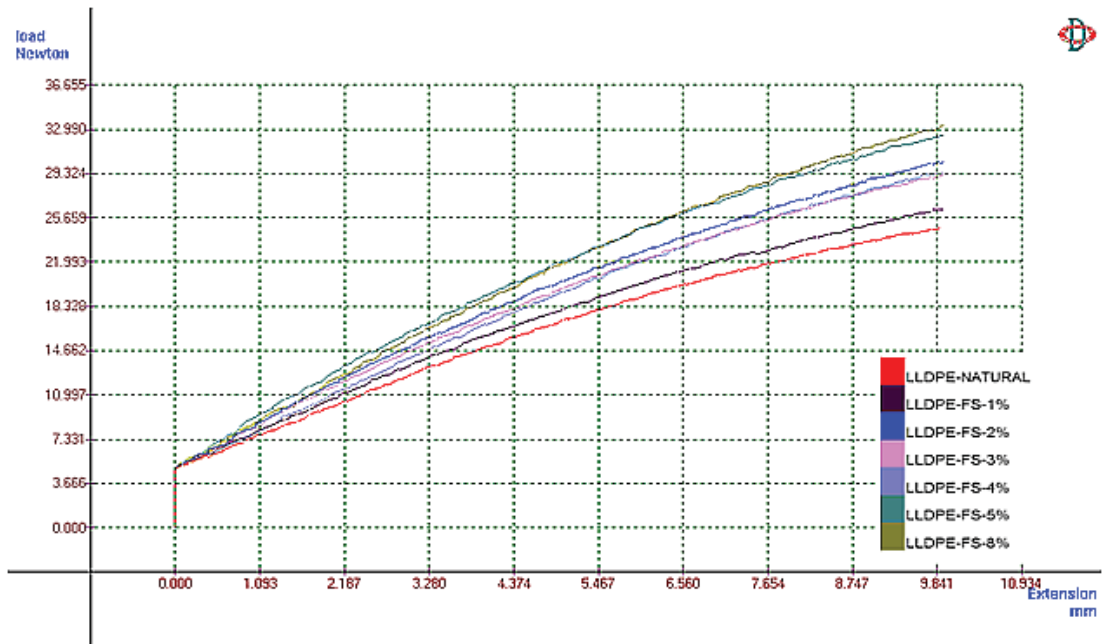
Figure B.10: Flexural testing graphs of natural LLDPE and LLDPE-FS blends at 5 mm/min cross head speed
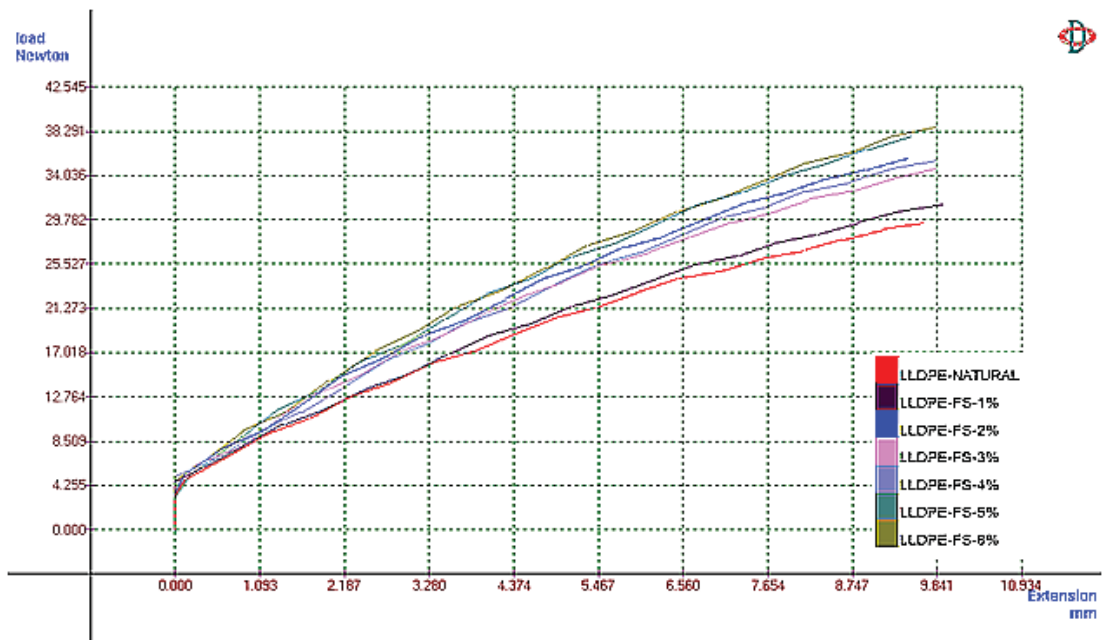
Figure B.11: Flexural testing graphs of natural LLDPE and LLDPE-FS blends at 50 mm/min cross head speed

B.4   Mold Drawings
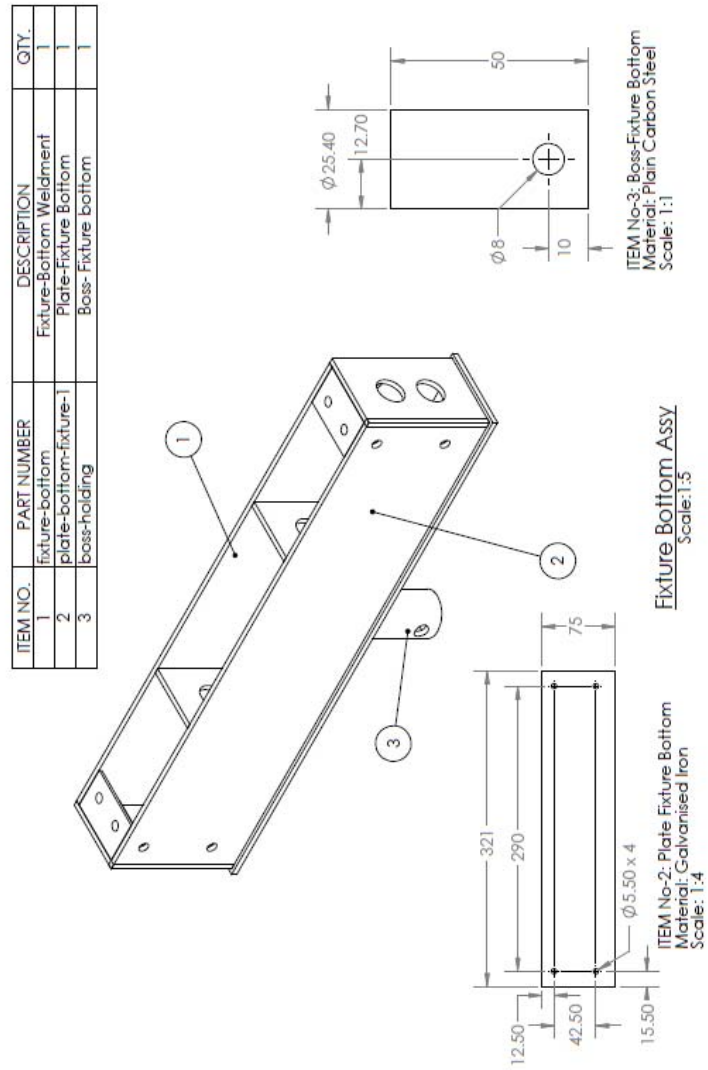
Figure B.12: Mold bottom assembly drawing
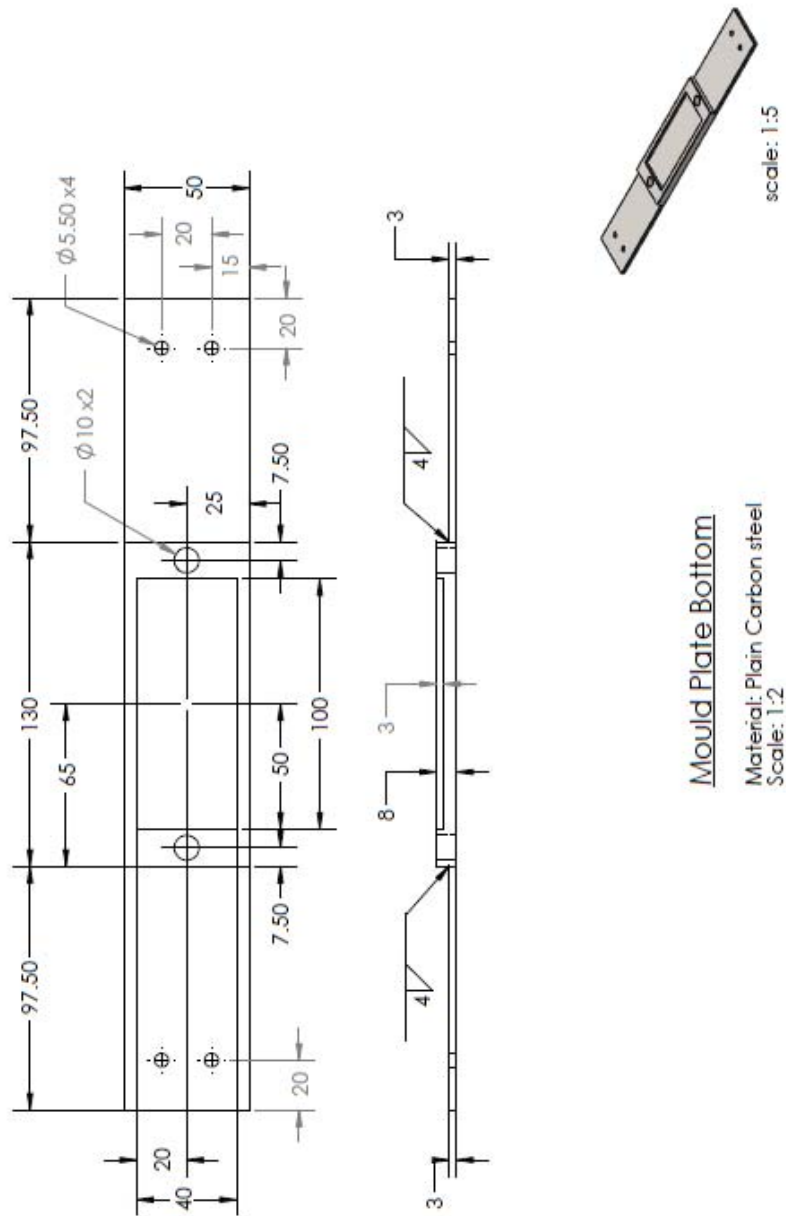
Figure B.13: Mold drawing

Figure B.14: Fixture assembly
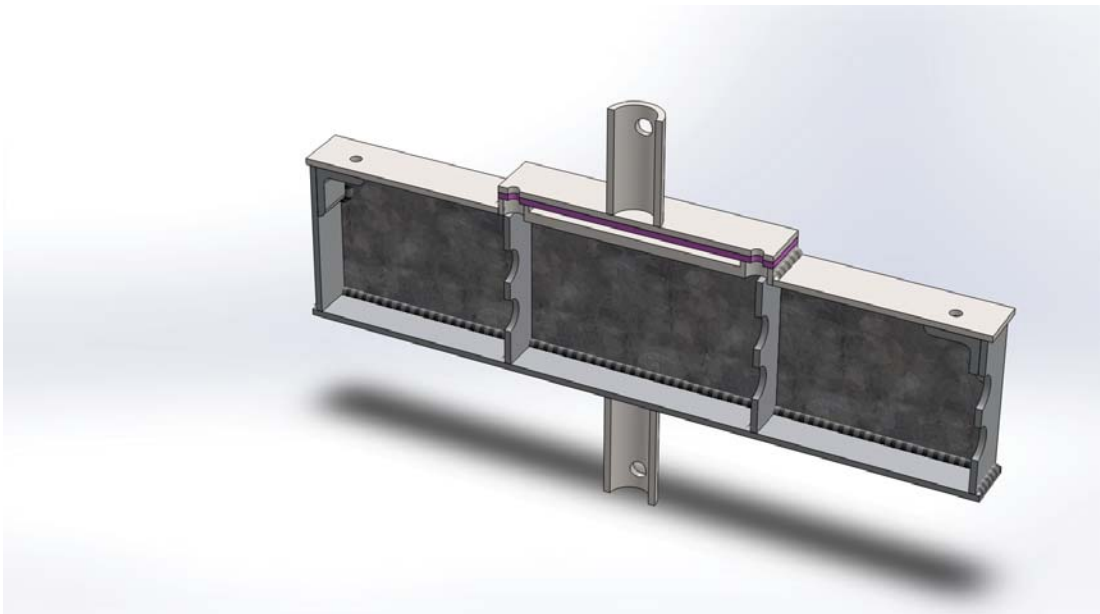
Figure B.15: Fixture cut section

List of Publications

International / National Journals

[1] Girish Chandran V and Sachin D. Waigaonkar. Mechanical properties and creep behavior of rotationally moldable linear low density polyethylene-fumed silica nanocomposites. *Polymer Composites*, In Press, DOI. 10.1002/pc.23600,**IF=1.632**.

[2] Girish Chandran V and Sachin D. Waigaonkar. Rheological and dynamic mechanical characteristics of rotationally moldable linear low-density polyethylene fumed silica nanocomposites. *Polymer Composites*, In Press, DOI. 10.1002/pc.23496, **IF=1.632**.

[3] Girish Chandran V and Sachin D. Waigaonkar. Effect of fumed silica nano particles on lldpe used for rotational molding. *Popular plastics and packaging*, 60:723–26, 2015.

[4] Girish Chandran V and Sachin D. Waigaonkar. Investigations on cycle time reduction, dynamic mechanical properties and creep for rotationally moldable nano composites of polyethylene and fumed silica. *Nano system: Physics, chemistry, Mathematics*, Under Reveiw.

[5] Girish Chandran V and Sachin D. Waigaonkar. Rotational molding of linear low density polyethylene (lldpe) fumed silica nano composites. *International Polymer Processing*, Under Revision.

International Conference

[1] Girish Chandran V and Sachin D Waigaonkar. Rheological Characteristics of Linear Low Density Polyethylene – Fumed Silica Nano composites, International conference on Advanced Polymeric Materials (ICAPM-2013)), Page No: 90-91, OCT: 11-13, 2013.

[2] Girish Chandran V and Sachin D Waigaonkar. Simulation of Rotational Moulding of Plastics for a Rock and Roll Rotational Moulding Machine using ROTOSIM 9th International Materials Technology Conference and Exhibition (IMTCE-2014), May:13-16, 2014.

[3] Girish Chandran V and Sachin D Waigaonkar. Experimental investigations on mechanical properties of Linear Low Density Polyethylene - Fumed Silica nano composites, Proceedings of the 3rd World Conference on Applied Sciences, Engineering and Technology (WCSET-2014),27-29 September 2014, Kathmandu, Nepal, ISBN 13: 978-81-930222-0-7, pp 419-422

[4] Girish Chandran V and Sachin D Waigaonkar. Effect of Fumed Silica Nano-particles on Linear Low Density Polyethylene (LLDPE) used for Rotational Molding, PlastIndia-2015 on Feb: 6-7, 2015.

[5] Girish Chandran V and Sachin D Waigaonkar. Effect of Fumed Silica Nano composites on Linear Low Density Polyethylene (LLDPE) used for Rotational Moulding of Plastics, 35th Australian Polymer Symposium oragnised by Royal Academy of Chemical Engineers , Australia, July 12-15, 2015

[6] Girish Chandran V and Sachin D Waigaonkar. Investigations on cycle time reduction, dynamic mechanical properties and creep for rotationally moldable nano composites of polyethylene and fumed silica, International Conference on Nano materials and Nano technology (NANO-2015), 07-10 Dec 2015.

[7] Girish Chandran V and Sachin D Waigaonkar. Creep and stress relaxation characteristics of rotationally molded linear low density polyethylene (LLDPE) fumed silica nano composites, National Conference on Recent Advances in Manufacturing and Robotics (RAMR-2016), 22 -23 April 2016.

Book chapter

[1] Girish Chandran V and Sachin D Waigaonkar. Chapter 4, Rheological Characteristics of Linear Low Density Polyethylene – Fumed Silica Nano composites, Advanced Polymeric Materials (From Macro to Nano Length Scales),Apple Academic press - USA, Hard ISBN: 9781771880961

Brief Biography of the Candidate

Girish Chandran V is working as full time research scholar in Department of Mechanical Engineering at BITS Pilani - K K Birla Goa Campus, Goa, India. He has completed his Bachelor's degree in Production Engineering and management from REC Calicut (currently NIT Calicut), Calicut University, Kerala, India in 1997 while Masters Degree in Engineering Management from BITS Pilani, Rajasthan, India in 2004. He started his research work in processing of polymers and composites at BITS Pilani - K K Birla Goa Campus in 2012. His research interests are Polymer and Composite Processing, Design and Engineering, Melt Rheology and Optimization.

He has 1 year of teaching experience as Assistant Professor. He has taught different subjects in Department of Production Engineering at PSG College of Technology, Coimbatore, Tamil Nadu, India (2011 - 2012). He has also provided Teaching Assistance for different subjects at BITS Pilani - K K Birla Goa Campus, Goa, India (2012 - till date). He has 13 years of industry experience at different companies in India and USA. He worked as Engineering / Production Planning Manager at KEM-TRON Technologies – Houston, TX, USA (2007 - 2010) responsible for design and development along with production planning for centrifuges, linear motion shale shakers and custom units for mud cleaning. He worked as Mechanical Design Engineer for Hope Consulting Inc – NJ, USA (2006 - 2007) providing design support for off-shore drilling platforms and equipment at Vetco Grey (GE Oil and Gas). He worked as Team Lead (E3) at Larsen and Toubro e-Engineering Solutions (2004-2006) and provided on-site support for Kenworth Trucks, Seattle, WA, USA. He worked as Senior Development Engineer at Ashok Leyland Ltd – Chennai, India (1997 - 2004) assisting chassis design for medium duty commercial vehicles.

He has published 3 papers in journals of national and international repute. He also presented 7 papers in international conferences and has published a book chapter in Nano composites, Advanced Polymeric Materials (From Macro to Nano Length Scales), Apple Academic press, USA.

Brief Biography of the Supervisor

Dr. Sachin Damodharrao Waigaonkar is working as Assistant Professor in Department of Mechanical Engineering at BITS Pilani K K Birla Goa Campus. He has completed his doctoral studies in Polymer and composite Processing from BITS Pilani. He has completed his Masters Degree in Production Engineering from College of Engineering, Pune. He joined BITS Pilani K K Birla Goa Campus in 2004 and teaches the subjects related to Manufacturing and Production Engineering. He has 16 years of teaching experience at first degree, higher degree levels as well as off campus students from industries. His key research areas include Structure-Property-Processibility studies on Polymeric materials, Rotational Molding of Plastics, Fiber Reinforced Composites (FRPs), Analysis of Material Processing Techniques, etc.

He has received research grants from Department of Science and Technology (DST), Govt. of India as well as University Grant Commission (UGC) for the project related with Rotational Molding of Plastics using nano composites. Apart from active participation in course and curriculum development in BITS, he has several publications in journals of national and international repute like Polymer composites, Journal of Reinforced Plastics and Composites, Indian journal of engineering and Material Science ,etc. He has also presented his work in reputed conferences in India as well as abroad like Australian Society of Chemical Engineers, Institute of Materials, Malaysia, ALL India Manufacturing and Design Conference (AIMTDR), etc. The present Ph.D. thesis is the first doctoral thesis under his supervision.

Index